UNIVERSITÉ DU LUXEMBOURG

PhD-FSTM-2024-018
The Faculty of Science, Technology and Medicine

DISSERTATION

Defence held on 29/04/2024 in Esch-sur-Alzette

to obtain the degree of

DOCTEUR DE L'UNIVERSITÉ DU LUXEMBOURG

EN SCIENCES DE L'INGÉNIEUR

by

Samuele CEOLIN
Born on 25 March 1994 in Treviso (Italy)

ROOT DYNAMICS UNDER VARYING WATER AND NUTRIENT SUPPLY

Dissertation defence committee

Dr Stanislaus Schymanski, dissertation supervisor
Luxembourg Institute of Science and Technology

Dr Julian Klaus, dissertation co-supervisor
Professor, University of Bonn

Dr Xavier Draye
Professor, Université catholique de Louvain

Dr Andrea Schnepf
Professor, University of Bonn

Dr Christian Vincenot, Chairman
Professor, Université du Luxembourg

Abstract

Plant roots are dynamically evolving organs able to undergo morphological and physiological changes to overcome water and nutrient limitation. The availability of these resources in the soil environment is naturally heterogeneous and subject to fluctuations. These oscillations are expected to intensify under climate change and increased drought stress. In these circumstances, it is crucial to understand how dynamic roots are in modifying their properties in order to rapidly chase and acquire water and nutrients. Short-scale dynamic adjustments are also often overlooked but can be important for plant fitness and can strongly affect carbon fluxes between the above and belowground.

In the first chapter of this thesis I documented rapid shifts in root distribution in response to localized, short-term water injections in a lab experiment. In Chapter 2 I followed up on Chapter 1 and observed root distribution adjustments both at the seasonal scale and on a daily-basis following precipitation events in a minirhizotron study within a natural grassland. In Chapter 3 I detected a minute-scale increase in respiration rates and a decline in water uptake from roots exposed to pulses in ammonium concentrations in a split-root setup. Higher respiration rates might have been given by activation of proton pumps, facilitating the uptake of ammonium. The ammonium uptake could have then acidified the root environment and reduced aquaporin

activity.

The results provide evidence that roots are highly dynamic structures, capable of locally changing their properties and growth rates within days, following sudden shifts in surrounding resource availability. My findings expand our knowledge on plant morphodynamics and could point to new ways towards more water and nutrient-efficient agricultural practices. The observed mechanisms and adaptations could also be integrated in vegetation models to enhance their predictive capabilities.

Acknowledgments

I extend heartfelt gratitude to those who accompanied me on my PhD journey. To Stan, my supervisor, your support and guidance were crucial to my experience. Your teachings shaped me not only as a scientist but as a person. Your passion for science is truly inspiring. To Julian, my co-supervisor, your insightful inputs were invaluable and contributed immensely in shaping the trajectory of my PhD. I deeply appreciate your teachings and I plan to carry them with me into my future endeavors. To Olli, Adriano, Frank, Jérôme and Jeff, thank you for your incredibly helpful contributions in designing and setting up my experiments and for your assistance during the sampling campaigns. Dagmar, Robert and Daniel, working at Forschungszentrum Jülich was an amazing opportunity and I thank you for your guidance during my stay at IBG-2. To my family, partner, friends and colleagues, your unconditional support means the world.

I dedicate this thesis to my grandma, my biggest mentor, who taught me the joy of observing and appreciating the simple things.

Table of contents

General introduction

Among other functions such as anchorage and storage, roots are responsible for the task of water and nutrient uptake, necessary for photosynthetic and metabolic processes and for cellular activity. Water and nutrient availability in the soil is naturally heterogeneous both in space and time. Water distribution within the soil profile can fluctuate both horizontally and vertically at the centimeter scale and its temporal variation depends on soil drying and wetting cycles (Ritsema and Dekker, 1994 and Dekker et al., 2001 as cited in Hodge, 2010; Schwinning and Ehleringer, 2001; Bauerle et al., 2008; Padilla et al., 2013). Nutrient availability in the soil is subjected to temporal variability as much as it is to spatial variability (Hodge, 2004). Soil nitrogen concentrations in a deciduous woodland varied two to five-fold within a scale of 20 cm (Farley and Fitter, 1999). Overall, spatial and temporal heterogeneity in water and nutrient availability is mostly determined by seasonality, variations in physical and chemical properties of the soil, irrigation/rainfall variability and organic material decomposition rates (Hodge, 2004; Thomas, 2020; Tzohar et al., 2021).

Root systems can implement a series of plastic adjustments to capture water and nutrients and satisfy the plant physiological and metabolic needs under resource heterogeneity (North and Nobel, 1998; Hodge, 2004; Padilla et al., 2013; Fromm, 2019; Yu and Li, 2019; Singh et al., 2020). These plastic

adaptations are expressed as adjustments in both root system morphology and physiology. Physiological adjustments can consist of sub-daily shifts in root hydraulic conductivity regulated by aquaporin activity and abundance, used to favor water and/or nutrient uptake from resource-rich areas (Javot and Maurel, 2002; Gorska et al., 2008; Hodge, 2010; Ishikawa-Sakurai et al., 2014; Tzohar et al., 2021). They can also involve the activity of other protein channels and proton-pumping ATPases, which are cellular membrane structures able to create proton gradients that facilitate the absorption of certain ions (Taylor and Bloom, 1998; Bloom et al., 2002; Zhang et al., 2021).
Root system also display a large degree of malleability in morphology and architectural organization. Root architecture is defined as the spatial configuration of root systems, where roots are typically classified as primary, nodal, and lateral from a developmental viewpoint. Architectural development and organization is mostly determined by processes of new axis emission, branching, and axial growth and can adjust according to environmental conditions and resource availability (Hodge et al., 2009). These adjustments involve branching derivation, rooting depth and various architectural tradeoffs for resource acquisition (Ho et al., 2005; Robbins and Dinneny, 2015; Sebastian et al., 2016). At the single root scale morphological malleability is displayed through mechanisms such as Hydrotropism (root curvature towards wet soil) and Hydropatterning (growth of lateral roots towards wet soil) (Fromm, 2019). At the whole root system level, plasticity is expressed as full scale dynamic shifts following the effects of seasonality on resource availability (Hayes and Seastedt, 1987; Wan et al., 2002; Peek et al., 2006; Saelim et al., 2019).

In agricultural settings, resource availability is often drastically modified to favor crop growth and yield through fertilization and irrigation. Current phosphorus fertilizers are obtained from phosphate rocks, which reserves may be depleted in 50-100 years (Cordell et al., 2009). This highlights the necessity of modifying agricultural practices to limit phosphorus demand and

usage.

Unfortunately, present climate change, increased drought stress and the looming phosphorus crisis are causing pronounced fluctuations in water and nutrient availability to plants and are projected to lead to significant yield loss globally (Cordell et al., 2009; Daryanto et al., 2017; Farrant and Hilhorst, 2022; Torbenson et al., 2023). Consequently, we need a more profound understanding of the dynamics of such plastic adjustments and the plants' ability to withstand and leverage severe fluctuations in resource supply (Chaves and Davies, 2010). Furthermore, while root distribution shifts following seasonal oscillations are well studied, it is necessary to investigate the dynamics of these adjustments reflecting daily fluctuations in resource availability. In fact, short-term root growth dynamics can have a strong impact on plant fitness and are often overlooked and underestimated in root growth dynamics studies (Nguyen et al., 2017; Stewart and Frank, 2008). An improved knowledge in this context could lay the groundwork for achieving food security while minimizing agricultural inputs and for fostering plant breeding programs targeting plastic traits enhancing resilience to water and nutrient scarcity (Eshel and Beeckman, 2013).

The study of these dynamics may have important implications in forestry too, and, at a wider scale, in hydrology and climatology. Plants' roots, together with stem and leaves, are in fact one of the main players in the process of water transfer from soil to atmosphere in vegetation, ecosystem and climate models. Incorporating root adjustments to cope with resource fluctuations into such models might improve their predictive power (Kleidon and Heimann, 1998; Schymanski et al., 2008). This is particularly true for long-term climate change predictions, where models considering static root systems are not suitable and can lead to errors in ecosystem model outputs (Jackson et al., 2000 as cited in Schymanski et al., 2008). Schymanski et al. (2008) developed a vegetation model programmed for root systems to adjust their vertical distribution according to water demand, and its predictions

were much more accurate than models using static root systems. However, further process representation of root dynamic morphological and physiological adjustments is still needed in the model (Schymanski et al., 2008; Wang et al., 2018), especially in the context of strongly fluctuating soil water and nutrient supply and high atmospheric demand.

Another reason highlighting the importance of studying such dynamics is a potential improvement in the understanding of the processes behind carbon cycling and sequestration in soil (Gill et al., 2002a).

The study of dynamic root adjustments to varying resource supply could also enhance the understanding of plant trade-offs, as these dynamics may involve re-routing of carbon allocation to aid the acquisition of the most limiting resource (Eissenstat, 1992). In this context, the estimation of the carbon costs of certain root properties adjustments (i.e., hydraulic conductivity) could again be beneficial for expanding the representation of root processes and properties in dynamic vegetation models. However, to complicate matters, roots seem to implement different physiological adjustments (with different C costs) for the uptake of different nutrients, for example NO_3^- and NH_4^+ (Bloom et al., 1989; Bloom et al., 1992; Cramer and Lewis, 1993).

The overall goal of this thesis is to investigate to what extent, how quickly and how dynamically root distribution and properties adjust in order to chase and capture water and nutrients under rapidly changing availability in space and time. Findings from such investigation hold the potential of improving the overall knowledge of plant morphodynamics. Additionally, they could be built upon for the development of agricultural methods and plant breeding programs aiming at increasing water and nutrient use efficiency. Such findings would also shed more light on root adaptations and mechanisms to be incorporated in vegetation models for an improved performance.

0.1 Thesis outline

This thesis is composed of three main chapters and a general discussion and outlook section:

- Chapter 1: "Root growth dynamics and allocation as a response to rapid and local variations of soil moisture". In this chapter I aimed at assessing daily-time scale root growth dynamics as a response to rapid and local variations in soil moisture. I also intended to estimate the speed of the response and the reversibility of the dynamics under an abrupt shift in soil moisture conditions. In order to do so I carried out a laboratory experiment where I monitored daily root growth with a magnetic resonance imaging (MRI) technology.

- Chapter 2: "Monitoring seasonal root distribution shifts and daily growth dynamics following precipitation events in a natural grassland". This chapter is a continuation of Chapter 1, as it reports a field study where I aimed at assessing if the daily time-scale root growth dynamics observed in the previous chapter were also observable at the plant community level. In this study I also strove to observe seasonal shifts in vertical root distribution and to understand whether soil moisture was the main driver of root growth in the studied plant community. I approached these goals by designing a minirhizotron experiment in a temperate grassland subjected to naturally changing moisture conditions.

- Chapter 3: "Dynamics of garlic root respiration in response to pulses of nitrate and ammonium". In this chapter I aimed at shedding light on the carbon consumption rates derived from physiological adjustments related to nutrient acquisition. I did so by investigating the real-time dynamics of root respiration and water uptake rates following localized applications of NH_4^+ and NO_3^- in a split-root experiment.

- General discussion and outlook: in this section I discuss the results and the insights gained from the three main chapters and contextualize them from a broader perspective. Additionally, I provide directions for future studies to be built upon my research findings.

The 3 main chapters are written in "we" form, as they are intended for submission to journals as articles co-authored with my supervisors and other external collaborators.

Chapter 1

Root growth dynamics and allocation as a response to rapid and local variations of soil moisture

This chapter will be submitted in modified form as a paper to the journal "Biogeosciences" as "Ceolin, S.; Schymanski, S.; van Dusschoten, D.; Koller R.; Klaus, J.". The work presented in this chapter was made possible by the contributions of Dr. Stanislaus Schymanski (SJS), Dr. Julian Klaus (JK), Dr. Dagmar van Dusschoten (DVD), Dr. Robert Koller (RK), Oliver O'Nagy (OON) and Frank Minette (FM).
Contribution in concept and experimental design: SC (me), SJS, OON, FM, JK, DVD, RK. Contribution in experimental preparation and measurements: SC, SJS, DVD, OON, FM. Contribution in data analysis: SC. Contribution in results interpretation and discussion: SC, SJS, JK, DVD, RK.

1.1 Abstract

Roots exhibit plasticity in morphology and physiology when exposed to fluctuating nutrient and water availability. However, the dynamics of daily timescale adjustments to changes in water availability are unclear and experimental evidence of the rates of such adjustments is needed. In this study we investigated how the root system responds within days to a sudden and localized increase in soil moisture ("Hydromatching"). Root systems of maize plants were grown in soil columns divided into four layers by vaseline barriers and continuously monitored using a magnetic resonance imaging (MRI) technology. We found that within 48 hours after application of water pulses in a given soil layer, root growth rates in that layer increased, while root growth rates in other layers decreased. Our results indicate local root growth was guided by local changes in soil moisture and potentially even by changes in soil moisture occurring in other parts of the soil profile, which would result in a coordinated response of the entire root system. Hydromatching in maize appears to be a dynamic and reversible phenomenon, for which the investment in biomass is continuously promoted in wet soil volumes and/or halted in drier soil volumes. This sheds new light onto the plasticity of root systems of maize plants and their ability to adjust to local and sudden changes in soil moisture, as would be expected due to patchy infiltration after rainfall or irrigation events.

1.2 Introduction

Plant water uptake can be a key limitation to plant growth, above-ground net primary productivity and crop yields. Droughts are expected to increase in frequency, duration and intensity in the future with potentially severe effects on vegetation (Van Loon et al., 2016; Klaus et al., 2022). Crop yields

that are sensitive to water shortage are expected to decline in the future and research to increase drought tolerance and root water uptake efficiency is intensifying (Chaves and Davies, 2010; Daryanto et al., 2017; Farrant and Hilhorst, 2022). One promising mitigation strategy to cope with increased drought stress is to implement plant breeding programs that enhance water uptake through root traits selection (Eshel and Beeckman, 2013).

Roots are known to display plasticity in morphology and physiology under environmental fluctuations (Hodge, 2004; Fromm, 2019). In the presence of spatial variability in soil moisture, plants rely on compensatory mechanisms to meet their transpiration demand. These mechanisms consist of enhanced water uptake from zones with higher moisture that compensate for the lower uptake from the drier zones (Thomas, 2020). In the short-term (hours), local adjustments in uptake rates are mostly driven by water potential gradients (Jarvis, 2011). It can be assumed that the root-soil water potential difference drives root water uptake, while the radial root conductivity and root surface area determine the main resistance to water uptake in relatively wet soils (Schymanski et al., 2008). At the same time, root hydraulic conductivity can be regulated by aquaporin activity locally at sub-hourly time scales to promote water uptake in water-rich areas (Carvajal et al., 1996; Gorska et al., 2008; Ishikawa-Sakurai et al., 2014).

On a longer term (days), root systems can undergo morphological adjustments consisting of promotion of root growth within wetter soil zones, increasing the surface area available for water adsorption (Pregitzer et al., 1993; Majdi and Andersson, 2005; Wang et al., 2005; Bauerle et al., 2008; Zhang et al., 2019a; Tzohar et al., 2021). Among such morphological adjustments of roots, we find “Hydrotropism” and “Hydropatterning” that refer to root curvature towards zones of high water potential and to the promotion of asymmetrical lateral root formation towards wet soil patches, respectively. “Xerobranching”, in contrast, refers to the inhibition of lateral root development in dry soil areas (Giehl and von Wirén, 2018; Fromm, 2019).

Studies also reported another type of morphological adjustment consisting of root proliferation within a wet soil patch and in decline of root growth in drier areas (Engels et al., 1994; Gallardo et al., 1994). As a combination of these latter responses has the capacity to adjust the entire root system to spatial variation in soil water availability, we call this process "Hydromatching" for ease of reference. Hydromatching differs from Hydrotropism, Hydropatterning and Xerobranching as it does not dictate the direction of individual root growth or lateral root emergence. Instead, it considers a larger scale and includes changes to both the elongation rate of pre-existing roots and emergence rate of new roots (of any order) from portions of root systems experiencing a change in soil moisture. Under temporal heterogeneity in soil moisture, studies have mostly focused on seasonal time scales and have shown that plants are able to dynamically shift their root length distribution in response to seasonal fluctuations (Hayes and Seastedt, 1987; Wan et al., 2002; Peek et al., 2006; Saelim et al., 2019).

Although the morphological adjustments under spatial soil moisture changes and the root growth dynamics to seasonal oscillations are well studied, little is known about the dynamics and flexibility of root growth patterns under rapid (daily) changes of soil moisture. Such daily patterns are in fact often overlooked (Stewart and Frank, 2008) and can strongly affect plant fitness (Nguyen et al., 2017). In addition, studies have yet to prove the ability of plants to deploy morphological adjustments according to multiple abrupt, daily changes in soil moisture in different parts the soil profile. A better understanding of such dynamics could lay the groundwork to improve irrigation management and the performance of soil-vegetation-atmosphere models. In fact, it was already shown that models with dynamic root systems performed better than models with static root systems (Schymanski et al., 2008; Wang et al., 2018).

The overarching aim of this study is to decipher the dynamics of the Hydromatching phenomenon at daily time scale. Specifically, we build on previous

studies (Gallardo et al., 1994; Engels et al., 1994; Wang et al., 2005) by analyzing the Hydromatching dynamics such as timing of occurrence, depth independence and local root allocation patterns following abrupt changes in soil moisture. We monitored these dynamics following rapid spatial (different depths) and temporal changes in soil moisture induced by consecutive water pulses applied in different soil layers. The following research questions were addressed:

- Question 1 (onset time of Hydromatching): How quickly does Hydromatching occur following a rapid and local change in soil moisture availability?
- Question 2 (vertical responsiveness): Do roots at different depths respond equally when subjected to local changes in soil moisture availability?

To address these questions we designed an experiment involving the use of maize plants grown under highly controlled conditions in a horizontal split-root setup consisting of layered soil columns. Root development was monitored at a high frequency (every two days) using a Magnetic Resonance Imaging (MRI) technology. This produces 3D images of root systems and allows to measure root distribution repeatedly and non-destructively.

1.3 Materials and methods

1.3.1 Magnetic Resonance Imaging (MRI)

We carried out the experiments using the PlantMRI installation in IBG-2 at the Forschungszentrum Jülich (FZJ). The PlantMRI is suitable for repetitive and non-destructive 3D imaging and measurement of root traits. Magnetic Resonance Imaging (MRI) uses the magnetic moment of atomic nuclei such

as H^1 (protons), which are highly present in water molecules and hence in living tissues. The technology exploits magnetic and radio frequency fields and contrast parameters to differentiate between roots and the background. The software NMRooting was used to translate the MRI signal into 3D images of root systems and into root length values (Dusschoten et al., 2016).

1.3.2 Experimental design

Setup

We used *Zea mays* as the species of interest, as its roots are well suited for MRI detection (Müllers et al., 2023) and pre-experiment showed that it grows well in our experimental setup.
The plants were grown in 45 cm long plexiglass tubes filled with soil and divided in four layers (top three layers of 9 cm and the bottom layer of 14 cm). Layers were hydraulically isolated from each other by vaseline barriers. Each layer had an opening fitting "rhizons", small tubes made of a porous material (10 cm length, 0.15 μm pore size), which are designed for water sampling in soil (Rhizon MOM 19.21.21, Rhizosphere Research Products). We used the rhizons to inject water in the soil layers. The vertical soil moisture distribution was recorded using the Soil Water Profiler (SWaP) available at IBG-2 (van Dusschoten et al., 2020). This sensor allows the determination of volumetric soil moisture (VWC) profiles with a one-dimensional vertical resolution of 1 cm.

Preparatory stage

For the experiment, we selected seeds with a weight between 0.36 and 0.46 g and placed them in wet filter paper in the dark at 20 °C for four days prior to planting. Subsequently, two seeds were planted per column at a depth of 0.5 cm and covered with 2 cm of soil, for a total of 24 columns.

We used a silty sand soil (LUFA Speyer 2.1, LUFA, Speyer, Germany) packed at a bulk density of 1.48 g cm^{-3} in each layer. We added tap water to the soil to reach 15% volumetric water content. The added water contained 1.5 g l^{-1} of NPK fertilizer (20% Nitrogen Total, 20% Phosphorus Pentoxide (P_2O_5), 20% Potassium Oxide (K_2O) and trace elements, Allrounder Peters Professional, ICL). This means that each layer contained 0.1 g of fertilizer at the start of the experiment. The soil surface was covered with perforated parafilm to reduce evaporation. The perforations favored aeration and reduced mold formation.

The soil columns were placed in a room at 30 °C to boost seedling growth. Once one of the sprouts grew through the parafilm (approximately after three days), the shorter sprout was removed. The columns were transferred to a room at 24 °C and exposed to a light/dark period of 10/14 hours. In order to guarantee the same light intensity for each plant, each soil column was placed inside a 90 cm high white PVC column with a larger diameter of 15 cm. The top of the PVC columns was open to allow air circulation. The PVC columns were elevated by 10 cm so that air could also circulate from the bottom up. Each PVC had a LED mounted on top. The LED was programmed in order to produce a PAR of 600 μmol s^{-1} m^{-2} at 30 cm above the soil surface (approximately halfway between the soil surface and the light source). This height corresponds to the one that previously tested plants reached after a period of three weeks. Air humidity was not recorded. Each column was weighed every second day to determine the amount of transpired water. The amount of transpired water was replenished in the top layer right after the weighing. Two weeks after sowing, the plants were placed in a well ventilated growth room with a constant temperature range of 21-23 °C, humidity of 60% and the same lighting conditions as before.

Core experimental stage

In order to efficiently manage the workload and accommodate to the MRI imaging schedule, we selected 18 plants (out of 24) that performed the best in terms of shoot growth, transpiration and root abundance. In the chosen plants, we started recording the volumetric water content (VWC) in each soil layer every two days by using the SWaP. As we could image a maximum of 9 root systems per day with the MRI, the plants were sub-divided into two groups and MRI scans of the root systems were performed every day on one group, such that each root system was imaged every two days. Only layers containing roots were imaged, starting at the top and adding another layer only when the first root reached the bottom of the image. We let the plants acclimate and grow their root systems for two weeks, during which we replenished each layer of each column every two days to 15% VWC by injecting water through the rhizons. Whenever the amount of water to be replenished in the top layer exceeded 20 ml, watering occurred directly by pouring water from the top to speed up the process. Water uptake rates were inferred from the decline in VWC since the water replenishment on the previous day.

Four weeks after sowing, we re-organized the plants into two new groups. Each group was composed of plants that had high, medium and low abundance of roots in Layer 2 (determined visually using the MRI images). We stopped the replenishments of water and let the plants draw down soil moisture to induce water stress for six days. We kept scanning each group every two days. We measured the VWC of each layer of every plant everyday with the SWaP. To avoid excessive damage to the root system, VWC was not allowed to remain below 6% VWC in any layer, i.e. water was replenished back to 6% VWC whenever it declined below this value. Shoot length and leaf number were also recorded daily.

At the end of this water stress period, the plants that did not grow roots in Layer 2 were discarded.

The experiment consisted of two treatments and a control. Only Layer 1 (L1) and Layer 2 (L2) were treated. Layer 3 and Layer 4 were not considered for the treatments because most of the plants did not grow roots there by the end of the water stress period. Treatment 1 (T1) group received a first series of water pulses in Layer 2 (L2) followed by a second series of pulses in Layer 1 (L1), whereas the T2 group received the series of pulses in reverse order. A series of pulses consisted of one water injection per day in a layer, causing a sudden increase in soil moisture that was then maintained for four days. During these four days, soil water in the selected layer was replenished daily to 15% VWC. The other layers were only replenished to 6% VWC if necessary. With Phase 0, Phase 1 and Phase 2, we refer to the three main periods of the experiment, namely the drought period, the period of the first series of pulses and the period of the second series of pulses. This means that Layer 1 and Layer 2 both received one series of pulses, either during Phase 1 or Phase 2 depending on the treatment group (T1 or T2). Phase 0 consisted of the four days prior to Phase 1 (Fig. 1.1), coinciding with the water stress period.

The start of Phase 1 was pre-determined. To determine when to start Phase 2, a SWaP Guided Experimental Design Optimization (SGEDO) approach was used. This consisted of adapting the timing of the start of Phase 2 and of the end of the experiment to the individual plant water uptake rates inferred from the SWaP measurements. This means that each plant had its own start of Phase 2. This started only after the VWC of the layer receiving the pulses (treated) during Phase 1 dropped below 7.5% after the fourth day of pulse. This also means that the experiment ended only when the VWC in the layer treated during Phase 2 was depleted to half its maximum (refer to Fig. 1.6 in the Supplementary information section for examples of the SGEDO approach).

The plants in the control group were also subjected to the draw-down of soil moisture in Phase 0, but afterwards, VWC was raised again to around

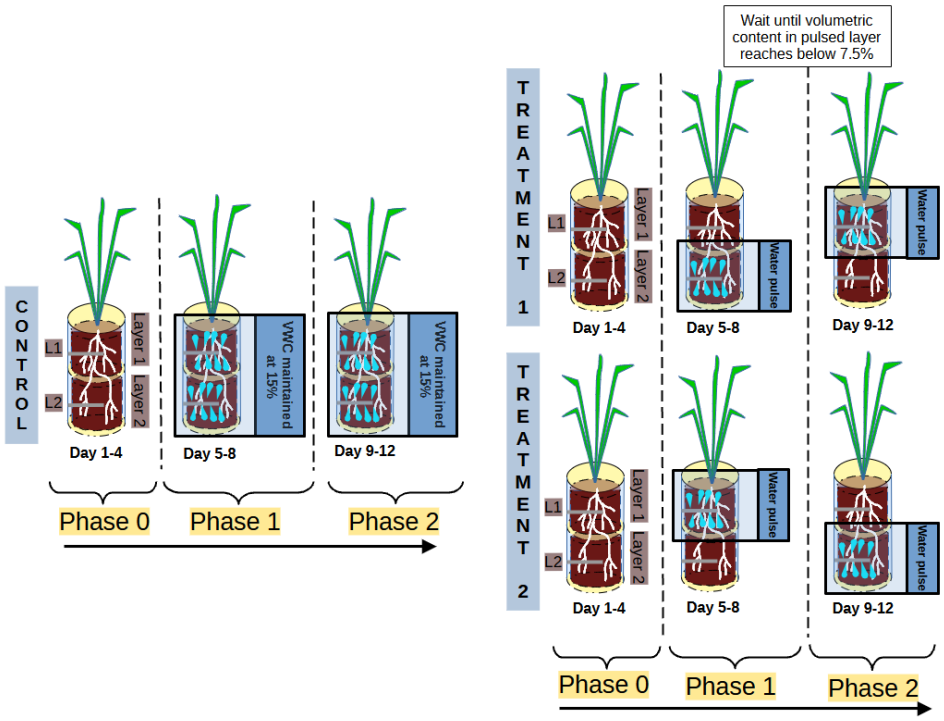

Figure 1.1: Summary of the treatments in the two treatment groups and of the temporal organization into phases in treatment and control groups.

15% in all soil layers and maintained at this level.

1.3.3 MRI image analysis

We used the software NMRooting (Dusschoten et al., 2016) to estimate root lengths from the MRI scans. In many images the estimated root length in L1 was prone to artifacts and a global analysis of the layer resulted in erroneous estimates. Most of the artifacts were related to the watering, which was applied from the top several times in L1, seeping through the perforations in the parafilm. These water leaks generated noisy "clouds" in the MRI

signal which would hinder root detection. Since the MRI can reliably detect roots with diameters above 0.2 mm, fine roots below this detection threshold were not visible in our columns throughout the software outputs. Finer roots could have been particularly difficult to detect in L1, due to the fact that L1 periodically experienced severe levels of dryness ($< 4\%$ VWC), which likely drought out finer roots (making them invisible to the MRI) faster than thicker roots. To overcome the problems of the noisy clouds and of the MRI detection threshold, we selected and measured the root length of clearly visible individual roots in L1.
To limit our analysis to roots that showed some growth during the treatments, we compared the root systems right before Phase 1 and at the end of Phase 2. We selected roots of any order that either appeared or visibly increased their length within this time window.
Individual root selection was not performed in L2 due to the high presence of intertwined lateral roots that would make such selection very difficult and prone to errors. Layer 1, in contrast, had less tangled laterals and a higher presence of visible thicker roots (mostly nodal), easy to trace manually (Fig. 1.7).

In order to ensure that the measurements obtained with the software were consistent and were not influenced by the parameter threshold selection, we varied the noise cutoff and the max gap (two main parameters used by the software to construct the root system) within a given range. We confirmed that our qualitative results and conclusions were not affected by these variations (Fig. 1.12).

1.3.4 Statistical analysis

Growth rates (mm d^{-1}) of each selected root in L1 and of each root system portion in L2 were calculated by subtracting the previous root length

measurement from the subsequent measurement, divided by days between measurements. Comparability of growth rates between different plants and between layers was enabled by normalizing each growth rate time series by its maximum value ("scaled growth rate"). We calculated then the median of the scaled growth rates in L1 and in L2 in each treatment group and control. Since the imaging of each root system was performed every two days, each layer had two data points in each phase of the experiment. Measurements of volumetric water content were used to calculate water uptake in each layer as ml d^{-1}.

The non-parametric Mann-Whitney U test was used in our analysis to compare groups of scaled growth rates and assess if their distributions differed significantly. This test was part of the package "stats" of the Python library "scipy" (version 1.6.0) (Virtanen et al., 2020). The test was used to evaluate the occurrence of Hydromatching as a response to our treatments by comparing the growth rates before and after the pulse. Question 1 (onset time of Hydromatching) was then address by comparing the growth rates before and two days after the start of the pulse in each layer. Question 2 (vertical responsiveness) was tackled by comparing the growth rates before and after the pulse separately for L1 and L2. We also compared the growth rates in L1 with the ones in L2 within the same treatment group and within the same phase to estimate root allocation switches between layers from Phase 1 to Phase 2.

Hydromatching was considered to have occurred when growth rates increased in a pulsed treatment layer and/or when growth rates decreased in a non-pulsed treatment layer.

To assess whether root growth was only affected by local soil moisture or also by changes in soil moisture in a neighbouring soil layer, we carried out correlation analyses between these covariates. The correlations were analysed between scaled growth rates (of each individual root in L1 and of the whole root system portion in L2 of each treated plant) and the volumetric

water content (VWC) in their own layer and between the scaled growth rates and the VWC in the other layer. We used the Pearson correlation coefficient when both sample groups were normally distributed. We used the Spearman rank-order correlation coefficient when at least one of the two sample groups was not normally distributed. We considered the correlation significant if the p-value was below 0.05. Both correlation functions are part of the package "stats" of the Python library "scipy" (version 1.6.0). We ended up performing 60 correlations of scaled growth rates vs local VWC and 60 correlations of scaled growth rates vs VWC in the other layer. Additionally, we visually investigated the evolution of volumetric water content (VWC, %), water uptake rates (ml d^{-1}) and scaled growth rates in time series plots in order to shed light on potential links between root growth dynamics and water acquisition.

The dataset of Chapter 1 can be found on Zenodo at https://zenodo.org/records/10602424 .

1.4 Results

1.4.1 Occurrence of Hydromatching

The occurrance of Hydromatching was determined by comparing the scaled growth rates between phases for the treatment layers pulsed during Phase 1 (L2 of T1 plants and L1 of T2 plants, see Fig. 1.1) and for the treatment layers pulsed during Phase 2 (L1 of T1 plants and L2 of T2 plants). The scaled growth rates of treatment layers pulsed during Phase 1 significantly increased from Phase 0 (median of 0.06) to Phase 1 (median of 0.55) and significantly decreased in Phase 2 (median of 0.01, purple line in Fig. 1.3, Table 1.1, Fig. 1.2). The scaled growth rates of treatment layers pulsed during Phase 2 significantly increased from Phase 1 (median of 0.01) to Phase

2 (median of 0.61, brown line in Fig. 1.3, Table 1.1, Fig. 1.2). The scaled growth rates in both layers of the controls increased significantly from Phase 0 (median of 0) to Phase 1 (median of 0.74) and significantly decreased in Phase 2 (median of 0.45, black line in Fig. 1.3, Table 1.1). These results indicate that growth rates in a layer increased markedly after transitioning from non-pulsed to pulsed in both treatments and controls. Growth rates in treatment layers also decreased markedly after transitioning from pulsed to non-pulsed. In the controls, growth rates decreased in Phase 2 even though volumetric water content (VWC) was kept at the same level as in Phase 1. During Phase 1 the scaled growth rates in the controls and in the pulsed treatment layers did not differ significantly (Table 1.2), but were both significantly higher than the scaled growth rates in the non-pulsed treatment layers (namely the layers pulsed in Phase 2, Table 1.2). The same was found for Phase 2. During Phase 1 the median of the scaled growth rates was 0.74 for the controls, 0.55 for the pulsed treatment layers and 0.01 for the non-pulsed treatment layers (Fig. 1.3 and Table 1.1). During Phase 2 the median of the scaled growth rates was 0.45 for the controls, 0.61 for the pulsed treatment layers and 0.01 for the non-pulsed treatment layers (Fig. 1.3 and Table 1.1). The fact that the scaled root growth rates in the control layers were similar to those in pulsed treatment layers and significantly greater than those in non-pulsed treatment layers indicates that the treatments were responsible for the changes in growth rates.

Note that the median lines in Fig. 1.3 are more representative of the behavior of roots in L1. This was due to the much higher availability of data from L1 than from L2 (5 data points per plant per day from L1 versus only 1 data point per plant per day from L2). This explains the strong resemblance of the median lines in Fig. 1.3 with the median lines in Fig. 1.4a and c.

1.4.2 Onset time of Hydromatching after pulse

We compared the scaled growth rates in both pulsed treatment layers and control layers on the first day of pulse and 48 hours after to determine the onset time of Hydromatching. The scaled growth rates increased significantly during this time interval (median increased from 0.05 to 0.75, p-value$<$0.01 not shown in tables). Refer to Fig. 1.8, 1.9 and 1.10 for the growth rates over time in each individual plant. This, along with the evidence described at the end of subsection 3.1, implies that Hydromatching occurred within two days from a pulse. Note that in this analysis scaled growth rates of control layers and of treatment layers pulsed during Phase 1 and Phase 2 were grouped together (refer to Fig. 1.8, 1.9 and 1.10 to see what data were considered in this analysis).

Note that we experienced recurring technical difficulties with the automatic robot arm carrying the plants into the MRI. For example, the robot arm would sometimes get jammed after only carrying one plant into the MRI machine and would stop working for the rest of the imaging sessions, which were scheduled at night. In such case, only one plant was imaged on that day and the rest of the plants had to be imaged the following morning. This explains why in Fig. 1.3 and Fig. 1.4 there are days with only one measurement of growth rate available. These technicalities also did not allow us to maintain a constant 48 h interval between imaging events for each root system, which, at times, occurred 24 and 72 hours apart. In any case, growth rates (d^{-1}) were calculated by dividing the change in root length between two measurements by the time interval between measurements.

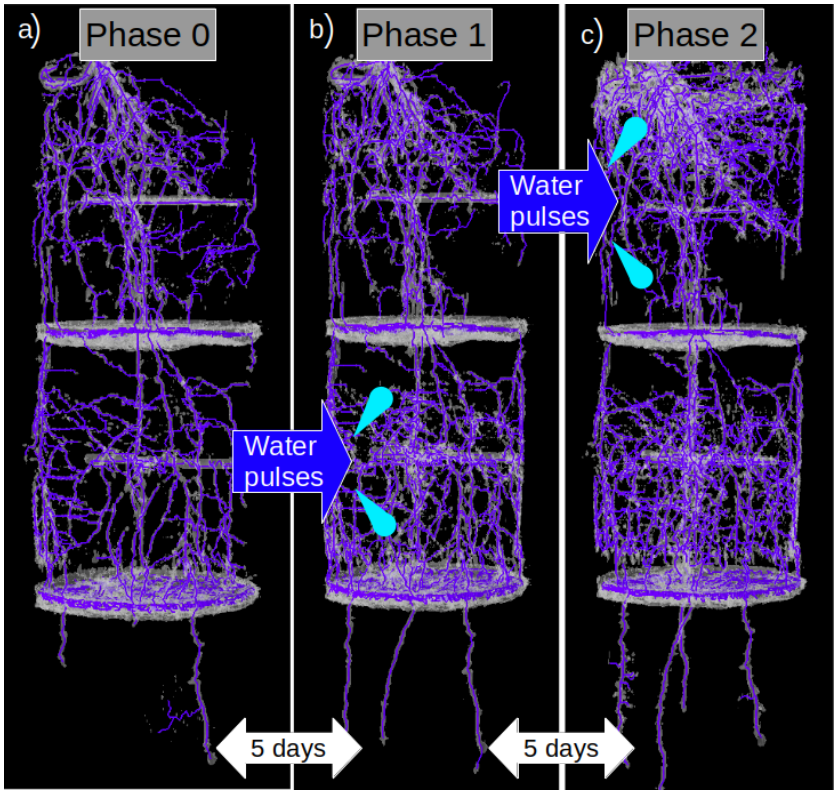

Figure 1.2: Selected MRI images of the same root system at the end of Phase 0 (a), in the middle of Phase 1 (b) and in the middle of Phase 2 (c). A water pulse was a applied in Layer 2 during Phase 1 and another pulse was later applied in Layer 1 during Phase 2. An increase in the root abundance in the pulsed layer is observable during both Phase 1 and Phase 2.

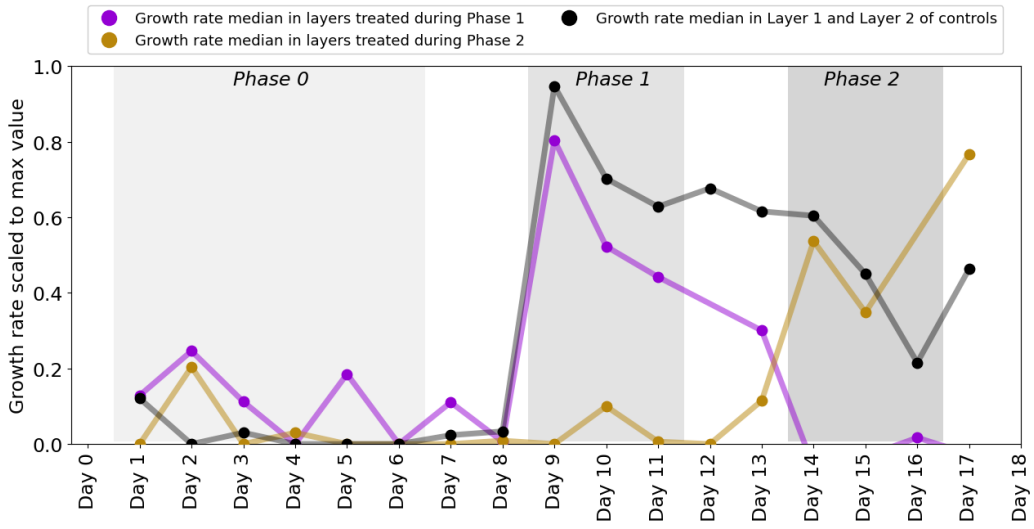

Figure 1.3: Median of the scaled growth rates in the treatment layers pulsed during Phase 1 (Layer 1 in Treatment 2 plants and Layer 2 in Treatment 1 plants), Phase 2 (Layer 1 in Treatment 1 plants and Layer 2 in Treatment 2 plants) and in the controls (where both layers were kept at 15% VWC during Phase 1 and 2). Each median point was calculated from sets of daily data which size ranged from 5 to 29 data points. Each median point contains mixed information of both treatments and layers. The medians of the control group contain mixed information of both layers. Only single data points of scaled growth rate were available on Day 12 for the layers treated during Phase 1 (brown line) and on Day 16 for the layers treated during Phase 2 (purple line). These values were excluded from the plot. The areas of different gray shades indicate the three phases containing the data points used in the analysis. Negative scaled growth rates are not shown. Differences in number of data points per measurement day are due to technical limitation.

Table 1.1: Medians of the scaled root growth rates (with 25th and 75th percentiles) and p-values of the comparisons between the scaled growth rates during different phases for treatment layers pulsed during Phase 1, treatment layers pulsed during Phase 2 and control layers. For the controls, medians and scaled growth rates used in the comparisons refer to both Layer 1 and 2. P-values indicate the probability that an observed difference between the groups considered is coincidentally sampled from the same distribution.

	Treatment layers pulsed in Phase 1	Treatment layers pulsed in Phase 2	Layers of controls
Median of scaled growth rates in Phase 0 (25th - 75th percentile)	0.06 (0 - 0.23)	0 (0 - 0.22)	0 (0 - 0.16)
Median of scaled growth rates in Phase 1 (25th - 75th percentile)	0.55 (0.27 - 1)	0.01 (0 - 0.21)	0.74 (0.42 - 1)
Median of scaled growth rates in Phase 2 (25th - 75th percentile)	0.01 (−0.11 - 0.19)	0.61 (0.19 - 1)	0.45 (0.25 - 0.75)
Scaled growth rates in Phase 0 vs Phase 1 (p-value)	<0.01	0.38	<0.01
Scaled growth rates in Phase 1 vs Phase 2 (p-value)	<0.01	<0.01	<0.01

Table 1.2: P-values of the comparison of the scaled growth rates of the control layers with the scaled growth rates of the non-pulsed treatment layers, from the comparison between control layers and pulsed treatment layers and from the comparison between pulsed and non-pulsed treatment layers. The comparison was done between scaled growth rates within the same phase. Refer to Table 1.1 for the medians of the scaled growth rates during each phase.

	Scaled growth rates in controls vs non-pulsed treatment layers	Scaled growth rates in controls vs pulsed treatment layers	Scaled growth rates in non-pulsed treatment layers vs pulsed treatment layers
Phase 1	<0.01	0.13	<0.01
Phase 2	<0.01	0.19	<0.01

1.4.3 Vertical responsiveness of Hydromatching

Scaled growth rates during the pre-pulse and post-pulse were compared separately for L1 and L2 to determine whether roots at different depths would respond equally. The scaled growth rates increased significantly in L1 after the start of the treatment, both in Phase 2 of T1 plants and Phase 1 of T2 plants, with median growth rates from 0 to 0.64 and from 0.01 to 0.55, respectively (purple area in Fig. 1.4a and c and Table 1.3). However, the response of growth rates in L2 to water pulses was not statistically significant, neither in Phase 1 of T1 plants, nor Phase 2 of T2 plants (brown area in Fig. 1.4b and d, and Table 1.3), although a small second peak is visible during Phase 2 in L2 of T2 plants (brown area in Fig. 1.4d). In addition to the significant increase in root growth in L1 in response to the pulse, a significant decrease in growth rate was found in non-pulsed treatment layers (both L1 and L2), when the pulse was applied in the other layer. Some growth rates reached negative values, potentially indicating root disappearance. Scaled growth rates in L1 of T2 plants significantly decreased from a median of 0.55 in Phase 1 to 0.04 in Phase 2 (purple area in Fig. 1.4c, Table 1.3). Scaled growth rates in L2 of T1 plants also significantly decreased from a median of 0.56 in Phase 1 to -0.16 in Phase 2 (brown area in Fig. 1.4b, Table 1.3). Scaled growth rates in L2 of T2 plants decreased from a median of 0.60 in Phase 0 to 0.20 in Phase 1 (solid brown line in Fig. 1.4d). Although L1 clearly responded when receiving water pulses while L2 did not, we observed in both layers a significant decline in growth rate (unless already at 0) in response to a water pulse in the other layer.

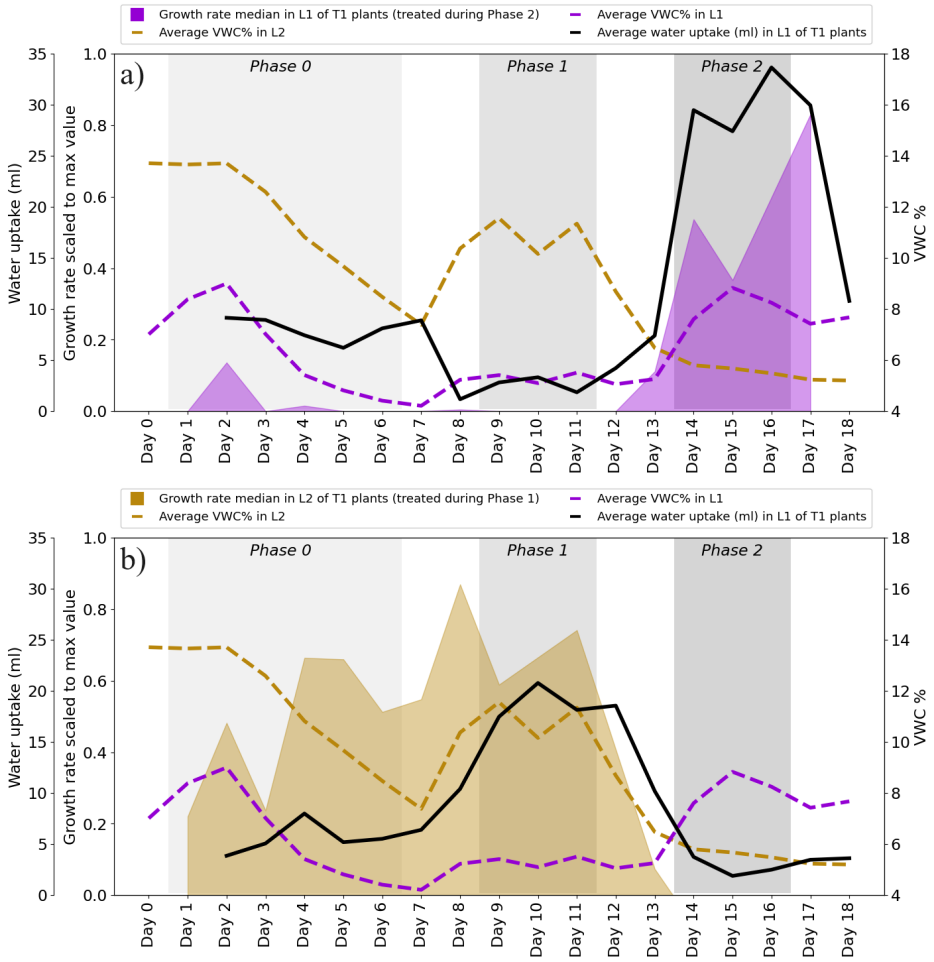

Figure 1.4: Medians of scaled growth rates, volumetric water content (VWC, %) and water uptake rates (ml $24h^{-1}$) throughout the phases. (a) L1 of T1 plants. (b) L2 of T1 plants. Each median was calculated from a range of 5-20 data points per day for L1 and 2-5 data points per day for L2. Note that during the pulse VWC was increased to 15% and that the values of VWC in the plots are lower because the measurements were taken right before the watering. Only single data points of scaled growth rate were available on Day 10 and Day 12 in L2 of T1 plants (b). These values were excluded from the plot.

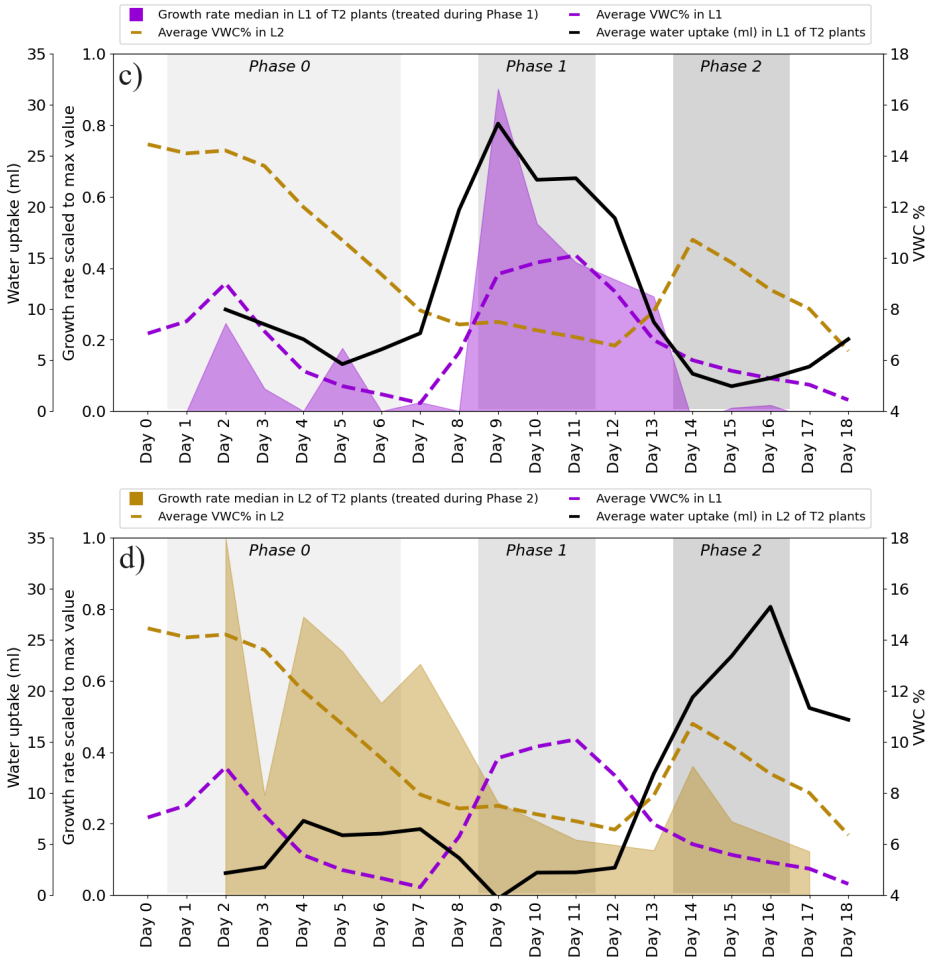

Figure 1.4: Medians of scaled growth rates, volumetric water content (VWC, %) and water uptake rates (ml $24h^{-1}$) throughout the phases. (c) L1 of T2 plants. (d) L2 of T2 plants. Only single data points of scaled growth rate were available on Day 1, Day 10 and Day 16 in L2 of T2 plants (d). These values were excluded from the plot.

Table 1.3: Medians of the scaled growth rates (with 25th and 75th percentiles) and p-values of the comparisons between the scaled growth rates during different phases for the treatment layers pulsed during Phase 1 considered separately (L1 in T2 plants and L2 in T1 plants) and for the treatment layers pulsed during Phase 2 considered separately (L1 in T1 plants and L2 in T2 plants).

	Treatment layers pulsed during Phase 1		Treatment layers pulsed during Phase 2	
	L1 in T2 plants	L2 in T1 plants	L1 in T1 plants	L2 in T2 plants
Median of scaled growth rates in Phase 0 (25th - 75th percentile)	0.01 (0 - 0.16)	0.60 (0.31 - 0.73)	0 (0 - 0.06)	0.60 (0.37 - 0.75)
Median of scaled growth rates in Phase 1 (25th - 75th percentile)	0.55 (0.28 - 1)	0.56 (0.28 - 0.75)	0 (0 - 0.12)	0.20 (0.06 - 0.38)
Median of scaled growth rates in Phase 2 (25th - 75th percentile)	0.04 (−0.07 - 0.26)	-0.16 (−0.40 - −0.04)	0.64 (0.17 - 1)	0.32 (0.20 - 0.83)
Scaled growth rates in Phase 0 vs Phase 1 (p-value)	<0.01	0.50	0.20	0.07
Scaled growth rates in Phase 1 vs Phase 2 (p-value)	<0.01	<0.01	<0.01	0.14

1.4.4 Switches in local root growth allocation from Phase 1 to Phase 2

Scaled growth rates in L1 were compared with the ones in L2 within the same treatment group and within the same phase. This was done to estimate to what extent root growth allocation switched between layers when moving from Phase 1 to Phase 2. During Phase 1, scaled root growth rates in the pulsed treatment layers (L2 in Treatment 1 and L1 in Treatment 2) were significantly higher than in the non-pulsed treatment layers (Fig. 1.5 and Table 1.4). In Phase 2, when the water pulses were reversed, so were the scaled growth rates, again resulting in higher scaled growth rates in the pulsed treatment layers. This was achieved by both decreased growth rates in non-pulsed treatment layers (observed in both L1 and L2), and increased

growth rates in pulsed treatment layers (observed only in L1). This means that roots clearly switched growth allocation patterns between layers when moving from Phase 1 to Phase 2.

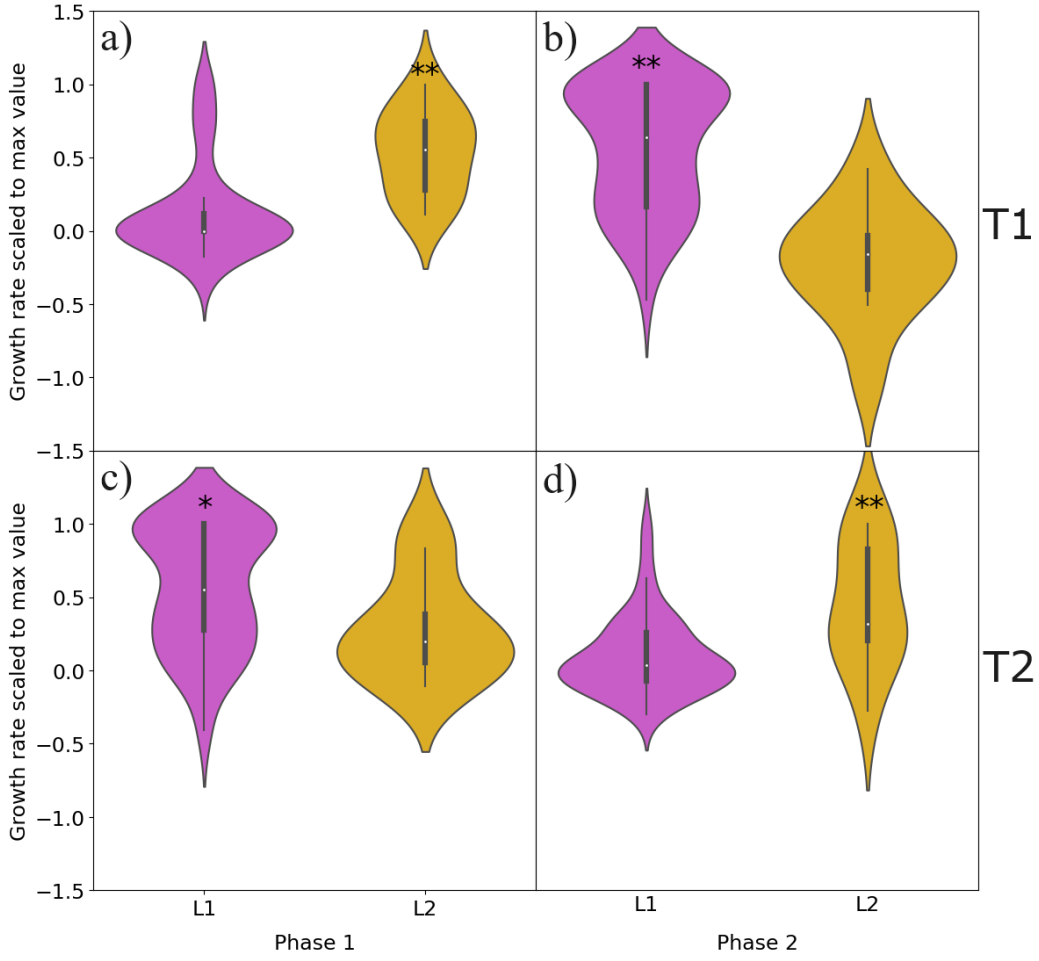

Figure 1.5: Growth rates in L1 and L2 during Phase 1 and Phase 2 of T1 and T2 plants. Panels on the left refer to Phase 1 and on the right to Phase 2. (a)-(b): T1; (c)-(d): T2. Each violin contains 10 data points for L2 and 50 data points for L1. The thick black line inside each violin indicates the range between the 25^{th} and 75^{th} quartiles, while the white circles mark the median values.

Table 1.4: P-values of the comparisons between the scaled growth rates in L1 and L2 during the same phase for each treatment group (T1 and T2). Refer to Table 1.3 for the medians of the scaled growth rates in L1 and L2 of T1 and T2 during each phase.

	Treatment 1	Treatment 2
Scaled growth rates in L1 vs L2 during Phase 1	<0.01	0.01
Scaled growth rates in L1 vs L2 during Phase 2	<0.01	<0.01

1.4.5 Links between VWC, growth rates and water uptake rates

Out of the 60 correlation analyses between scaled root growth rates and volumetric water content (VWC), 17 of them revealed significant positive correlations between root growth and local VWC while 7 of them revealed significant negative correlations between root growth and VWC in the other layer (data not shown). Out of the 50 correlation analyses between scaled root growth rates of individual roots in L1 and VWC, 5 of them revealed both a positive correlation with VWC in L1 and a negative correlation with VWC in L2.

The dynamics of responses in root growth to variations in soil moisture can be seen clearly when visually inspecting the time series in Fig. 1.4. For example, it is interesting to observe how the scaled growth rates and water uptake rates in L2 of T1 plants (Fig. 1.4b) declined during the transition to Phase 2, when the soil moisture reached lower levels (on Day 12 and 13) and the treatment in L1 still had not been applied for any of the plants yet. In L2 of T2 plants (Fig. 1.4d), the scaled growth rates started decreasing during Phase 1 (when the treatment was applied in L1) and the VWC remained almost unvaried until the end of Phase 1. Water uptake rates decreased during Phase 1 and were even close to 0 ml day^{-1} on Day 9. L1 of T2 plants

(Fig. 1.4c) showed a similar behavior as the scaled growth rates and water uptake rates dropped at the onset of Phase 2, when the treatment was applied in L2. Water uptake was lower during Phase 2 (on Day 14 and Day 15) than at the end of Phase 0 (on Day 5 and 6) even though the soil moisture was higher during Phase 2.

1.5 Discussion

1.5.1 Hydromatching observable within two days of a water pulse

Our results provide evidence that maize roots responded to a water pulse by locally increasing their growth rates within the wetted soil layer (Fig. 1.3). Engels et al. (1994) measured root growth twice in maize and once in rapeseed over a period of six days after the re-wetting of a top soil layer. They attributed the observed root growth promotion in the top layer to mobilization of nutrients (only present in the top layer) and not to increased soil moisture itself. In our study Hydromatching occured within 48 h after applying a water pulse in a soil layer likely without the influence of nutrients. In fact, every soil layer was supplied with the same amount of nutrients at the beginning of the experiment, including deeper layers that always stayed relatively moister than the top layer (and where nutrients would therefore be expected to be more mobile). It is possible that changes occurred even faster than within our observation interval of 48 hours. Although enhanced local fine root production within water patches (Pregitzer et al., 1993) and preferential root growth in watered layers over drying layers (Gallardo et al., 1994; Pardales and Yamauchi, 2003) have been documented before, here we see for the first time just how quickly roots can respond to variations in soil moisture.

1.5.2 Growth rate is continuously promoted in wetter layers and inhibited in drier layers

The increase in root growth in response to the reception of water pulses was clear in L1 but it was less evident in L2. In L2 of T1 plants growth rates remained stable while transitioning from Phase 0 to Phase 1 (Fig. 1.4b). This is probably because roots were still establishing in L2 and had not drawn down the soil moisture as much as in L1 by the time the water pulse was applied. In L1, the soil moisture depletion at the end of Phase 0 was so severe that root growth had stopped prior to the first pulse (Fig. 1.4a and c). In addition to an increase in root growth in response to pulses in L1, we observed a consistent decline in root growth in both L1 and L2 when the pulse was stopped there and was applied in the other layer (Fig. 1.4b and c). This suggest that maize roots at different depths respond similarly to rapid changes in soil moisture. A similar behavior has been previously documented in maize and rapeseed. For these plants, root growth increased in the top layer and decreased in the bottom layer after a water pulse at the top (Engels et al., 1994). However, our results show that also the opposite occurs when switching the pulse order in the layers, and that root growth decline might even reach negative values indicating root disappearance. Similar to a previous study on Kiwifruit vines (Green and Clothier, 1995), our measured water uptake rates in a layer were rapidly influenced (within 24 hours) by a change in soil moisture in both that same layer and in the neighboring layer (Fig. 1.4). In fact Green and Clothier (1995) also documented daily-scale shifts in uptake patterns from drier to wetter parts of the soil after re-irrigation. They suspected that this was due to a rapid flush of new root growth and reactivation of existing roots. In our case, water uptake rose prior to the increase in root growth following the water pulse (Fig. 1.4). We hypothesize this was caused by the sudden change in soil-root water potential gradient, which is known to drive water uptake in the short term (hours) (Jarvis, 2011). The

change in gradient allowed the existing roots to markedly absorb the newly available water. Moreover, root water potential in the entire root system might become less negative when a part of the root system has access to a water source at higher water potential, according to modeling results (Amenu and Kumar, 2007; Schymanski, 2008). Hence, water uptake could decline in certain locations even though local soil moisture and canopy water demand did not change. Such situation could have occurred in our experiment as water uptake increased in the newly pulsed layer while almost coming to a halt in the other layer (Fig. 1.4).

In our study portions of maize root systems responded to multiple changes in soil moisture over daily (and potentially even shorter) timescales, by increasing the growth rates in wetted soil layers and/or by decreasing the growth rates in drier layers, inverting the local trends of growth rates between phases (Fig. 1.4 and Fig. 1.5). This demonstrates an exceptional level of dynamic morphological adaptation to rapidly varying moisture availability in young maize plants. The decline in root growth in response to increased soil moisture in another soil layer is one of the most intriguing findings of this study. Carbon allocation seemed to be continuously orchestrated and re-directed to match soil moisture availability, favoring the resourceful soil areas and neglecting the less beneficial ones. This behavior likely allows maize roots to chase dynamic soil moisture sources and take up enough water to meet the transpiration demand while being "cost-effective" in terms of root carbon expenditure. We suspect that carbon allocation for root growth might be dictated by both local soil moisture availability and moisture availability sensed elsewhere. In fact, the observed root growth decline in non-pulsed layers was potentially caused by locally reduced VWC and/or even triggered by an increase in the VWC in the pulsed layer. The identification of both positive correlations between local growth rates and local VWC as well as negative correlations between local root growth and VWC in another soil layer suggests that Hydromatching may not only be a result of root growth

responses to local conditions, but a consequence of a whole root system response. This coordinated response at the entire root system level could be part of a mechanism aimed at efficiently partitioning and targeting carbon allocation wherever and whenever water is more easily accessible. However, to conclusively test the hypothesis that roots respond to soil moisture variations elsewhere in the root system, soil moisture in one soil layer would need to be held constant while soil moisture in another soil layer is varied. This should be done in a follow-up experiment.

Our findings open new avenues for research on irrigation management. The method of patchy resource supply is already known to improve efficiency in resource uptake compared to uniform resource availability, although it was mostly studied for nutrients (Fransen et al., 1999, Hutchings et al., 2003, Wang et al., 2005). When considering alternating patchy supply (changing the location of a resource patch on a daily-basis), water uptake was mostly driven by physiological changes rather than morphological changes (Fransen et al., 1999). In fact, it was hypothesized that root proliferation within resource patches may be too slow to keep up with daily changes in patch location (Van Vuuren et al., 1996, Wang et al., 2005). However, our findings indicate that maize root systems can adjust their growth rates locally within 48 hours (potentially even faster) to match rapid soil moisture changes through Hydromatching. This high degree of morphological plasticity should be further studied to assess its influence on above-ground productivity, canopy water supply and overall plant fitness. Potentially, Hydromatching could be then targeted as a breeding trait and leveraged as a tool to enhance water use efficiency under patchy water supply, caused either by differential infiltration of rainfall or drip irrigation. Vegetation models could also benefit from our findings. They could incorporate the process of Hydromatching to improve predictions of plant water use and carbon uptake, as well as soil moisture dynamics in pulse-driven ecosystems (e.g. Schwinning and Ehleringer, 2001).

1.5.3 Limitations of the study

Non-destructive root imaging was crucial for the insights obtained in this study. Due to the number of treatments and replica and the time needed for measuring one root system, each plant could only be measured every 48 hours. Since we observed root growth responses already within the first 48 hours of a treatment, it is likely that the responses occurred faster than that. To get closer to the actual response time, a similar study should be conducted with fewer individuals and more frequent imaging.

The absence (or weakness) of a response in pulsed L2 could be related to the fact that we did not leave enough time for the root systems to establish before applying the water pulses. Overall, roots reached and explored L2 later than L1. Roots in L1 had already established, substantially consumed water and halted their growth by the time Phase 0 started. Meanwhile, four plants out of ten reached L2 only at the beginning of Phase 0, which then promoted root growth due to the encounter of a wet layer (while L1 was water-depleted). This led to a smaller difference in soil moisture between the pre-pulse and post-pulse in L2 (Fig. 1.4b and d). VWC reached 5% in L1 of T1 plants and 4% in L1 of T2 plants before the pulse (Fig. 1.4a and c). In contrast, VWC in L2 of T1 plants was still at 8% before the pulse and growth rate was promoted there already during Phase 0 because wetter than L1 (Fig. 1.4b). In L2 of T2 plants VWC was slightly above 6% before the treatment and here roots responded weakly to the pulse (small peak in growth rate visible during Phase 2, Fig. 1.4d). Overall, the initial higher levels of VWC in L2 compared to L1 may have affected the intensity of the response to the pulse in L2.

Note that a decrease in growth rates both in non-pulsed L1 and L2 suggests that roots in L2 do behave similarly to roots in L1, confirming that they likely would have increased their growth rates if pulsed following substantial water depletion. However, further testing on well-established root systems

after sufficient dehydration in each layer is needed to better support this interpretation.

In connection with this, another potential limitation of the study could have been the utilization of young plants, and a replication of our study on mature plants would be needed to further corroborate our results. This process might not be straightforward, as more mature root systems might display different degrees of plasticity and responsiveness to soil moisture availability and changes.

The MRI detection threshold of roots with diameter > 0.2 mm did not allow the identification of fine roots, which are known to play a significant role in water uptake (Wilcox et al., 2004). While this did not represent a problem in L1 as there we selected and analyzed well-visible individual roots, this detection threshold could have led to growth underestimation in L2. In fact, at the whole-layer scale including fine roots would have likely offered a more comprehensive view of root responsiveness to soil moisture changes.

Methodological challenges forced us to use different methods for root growth detection in Layer 1 (individual roots) and Layer 2 (portion of the root system). The selection of individual roots that exhibited growth throughout the entire experiment might have introduced a positive bias towards responsive roots. Interestingly, despite the methodological differences, we found similar responses to water pulses in both layers, indicating that our findings are likely not due to a methodological artefact. On the other hand, the use of these different methods precluded us from comparing absolute root growth rates between soil layers. Future studies should consider the same method of root sample selection (individual selection or whole layer selection) for a same-scale comparison of growth rates between layers. For example, a whole layer analysis in L1 should be feasible if watering from the top (causing artifacts) is avoided.

Additionally, targeted experiments should delve deeper into the possibility of local root growth responding to soil moisture variations in other parts

of the root system. This could be done by keeping soil moisture constant in one layer while applying a pulse in a different layer.

1.6 Conclusions

In this study we observed Hydromatching in maize roots as a fast-occurring phenomenon (within 48 hours), providing robust evidence in response to Question 1 regarding the onset time of Hydromatching. This phenomenon likely enables plants to explore dynamic soil moisture sources while economizing on root carbon investments. Hydromatching occurred at different depths of maize root systems, providing evidence in response to Question 2 regarding the extent of vertical responsiveness. Root systems also showed the ability to locally switch their growth allocation and water uptake rates to match rapid changes in soil moisture along the profile. Overall, root growth rates in maize plants were dynamically orchestrated according to temporal and spatial changes in moisture availability. Local growth was dictated by local changes in soil moisture and possibly even by changes in moisture occurring in other parts of the soil profile, which would suggest a whole-root system coordination. Targeted experiments will be needed to conclusively proof such a remote response to local changes elsewhere.
These findings are important indications on how root systems interact with their surroundings and reveal a new level of plasticity and dynamicity in root systems. Future studies should use more mature root systems, established in all the soil layers considered and depleting soil moisture significantly by the time the treatments are applied. It would also be interesting to compare root dynamics of different plant species. Our findings can pave the way towards new strains of research on irrigation management. These could assess the influence of Hydromatching on canopy water supply and potentially explore its use as a tool to improve water use efficiency under patchy water supply in agricultural settings. Future studies could also incorporate our findings into

vegetation-soil-atmosphere models to potentially represent a more realistic and dynamic role of root systems in affecting plant carbon and soil water fluxes.

1.7 Supplementary information

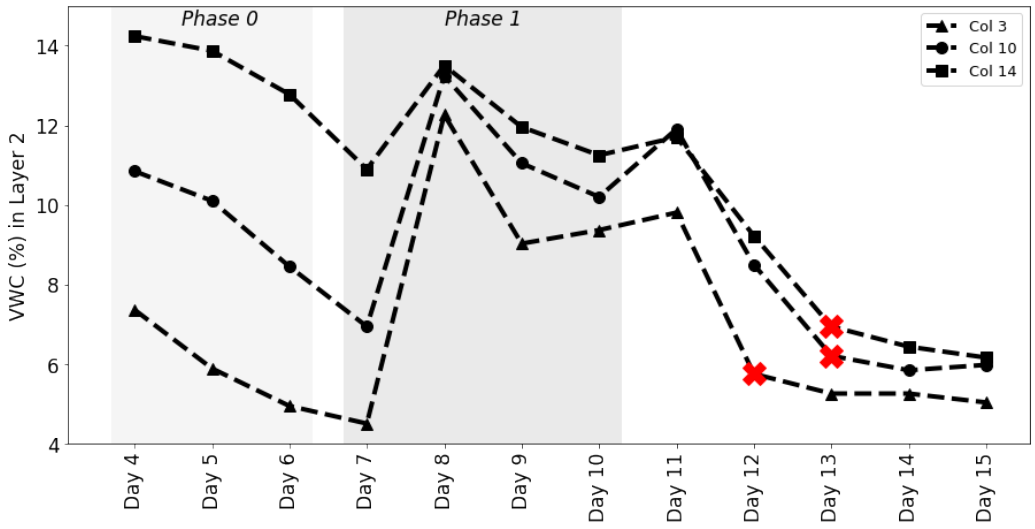

Figure 1.6: The SGEDO (SWaP Guided Experimental Design Optimization) approach in practice. This approach is used to determine when to start Phase 2. The horizontal axis represents the experimental days and the vertical axis displays the volumetric water content (VWC). The lines correspond to the VWC in Layer 2 (L2) of three columns in Treatment 1 (T1) (and so receiving the pulses in L2 during Phase 1 and receiving the pulses in L1 during Phase 2). The light gray block corresponds to Phase 0 (drought period) and the darker gray block corresponds to Phase 1 (when the first series of water pulses was applied). The red crosses correspond to the date when Phase 2 (when the second series of water pulses was applied) started for each of the three columns, i.e. when the VWC dropped below 7.5% in L2 after Phase 1 (it took 2 days in Column 3 and three days in Columns 10 and 14). Refer to Fig. 1 to understand the meaning of "L1, L2, T1, T2, Pulse, Phase".

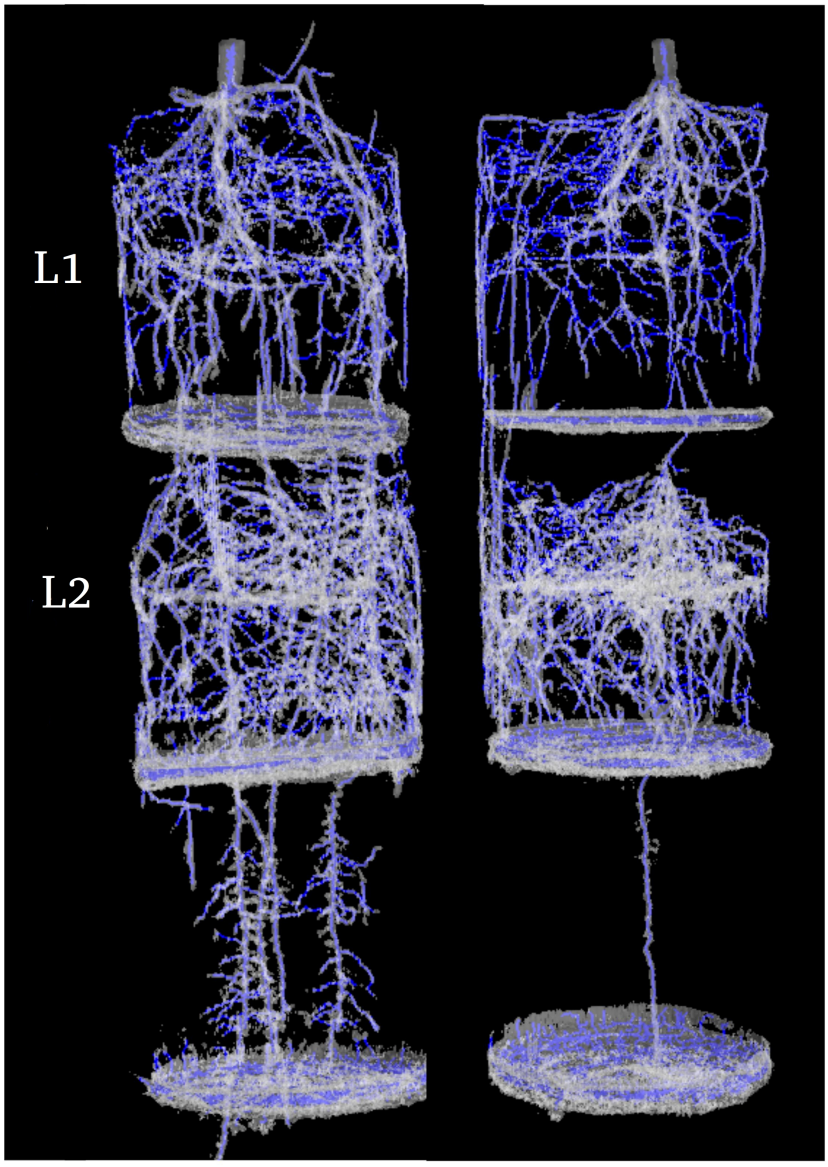

Figure 1.7: Higher presence of intertwined and clustered lateral roots in L2 compared to L1. Roots in L1 are easier to distinguish and to track all the way to the tip. This is the reason why individual root selection was not performed in L2, as such selection would have been difficult and prone to errors.

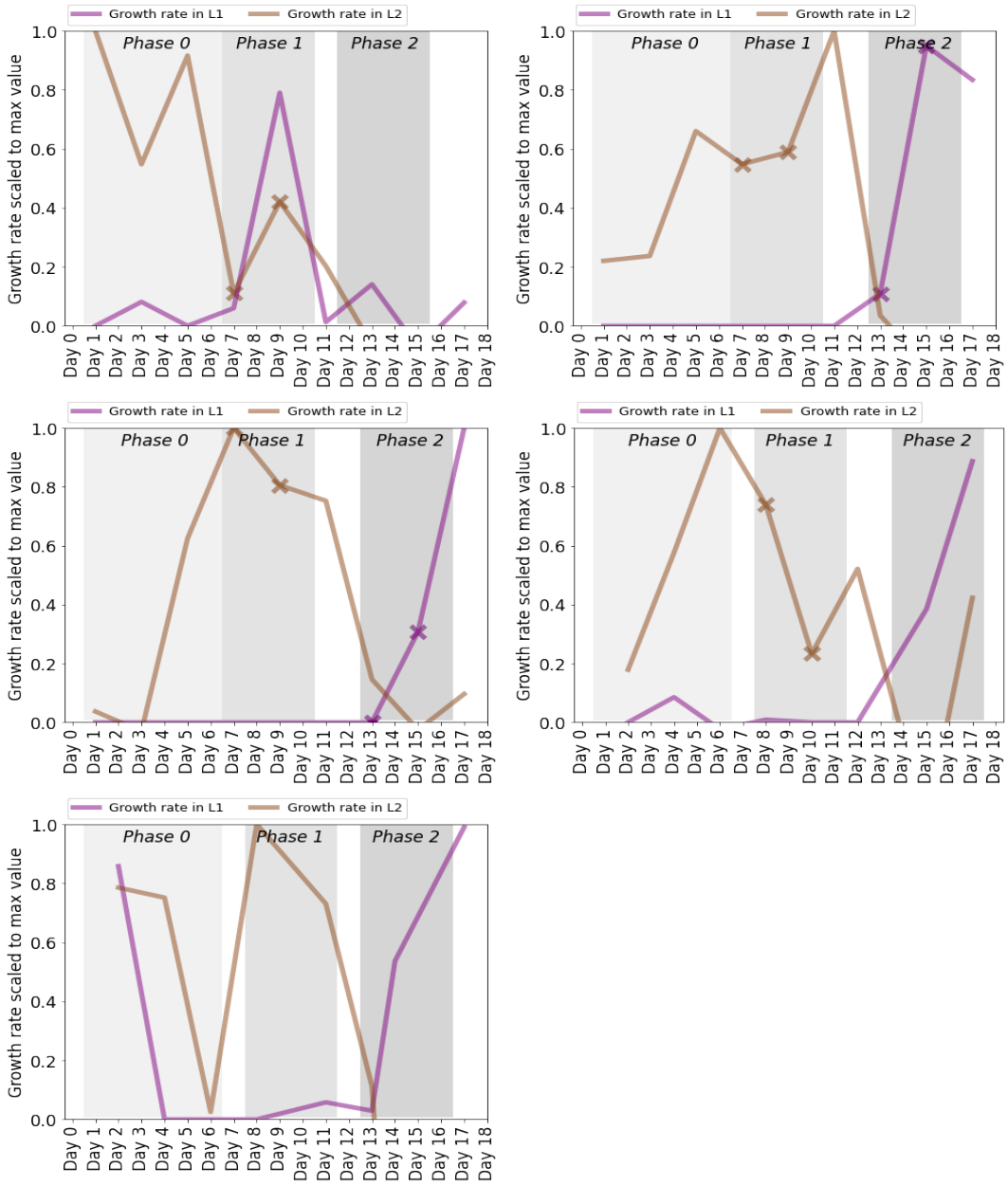

Figure 1.8: Medians of scaled growth rates for each T1 plant (treated in L2 during Phase 1 and in L1 during Phase 2). Purple lines are scaled growth rates in L1 and brown lines are scaled growth rates in L2. The crosses indicate the data points used in the statistical analysis of Question 1 (speed of Hydromatching). Only data points obtained on the first day of the pulse series and 48 hours later were considered, regardless of the phase.

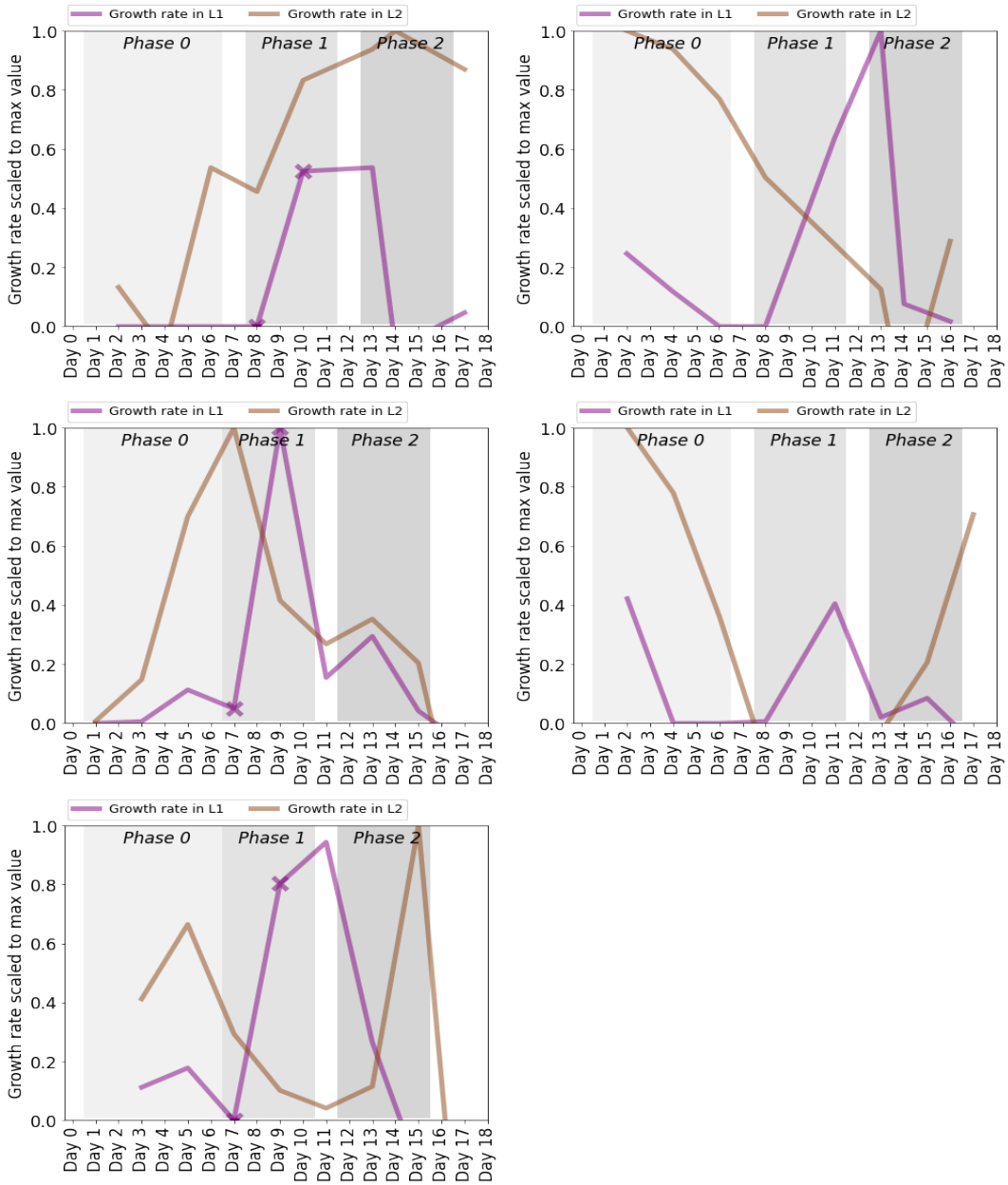

Figure 1.9: Medians of scaled growth rates for each T2 plant (treated in L1 during Phase 1 and in L2 during Phase 2).

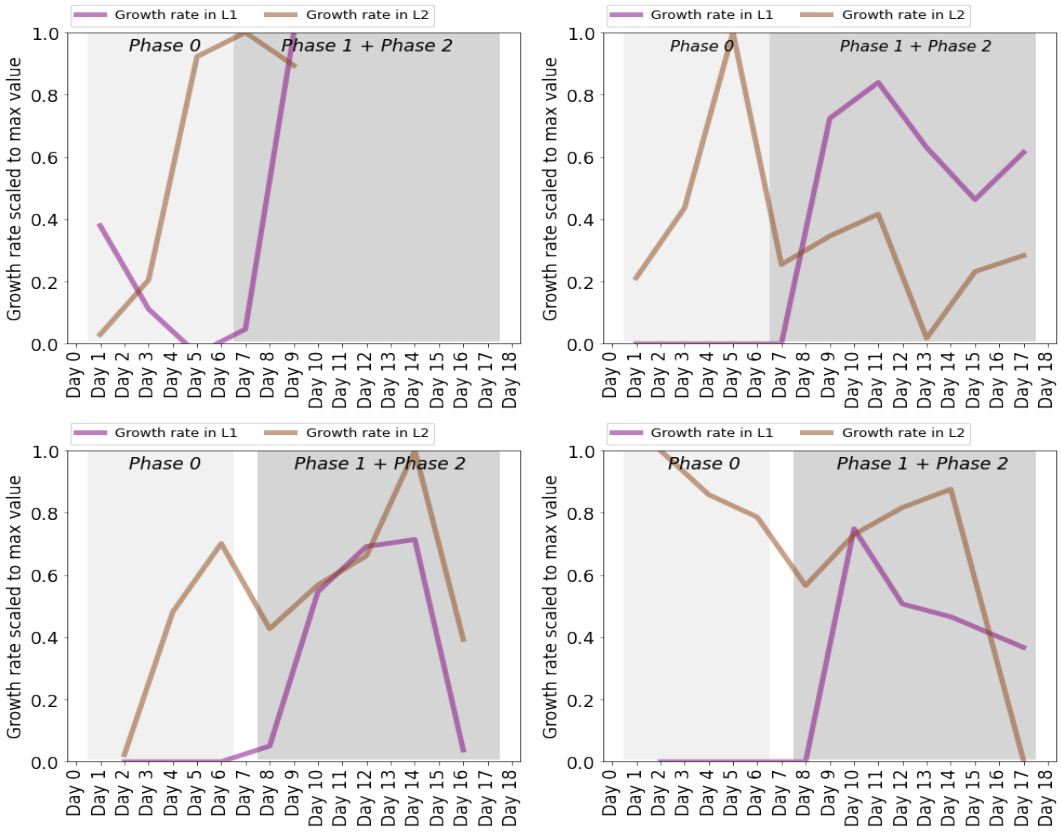

Figure 1.10: Medians of the scaled growth rates for each control plant (where VWC was kept at 15% in both L1 and L2 during both Phase 1 and 2)

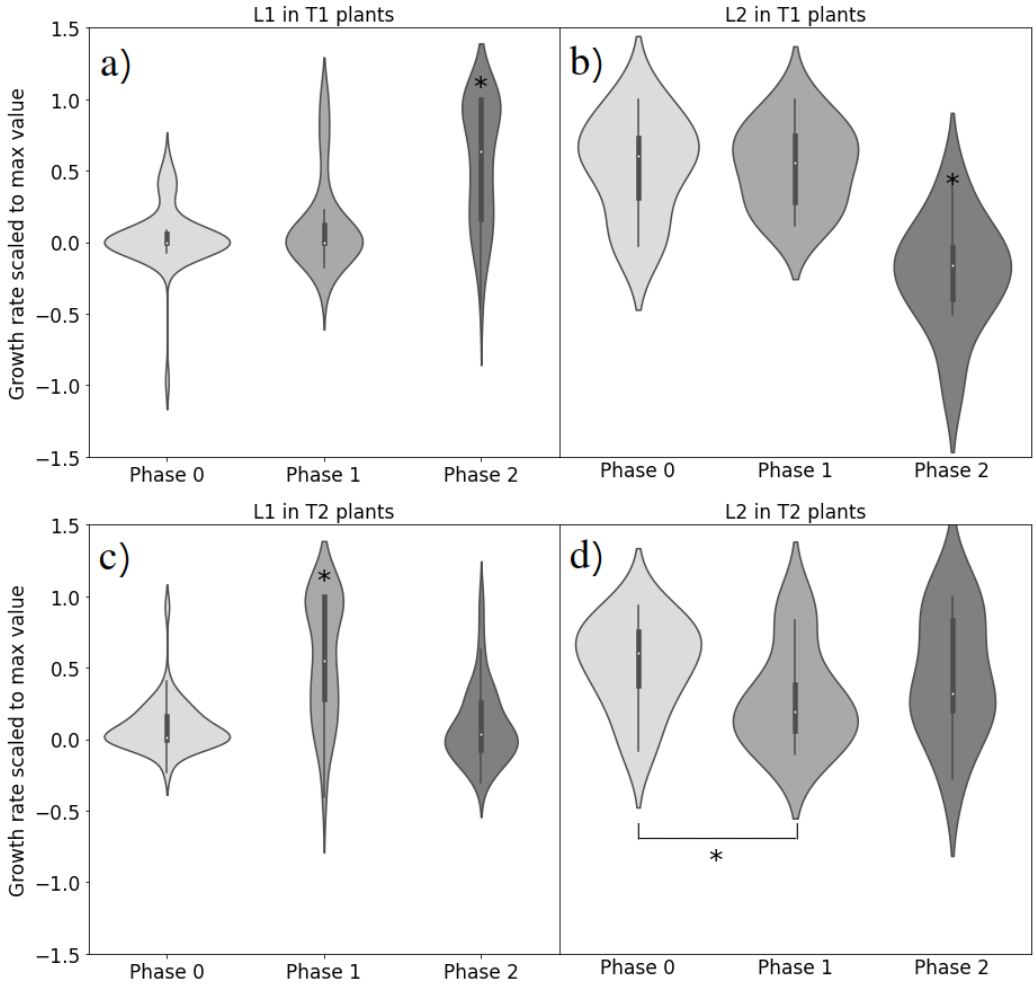

Figure 1.11: Violin plots of growth rates during the three experimental phases in T1, T2 and controls. Panels on the left refer to L1 (50 data points in each violin), and on the right to L2 (10 data points in each violin). (a)-(b): T1; (c)-(d): T2; (e)-(f): controls. The horizontal axis represents the different phases and the vertical axis the scaled growth rates. The thick black line inside each violin indicates the range between the 25^{th} and 75^{th} quartiles, while the white circles mark the median values. A violin marked with an asterisk has a higher mean rank compared to the other violins ($p<0.01$ for all plots, except for (d) where the difference exists only between the violin in Phase 0 and the violin in Phase 1).

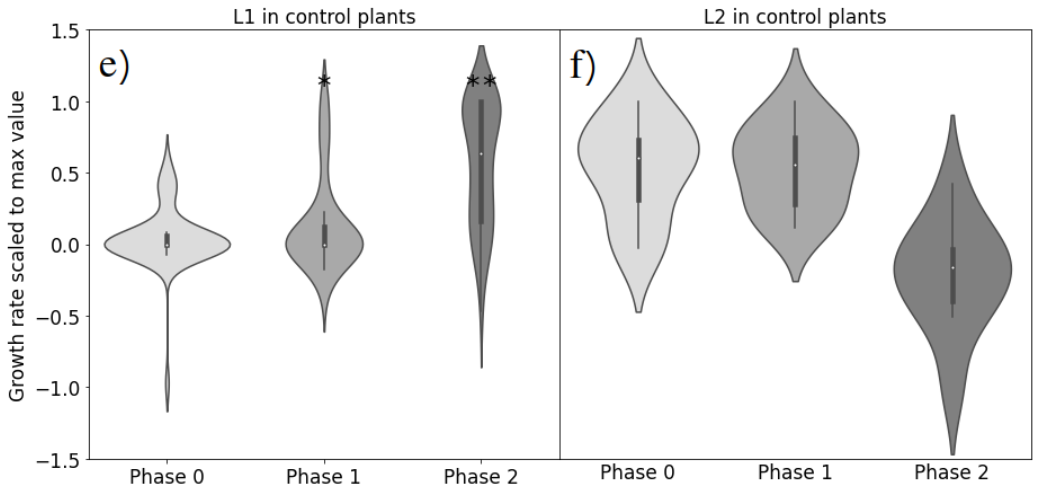

Figure 1.11: Refer to previous caption.

1.7.1 Results of sensitivity analysis

The results of the sensitivity analysis revealed that the choice of different values of maximum gap in NMRooting (from 2 till 7) led to visually similar curves (Fig. 1.12a). Different values of noise cutoff (0.04 to 0.12) also led to visually similar curves except for the value of 0.04 (Fig. 1.12b). So, aside from this value, the parameter choice did not obviously influence the trend of root length detection. The 3D image of the root system produced by the software when the noise cutoff level was set to 0.04 was not realistic (Fig. 1.13a). It overestimated root length by even recognizing roots outside the system. The image quality and realism increased significantly once the noise cutoff was increased to 0.06 (Fig. 1.13b). This further supports our parameter selection for the image analysis.

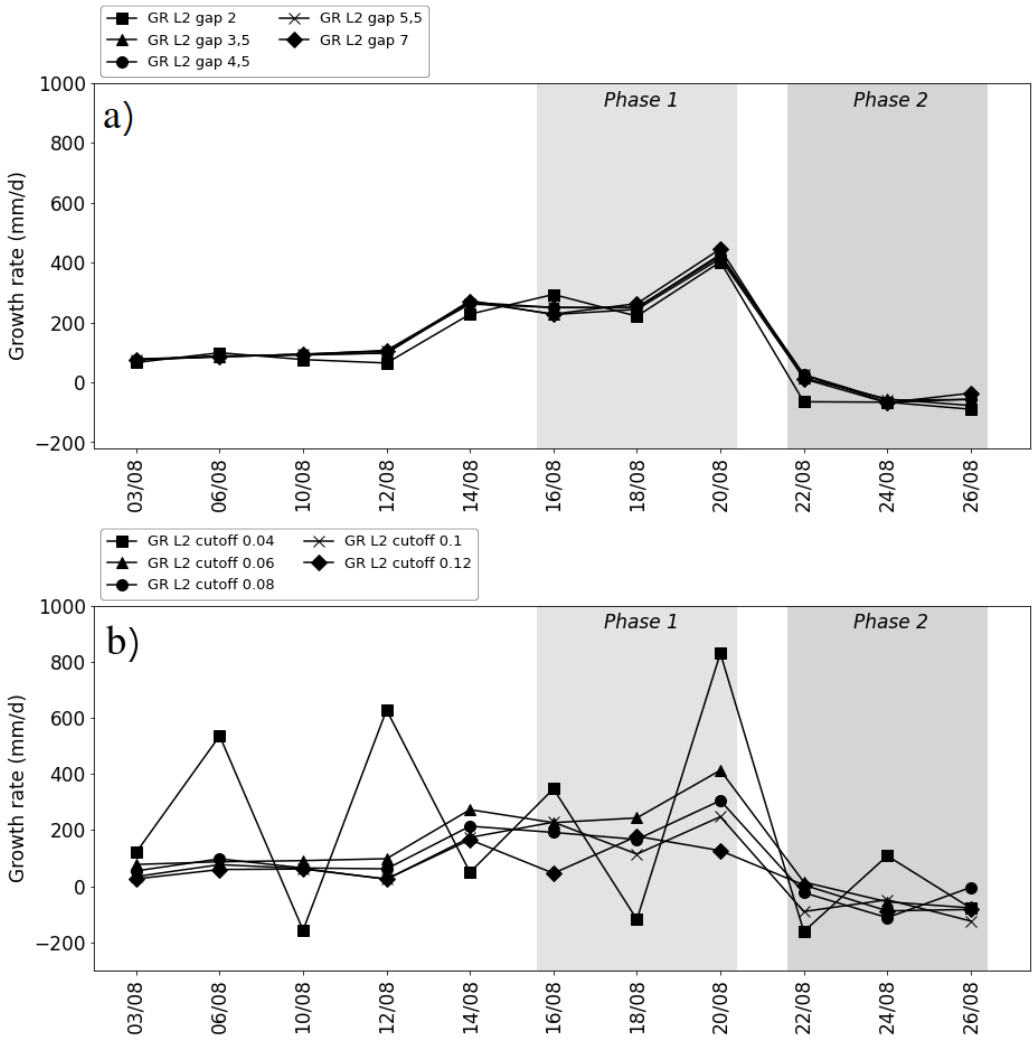

Figure 1.12: Growth rate in L2 of a root system under a) a range of values of maximum gap and b) a range of values of noise cutoff.

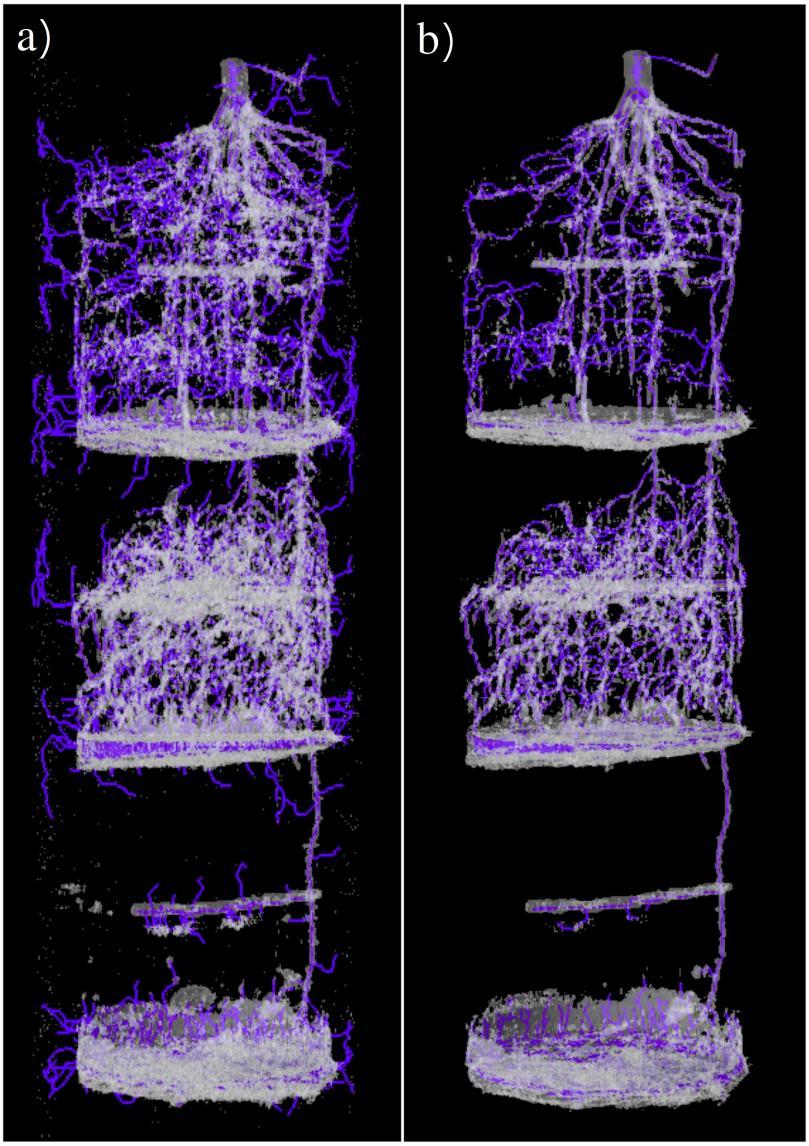

Figure 1.13: 3D representation of the same root system using two different levels of noise cutoff. a) Root system representation generated using a noise cutoff of 0.04. The root detection is erroneous and the signal has many artifacts. b) Root system representation generated using a noise cutoff of 0.06. The root detection is realistic.

Chapter 2

Monitoring seasonal root distribution shifts and daily growth dynamics following precipitation events in a natural grassland

This chapter will be submitted in modified form as a paper to the journal "Biogeosciences" or "Plant and Soil" as "Ceolin, S.; Schymanski, S.; Klaus, J.". The work presented in this chapter was made possible by the contributions of Dr. Stanislaus Schymanski (SJS), Dr. Julian Klaus (JK), Jérôme Juilleret (JJ) and Jean François Iffly (JFI).
Contribution in concept and experimental design: SC (me), SJS, JK. Contribution in experimental preparation and measurements: SC, JJ, JFI, SJS. Contribution in data analysis: SC. Contribution in results interpretation and discussion: SC, SJS, JK.

2.1 Abstract

Plants can alter their vertical root allocation according to seasonality and to soil moisture levels along the profile. "Hydromatching" was described as

the promotion of root growth in a newly wetted soil layer accompanied by a decline in root growth in drier layers, occurring at daily time scales in individual plants grown under controlled conditions.

In this study we investigated whether soil moisture or temperature is a major driver of the root growth dynamics in a central European temperate grassland. We then looked into root growth dynamics at daily time scales following 3 selected precipitation events to determine the occurrence of Hydromatching. Finally, we examined the extent of vertical root distribution shifts transitioning from spring to summer. In order to do so we installed twelve minirhizotron tubes in proximity of a weather station in a natural grassland in Luxembourg. We imaged the tubes from May 2022 until August 2023, adjusting the sampling frequency according to the season and increasing it following rain events.

Soil moisture availability turned out to be a more important predictor than temperature for growth rate at 10, 20 and 40 cm depth. At 60 cm interactions between soil moisture and temperature at the layers above appeared to have a larger control over root growth. We obtained indications of Hydromatching in 2 out of the 3 selected rain events, when root growth distribution shifted from deeper layers to shallow layers within 2-5 days following topsoil re-wetting.

We observed significant and profound shifts from shallower soil layers to deeper soil layers during the spring-summer transitions, consisting of both promotion of growth in the deeper layers and decline in root length in the shallower layers.

Root systems in grassland communities seem to respond to seasonality with drastic shifts at the whole root system level and to quick variations in soil moisture with smaller and localized but still significant and rapid shifts. Both types of response appear to adhere to an optimization strategy, consisting in the promotion of root growth in resourceful areas while discarding roots in areas where resources are less accessible.

2.2 Introduction

Roots are fundamental plant organs mediating water and nutrient uptake, among other functions. Root water uptake is one of the key aspects studied in the context of agricultural productivity. Management practices and selection of plant varieties that encourage water capture are some of the tools that can enable us to improve agricultural productivity to meet population growth (Eshel and Beeckman, 2013). Therefore, studying the limitations to water acquisition and the mechanisms implemented by plants to overcome such limitations is especially important.

Plants have evolved strategies and gained a degree of root morphological and physiological plasticity in order to deal with the fluctuations in soil water availability in time and space (Hodge, 2004; Fromm, 2019). Among those strategies we find "hydrotropism" and "hydropatterning". The former leads to root curvature towards zones of high water potential and the latter leads to promotion of asymmetrical lateral root formation towards wet soil patches (Fromm, 2019).

At the seasonal scale, several studies observed root systems shifting their root length distribution seasonally as a response to soil moisture changes under different plant communities and different climates. Overall, they reported that root length was higher in the shallow soil layers during the wet season. During the dry season, root distribution shifted towards deeper layers where soil moisture is usually higher (Hayes and Seastedt, 1987; Wan et al., 2002; Peek et al., 2006; Wedderburn et al., 2010; Saelim et al., 2019; Zhang et al., 2019a).

In Chapter 1 we investigated daily time-scale root responses to rapid and local variations of soil moisture along the soil profile. The study was carried out under controlled conditions on 5-week old individual maize plants. We observed and coined a phenomenon named "Hydromatching", which consisted of local root proliferation (involving both new root emergence and

elongation of pre-existing roots) occurring in a soil layer within 48 hours from a water pulse application. The increase in the treated layer was accompanied by a decrease in root growth in other untreated layers. The authors suspect this is a strategy enabling the plant to explore dynamic soil moisture sources while economizing on root carbon investments. The study also highlights the importance of considering root systems as highly dynamic entities. Modeling studies also agree on this, as they predicted more realistic soil moisture dynamics when considering dynamic, self-optimizing root systems than when considering static root systems (Schymanski et al., 2008; Wang et al., 2018).

In contrast to our previous observations on maize roots, in a study on ryegrass populations roots did proliferate following re-wetting of a dry topsoil, but started to do so only one month after the re-watering event (Wedderburn et al., 2010). The delay in the response was interpreted as a way to ensure that carbon is invested in layers with sustained resource availability.

Studying root growth dynamics as a response to changing conditions in soil moisture is particularly important in the context of climate change and drought stress. As a matter of fact, unprecedented summer droughts are becoming more frequent in central Europe (Torbenson et al., 2023). These are expected to increase in frequency, duration, and intensity in the future with potentially severe effects on vegetation (Van Loon et al., 2016; Klaus et al., 2022). For instance, the drought of summer 2022 in Europe was one of the most intense in recent history (Tripathy and Mishra, 2023). While the effects of drought stress on plant aboveground productivity are well-studied, the root growth dynamics during both drought and post-drought recovery are today considered the "elephant in the room" (Zheng et al., 2023).

Studying root growth dynamics in grasslands is also of crucial importance as grasslands are considered highly productive ecosystems and fundamental in carbon sequestration (Conant et al., 2001; Fay et al., 2015). In this context studying the effects of drought on root dynamics is also beneficial in

understanding how soil carbon and nutrient cycling are affected by drought, as dead roots are one of the main sources of soil nutrients and carbon (Gill et al., 2002b). Furthermore, insights into the spatial and temporal organization of root systems are needed in soil vegetation atmosphere transfer (SVAT) models to better predict water fluxes mediated by vegetation under pulsing availability (Schwinning and Ehleringer, 2001). Investigating root growth dynamics to water limitations and fluctuations is also paramount for predicting how water and bio-geochemical cycles in catchments respond to external stressors.

Studies on root growth responses to dry conditions in the field yielded contrasting results. Some studies detected increased fine root production under drought (Teskey and Hinckley, 1981; Leuschner et al., 2001). This is consistent with the "functional balance theory" which states that plants actively adjust shoot:root carbon allocation to improve the uptake of the most limiting resource (Thornley, 1972). Other studies observed a decrease in root production under drought (Metcalfe et al., 2008; Weißhuhn et al., 2011; Sebastian et al., 2016; Zwetsloot and Bauerle, 2021).
Different responses to dry conditions could be explained by different physiological adaptations and sensitivities and by niche separation among species within a community (Leuschner et al., 2001; Zwetsloot and Bauerle, 2021). Mixed species grasslands could be more resistant to drought effects in terms of ecosystem productivity (Isbell et al., 2015; Craven et al., 2016). The two main components of grasslands, grasses and forbs, are known to respond differently to drought and to occupy different niches to avoid competition for water. Grasses tend to grow their root systems in the topsoil, effectively extracting water even under conditions of scarcity. In contrast, forbs tend to avoid growing roots in upper soil strata and overcome water scarcity by tapping into deeper soil layers (Nippert and Knapp, 2007). Furthermore, it was discovered that water uptake was more correlated to moisture availability rather than root biomass in a sagebrush-steppe ecosystem, where most

of the water uptake was driven by aquaporin abundance rather than root biomass abundance (Kulmatiski et al., 2017). This means that the likelihood of detecting clear plant community-level root growth dynamics in response to water fluctuations could be low. On the other hand, in a greenhouse experiment 7 out of 9 co-occurring European grassland species (including both grasses and forbs) responded to drought in the same way by allocating less resources to roots compared to well-watered plants (Weißhuhn et al., 2011). This behavior was also observed across different vegetation types in the Amazon forest (Metcalfe et al., 2008). However, note that lower resource allocation to roots might not necessarily lead to decreased root abundance, as root turnover rates could also decrease and keep root abundance unaffected.

Considering the effect of succession of droughts is also important when studying the effects of water deficit on root growth dynamics. In a mesic grassland repeated drought events progressively decreased root productivity, indicating that adaptations to low-watered conditions (i.e., niche separation between forbs and grasses, involving different root distributions) might not be enough to overcome consecutive droughts (Slette et al., 2023). In the same study they also found out that above-ground post-drought productivity recovered faster than below-ground. Only above-average precipitation levels allowed the below-ground to recover, indicating the different impact of drought on above and below-ground productivity.

While it is well known that soil moisture highly influences root growth dynamics, it is not clear whether it is the main driver of root growth in temperate grasslands. In Chapter 1 we demonstrated that root growth dynamics in maize were highly responsive and driven by soil moisture variations. The study was carried out in the lab under controlled conditions, where only soil moisture varied while other factors such as irradiance, temperature and humidity were constant. The experiment also involved young maize plants, grown individually (without competition) and prevented from reaching levels of critical water stress (soil moisture always kept $> 6\%$). It is then important

to assess whether the dynamics observed in our moisture-manipulation study are also visible in an established plant community (i.e., a grassland), where variations of other environmental factors can potentially affect the dynamics. As a matter of fact, other studies identified different controllers of root growth in grasslands. In a mesic grassland root growth rates were strongly influenced by plant water status (Slette et al., 2023). In ryegrass populations temperature was controlling root growth peaks (Wedderburn et al., 2010). In a temperate grassland root growth was positively correlated to radiation but not temperature (Edwards et al., 2004). In an oak stand phenological factors were stronger than environmental variables in influencing root elongation rates (Joslin et al., 2001).

These scattered findings indicate that root growth dynamics might be dominated by different environmental (and phenological) factors in different plant communities. A comprehensive study considering the individual contributions of multiple environmental variables in determining shifts in root distribution within the same plant community is needed, especially at shorter (sub-weekly) time scales. In fact, most studies investigating root growth dynamics as a response to seasonal moisture fluctuations and to drought sampled at biweekly, monthly and even yearly intervals (Wan et al., 2002; Peek et al., 2006; Metcalfe et al., 2008; Wedderburn et al., 2010; Saelim et al., 2019; Zwetsloot and Bauerle, 2021; Slette et al., 2023). Such studies might have missed short-term dynamics potentially entailing high rates of root productivity and turnover, as it was demonstrated that one-month sampling intervals might lead to 60% underestimation of root growth and mortality (Stewart and Frank, 2008).

In this study we build upon the results of Chapter 1 and (1) verify if soil moisture is overall stronger than temperature in influencing root growth rates in a temperate grassland under natural conditions. We then aim to (2) test if the phenomenon of Hydromatching (observed on individual young plants under controlled conditions in unexplored soil) occurs also as a re-

sponse to natural rainfall variability in an established grassland community. Finally, our goal is to (3) capture vertical shifts in root distribution during the transition from a wetter late spring to a drier early summer. Specifically, we intend to answer the following research questions:

- Question 1 (importance of water or temperature): Is water availability or temperature the main driver of root growth dynamics in a central European temperate grassland?
- Question 2 (occurrence of Hydromatching): Can we observe Hydromatching within days from a precipitation event?
- Question 3 (allocation shift from spring to summer): Can we observe a vertical shift in root growth distribution following the onset of a dry early-summer period?

2.3 Materials and methods

2.3.1 Field site and data collection

The study was conducted in Schifflange, Luxembourg (49.5137°N, 6.0284°E), within the area of a well-instrumented weather station located in a natural grassland (Fig. 2.1) mowed once per year and sporadically subjected to grazing (never during the study period). The weather station is operated by the Hydro-Climatological Observation network (HOST), pole of the Luxembourg Institute of Science and Technology (LIST). At the site, the soil is clay loam down to 40 cm depth and heavy clay from 40 to 130 cm (Marx and Flammang, 2015). The species populating the area include both forbs and grasses and are common European temperate grassland species such as *Lolium perenne*, *Trifolium pratense*, *Trifolium repens*, *Taraxacum officinale*, *Jacobaea vulgaris* (or *erratica*), *Carduus crispus* and *Daucus carota*. The climate is temperate semi-oceanic and characterized by mild winters and moderate summers. The

long-term annual mean precipitation (1971 to 2000) in Luxembourg is 864 mm (Goergen et al., 2013).

Aboveground, the weather station is equipped with instruments measuring air temperature, humidity, wind speed and irradiance. Belowground, soil moisture and temperature sensors are located at depths of 10, 20, 40 and 60 cm. We defined these depths as "depths of interest". Near the weather station, we installed 12 acrylic minirhizotron tubes (180 cm long and 5 cm of diameter, CID Bioscience, Inc. Camas, WA, USA) at an angle of 45°, approximately 50 cm apart and with 20 cm of tube sticking out of the ground. This means that the tubes reached a soil depth of approximately 115 cm. The tubes were installed 3 months before data collection. When not sampled, polystyrene foam plugs were inserted inside the tubes and PVC caps were used to cover the protruding part of the tubes and avoid light disturbance.

Figure 2.1: The weather station located in a natural grassland in Schifflange, Luxembourg. The caps covering the minirhizotron tubes are visible along the fence.

Roots growing along the external wall of the tubes were imaged using the CI-602 Narrow Gauge Root Imager (CID Bioscience, Inc. Camas, WA, USA) from May 2022 till August 2023. Images down to 85 cm were collected till September 2022. We extended the measurements down to 115 cm from September 2022 on. As a rule of thumb we took images every two weeks but using an adaptive sampling strategy that consisted of increasing the sampling frequency shortly after major precipitation events during the growing season. Major precipitation events were defined as events that increased the soil water head by at least 3 m at 10 cm depth, equivalent to the effect caused by experimental water pulses in Chapter 1. In an effort to document the pre-existing root distribution before a major precipitation event, we imaged 1 to 4 days prior forecasted moderate rain events (>2 mm h^{-1}) and

we kept measuring every 2 to 4 days after the start of the event for a total of approximately 12 days. Such sampling scheme would lead to at least 3 measurements taken closely post-precipitation.
Hourly data of precipitation, air temperature, irradiance, humidity, soil temperature and half-hourly data of soil moisture were collected for the period May 2022 - August 2023 from the Schifflange weather station.

2.3.2 Image analysis

Root images from each depth of the minirhizotrons were corrected for overlaps and merged together to obtain single images of the entire root profiles growing along the 12 tubes. The entire root profiles were subdivided in 11 depths until August 2022 and in 14 depths starting September 2022. Depths 1 to 6 covered approximately 7 cm of tube length, corresponding to roughly 5 cm of vertical depth. Depths 7 to 14 covered approximately 14 cm of tube length, corresponding to roughly 10 cm of vertical depth. The subdivision was done in order to better capture the root growth occurring in proximity of the soil moisture and temperature sensors. For instance, we considered depth 2 and 3 to observe the roots growing 5 cm above and below the sensor located at 10 cm depth. Depth 4 and 5 were 5 cm above and below the sensor located at 20 cm depth. Depths 7 and 8 were 10 cm above and below the 40 cm deep sensor and depth 9 and 10 were 10 cm above and below the 60 cm deep sensor.
On certain sampling events image quality was lower due to issues with the scanner head. Such images were corrected for brightness and contrast in order to improve the image quality and strengthen the separation between roots and background. The Software "RootPainter" was used to detect alive roots in the images in an automated way (Fig. 2.2). The software is a Convolutional neural networks (CNN) that, once trained on a suitable dataset, is able to segment roots in soil and to extract them from the background

(Smith et al., 2020). During the training, roots were considered alive if they appeared bright white. The Software also provides the option to convert the segmented images into a format that is suitable for "Rhizovision Explorer", another software specialized in extracting root parameters from camera images. We used this software to extrapolate values of alive root length. The detection of alive roots allowed us not only to detect root growth but also root decline. However, we could not train RootPainter to accurately differentiate alive roots from dead ones, as it is a challenging task even for the human eye. For this reason we considered the detection of root appearance more accurate than the detection of root disappearance. Still, if trends in root disappearance were gradual (and not occurring abruptly from one day to the next) and validated through visual inspection of the images, we incorporated them in the overall interpretation.
Images taken from 21/07/2023 onward presented problems of noise coming from camera damages leading to the formation of straight bright stripes that were identified as roots by the Software. For these images, an additional noise cleaning process was implemented, which included both manual and automated corrections. While fixing the noise, these corrections also led to an underestimation of the total root length during this period.

We think it is important to underline that the quality of the images changed throughout the experimental period due to potential damages of the camera, fluctuations in temperature and humidity, and gradual soil establishment around the tube. This, in turn, affected the precision of RootPainter in segmenting the roots from the background. As previously mentioned, corrections through image manipulation have been implemented to reduce image noise as much as possible. While the data can be used to detect vertical (relative) distributions and sudden shifts in growth rates, the absolute values of root growth are not reliable.

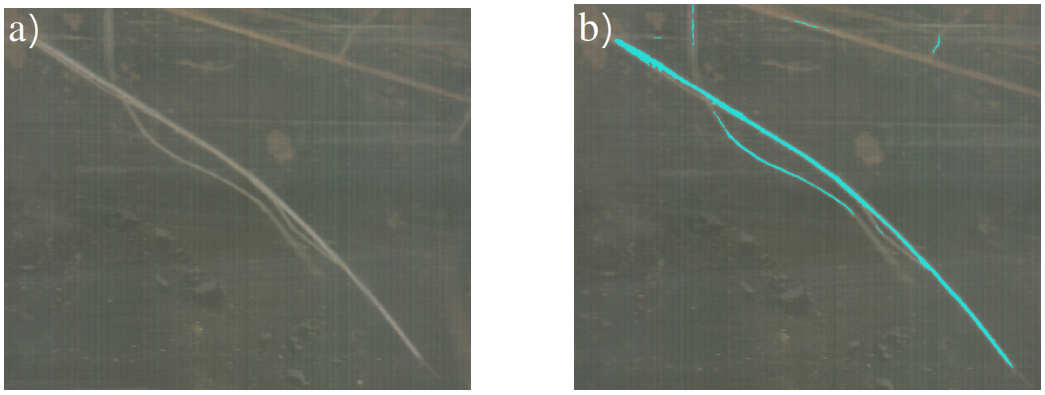

Figure 2.2: Root detection on RootPainter. a) Image before the Software processing and b) the processed image. The light blue area indicates the portion identified as alive root by the Software after being trained on white roots. Majority of the root on the upper right hand of the image was not identified as alive due to its less bright and more brown appearance.

2.3.3 Data and statistical analysis

Before the data analysis, we converted soil moisture data (measured as volumetric water content in m^3 m^{-3}) in meter of water head by using the equations of the water retention model formulated by Van Genuchten (1980). This was done in order to account for the role of textural classes in affecting soil water retention and availability to plants. Van Genuchten parameters for clay loam (down to 40 cm) and clay (from 40 cm downward) were obtained from Carsel and Parrish (1988) and specified in Table 2.1. Soil texture at the 40 cm moisture sensor depth was considered to be clay loam. The first step of the conversion consisted in transforming the measured volumetric water content (defined as θ in van Genuchten equations) into soil saturation degree ($s_{u,i}$) using the following formula:

$$s_{u,i} = \frac{\theta - \theta_r}{-\theta_r + \theta_s} \tag{2.1}$$

Where θ_r (cm^3 cm^{-3}) is residual soil water content and θ_s (cm^3 cm^{-3}) is saturated soil water content. We then converted the soil saturation degree ($s_{u,i}$) into soil water head, h (cm), utilizing the following equation:

$$h = \frac{\left(-1 + s_{u,i}^{-\frac{1}{m_{vG}}}\right)^{\frac{1}{n_{vG}}}}{a_{vG}} \tag{2.2}$$

Where a_{vG} (cm^{-1}), m_{vG} and n_{vG} are empirical parameters of the van Genuchten water retention model.

The water head values were then converted from centimeters to meters.

Van Genucthen parameters	θ_r (cm^3 cm^{-3})	θ_s (cm^3 cm^{-3})	a_{vG} (cm^{-3})	n_{vG} (-)
Clay loam	0.095	0.410	0.019	1.310
Clay	0.068	0.380	0.008	1.090

Table 2.1: Van Genucthen parameters used for the conversion from volumetric water content (m^3 m^{-3}) to soil water head (m). We considered the clay loam parameters for the soil depth 0-40 cm and the clay parameters for the deeper depths.

Root length (mm) values were converted into net growth rates (mm day^{-1}) by subtracting the root length of the previous sampling event from the next sampling event and by dividing that value by the number of days between events.

To answer Question 1 (importance of water or temperature), we considered root growth rate as the dependent variable of our system. Soil moisture (both as volumetric water content and as soil water head), air temperature, soil temperature, irradiance, air humidity and wind speed averaged over the periods between image sampling were considered as the independent variables. Soil moisture measurements would often go above detectable range

due to saturation. In that case, we considered the soil moisture equal to 0.52 m^3 m^{-3} (maximum value detectable for volumetric water content) or to 0 m (for soil water head). In the analysis we also considered as independent variables the interactions of soil moisture at different depths with air temperature and soil temperature at different depths. We calculated the interaction by multiplying the values of the interacting features. In this analysis we disregarded the data from the winter months (November, December, January and February) in order to avoid the impact of plant dormancy on the results. We then used the dependent and independent variables to perform a Random forest analysis, a Ridge regression analysis and a Partial Least Square (PLS) analysis using the Python library "scikit-learn". We chose these types of regression analyses because they are robust in the case of multicollinearity and high number of independent variables, which is our case. Random forest is a machine learning ensemble model that combines the predictions of several decision trees trained on a subset of data and features (dependent and independent) into a single result. It provides feature importance scores, indicating which independent features are the most influential in modeling the dependent one. Ridge regression is a regularized linear regression model that adds a regularization term penalizing large weights of independent variables that would normally result from a linear regression. This improves the accuracy and stability of the model in predicting the dependent variable. Partial Least Square regression identifies "latent components" by correlating linearly the independent features and the dependent feature and maximizing the co-variance between them. In both Ridge regression and PLS, features are assigned a coefficient describing the magnitude of contribution in predicting the dependent variable. With these methodologies we are able to compute the importance of the independent variables (in our case the environmental parameters) in explaining the dependent variable (in our case root growth rate). Random Forest, Ridge regression and PLS have been used for analysis of feature importance and feature selection in multiple studies and

fields (Hu et al., 2018; Shahhosseini et al., 2019; Toğaçar et al., 2020).
We performed the analysis with these three methods twice, considering volumetric water content and soil water head separately in order to avoid redundancy and an excessive amount of independent variables per analysis. In total, there were 32 independent variables for the analysis considering volumetric water content and 26 independent variables in the analysis considering soil water head (fewer variables because we disregarded soil water head at 60 cm as it was constantly equal to zero).
We utilized the above mentioned methods to assess the most important independent variables explaining root growth at each depth of interest. Specifically, we selected the analyses that yielded the highest R-squared when predicting root growth for each depth of interest. The R-squared is a way of evaluating how well the variance of the dependent variable is explained by the independent variables in a model. Specifically, R-squared of the Random Forest, Ridge regression and PLS regression models is calculated as reported in Richter et al. (2012) and Nakagawa and Schielzeth (2013):

$$R^2 = 1 - \frac{\sum_{i=1}^{n}(y_i - \hat{y}_i)^2}{\sum_{i=1}^{n}(y_i - \bar{y})^2} \tag{2.3}$$

Where n is total number of observations in the dataset, $\bar{y}$ is the mean of all the observed values of the dependent variable and $\hat{y}_i$ the predicted value of the dependent variable for the ith observation.

From the regression analyses that yielded the highest R-squared we then determined the five independent features that ranked as the best predictors of root growth rate at each depth of interest. We used this top five of most influential independent variables to draw our conclusions on what affected root growth the most at each depth.
In these analyses we used a total of 50 data points per variable. As this dataset is rather small and the number of independent variables considered is high, the used methods can face issues in establishing clear relationships

between independent and dependent variables. For this reason we would like to emphasize that the goal of this analysis is to obtain a broad and initial overview of the key features controlling root growth rate in our system.

To answer question 2 (occurrence of Hydromatching), we lumped together the growth rates 5 cm above and below the sensors at 10 and 20 cm and 10 cm above and below the sensor at 60 cm and considered them to investigate the link between root growth and soil water head. We also considered the differences between growth rate at 10 cm and 60 cm and the differences between growth rates at 20 cm and 60 cm (with positive values indicating growth rate favored in the topsoil and vice versa). This was done to better reveal changes in partitioning between the top and subsoil, especially in circumstances of high root mortality (ie: under dry conditions) when the differences in the partitioning between top and bottom soil could still be meaningful while no clear response is detected when considering the values of net growth rates only. In our investigation we considered the soil moisture changes occurring after 3 selected precipitation events that substantially increased the soil water potential by at least 0.3 MPa (0.3 m) of soil water head at 10 cm depth, during which we managed to frequently and closely monitor the root development over the next days. To determine if Hydromatching occurred, we first used the Shapiro test to check for normal distribution of the values of net growth rates and of growth rate partitioning for each sampling event. We then compared them between subsequent sampling events by either using the Mann-Whitney test (when at least one of the two compared groups did not follow normality) or the Student t-test (when both of the considered groups followed normality) to check for significant differences. For Hydromatching to occur, we expected a significant increase in growth rates in the topsoil and a significant decrease in the subsoil following major precipitation events. The Shapiro test, the Mann-Whitney test and the Student t-test were carried out using the Python library “scipy” and the package “stats” (Virtanen et al., 2020).

To answer question 3 (allocation shift from spring to summer) we compared the vertical root length distributions along each depth of the 12 tube profiles on two sampling days, one in May (late spring) and one in June (early summer) of both 2022 and 2023. To check for significant vertical shifts in root length allocation we lumped together the root lengths at each depth from all 12 tubes and compared the root lengths at each depth on the sampling event in May with the root lengths at the same depth in June for both years. We first used the Shapiro test to check for normal distribution of the root length values of all tubes at each depth and in each sampling event. We then carried out the comparison with the Mann-Whitney test (when at least one of the two compared groups of root length did not follow normality) or with the Student t-test (when both groups followed normality).

The dataset of Chapter 2 can be found on Zenodo at https://zenodo.org/records/10527733 .

2.4 Results

2.4.1 Question 1: importance of water or temperature

Question 1 was addressed by carrying out Random Forest, Ridge analysis and Partial Least Square (PLS) regressions to compute the importance of the independent variables in predicting root growth rates at each depth of interest. The independent variables considered were soil moisture (as volumetric water content or soil water head), soil temperature, air temperature, air humidity, irradiance, wind speed, interactions between soil moisture and air temperature and interactions between soil moisture and soil temperature. The three methods performed differently for each depth of interest and differently depending on whether we considered volumetric water content (VWC) or soil water head as an independent variable. The R-squared resulting from

the Random Forest, Ridge regression and PLS considering the growth rates at 10, 20, 40 and 60 cm and considering VWC and soil water head separately are shown in Table 2.2. Several reported R-squared values are negative. Although seemingly counter-intuitive, a negative value of R-squared computed by regression models is indeed possible according to Eq. 2.3 and Nakagawa and Schielzeth (2013). More specifically, a negative R-squared can occur when the regression model's predictions are worse than those of a null model that includes only an intercept and no predictors (Nakagawa and Schielzeth, 2013).

The growth rates at 10 cm were best predicted by the Ridge regression considering VWC (R2=0.5), the growth rates at 20 cm were best modeled by the Random Forest considering VWC (R2=0.26), the growth rates at 40 cm were best predicted by the Ridge regression considering soil water head (R2=0.55) and the growth rates at 60 cm were best predicted by the PLS considering soil water head (R2=0.24). The top 5 features appearing as the strongest predictors at 10 cm were, in order of strength, VWC at 10 cm (positive effect on growth rate), VWC at 20 cm (positive effect), soil T at 60 cm (positive effect), VWC at 60 cm x soil T at 60 cm ("x" indicates interaction, positive effect) and VWC at 10 cm x soil T at 40 cm (negative effect) (Fig. 2.3a, direction of the effect not shown). At 20 cm the best predictors were air humidity (positive effect), irradiance (negative effect), VWC at 10 cm (positive effect), soil T at 60 cm (negative effect) and VWC at 40 cm x air T (negative effect) (Fig. 2.3b). At 40 cm the best predictors were soil water head at 20 cm (negative effect), soil water head at 10 cm (negative effect), soil water head at 20 cm x soil T at 60 cm (positive effect), soil water head at 20 cm x air T (negative effect) and soil T at 60 cm (negative effect) (Fig. 2.3c). At 60 cm the best predictors were soil water head at 20 cm x air T (negative effect), soil water head at 20 cm x soil T at 10 cm (negative effect), soil water head at 20 cm x soil T at 20 cm (negative effect), soil water head at 10 cm x air T (negative effect) and soil water head at 20 cm x soil T at

40 cm (negative effect) (Fig. 2.3d).

Overall, we consistently observed soil moisture features (as VWC and soil water head) ranking higher than temperature features among the top 5 features at all depths except 60 cm. Soil moisture features appeared as the top two most influential at 10 cm and 40 cm. At 20 cm one soil moisture feature (VWC at 10 cm) ranked 3rd right after irradiance and air humidity. On the other hand, all of the top 5 most influential features at 60 cm were interactions between soil water head at 10 and 20 cm and temperatures from the above soil layers or air temperature. These results could indicate a larger influence of temperature on root growth at 60 cm, but are most likely shaped by the invariability of soil moisture at this depth.

R^2 values	Random Forest		Ridge Regression		Partial Least Square Regression	
Dependent variable	Considering VWC	Considering SWH	Considering VWC	Considering SWH	Considering VWC	Considering SWH
Growth rate at 10 cm	0.26	0.26	0.50	0.12	-2.22	-0.88
Growth rate at 20 cm	0.27	-0.65	-0.30	-0.43	-1.47	-0.41
Growth rate at 40 cm	-0.48	-1.04	0	0.55	-0.35	-1.02
Growth rate at 60 cm	0.03	0.08	-0.78	-0.74	0.15	0.24

Table 2.2: R-squared values deriving from the Random Forest, Ridge Regression and Partial Least Square Regression computed for each depth considering root growth rate as the dependent variable. We reported the results considering soil moisture both as volumetric water content (VWC) and as soil water head (SWH).

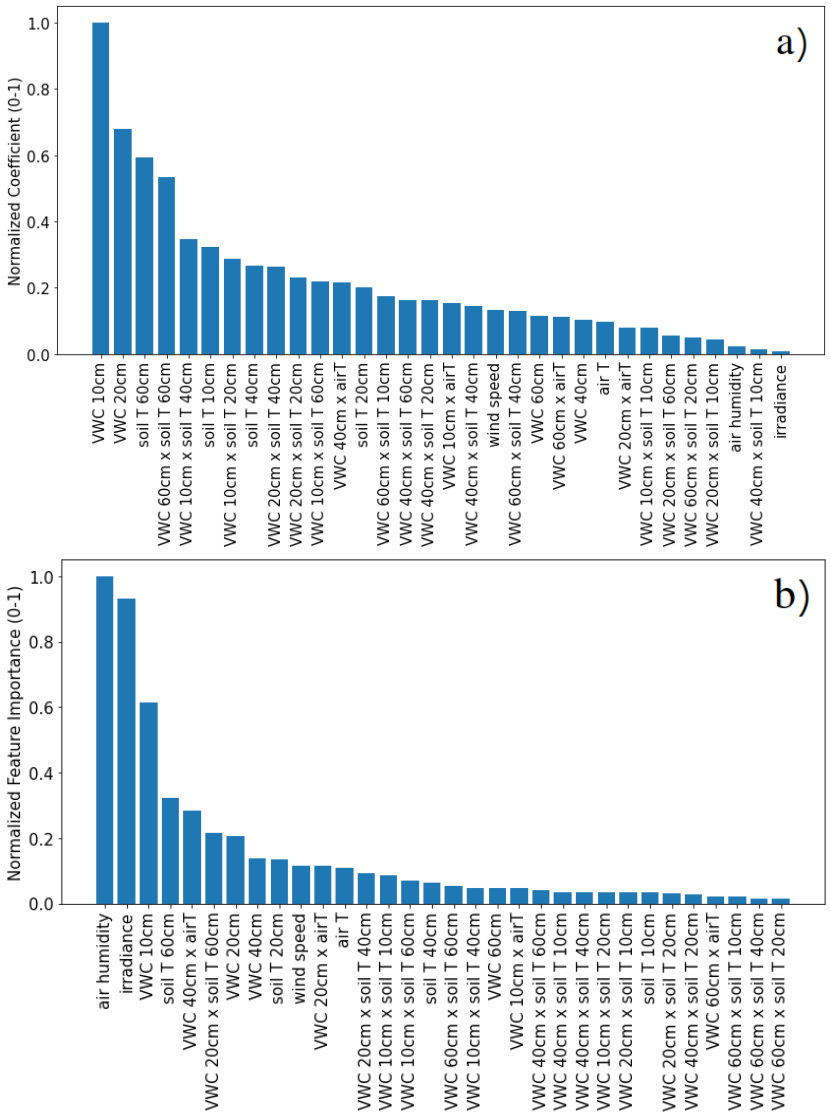

Figure 2.3: Feature importance and coefficients of contribution from the best-performing regression analyses to determine the most influential features on root growth. Coefficients were normalized within the range 0-1 for each selected analysis. a) Normalized coefficients of contribution of the independent variables from the Ridge regression model of root growth at 10 cm depth. b) Normalized feature importance of the independent variables from the Random Forest model of root growth at 20 cm depth. c) Normalized coefficients of contribution from the Ridge regression model at 40 cm depth. d) Normalized coefficients of contribution from the Partial Least Square (PLS) regression at 60 cm depth. These coefficients only represent the importance in affecting root growth rate but do not show the direction of the effect.

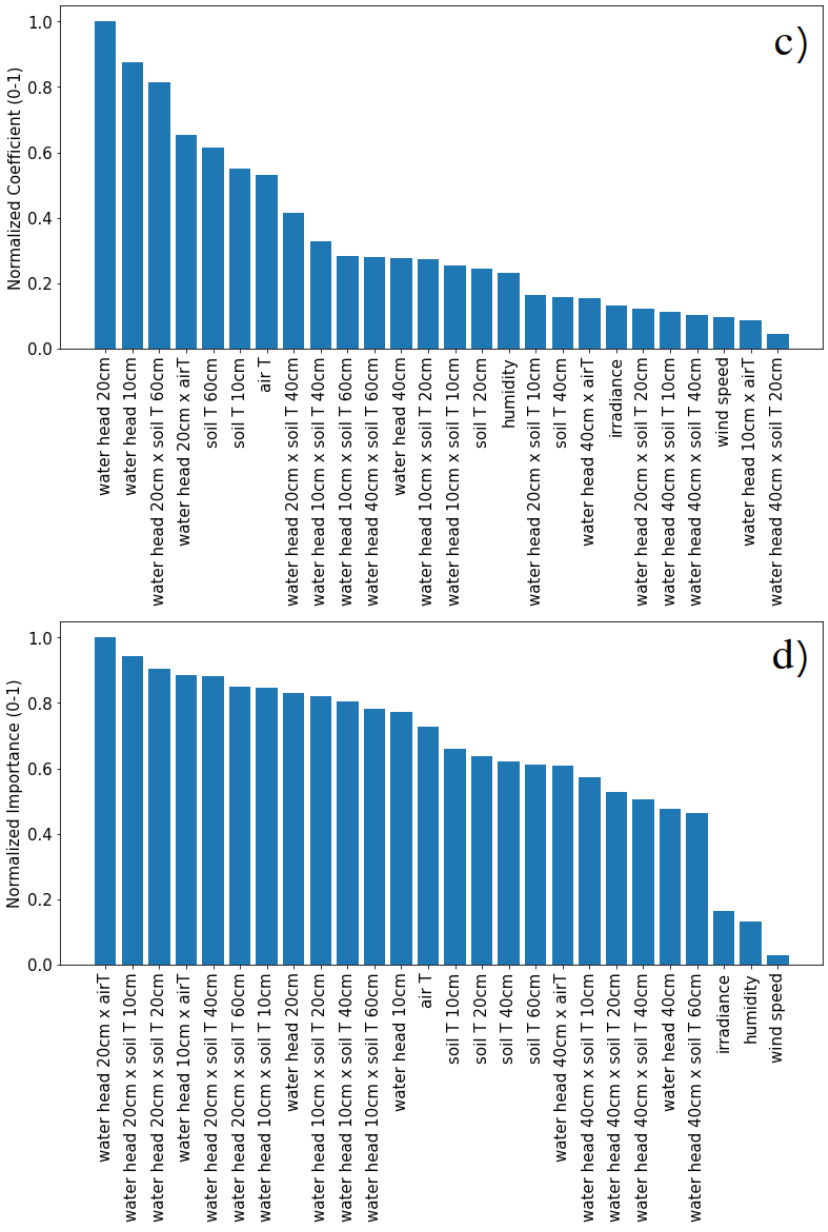

Figure 2.3: Refer to previous caption.

2.4.2 Question 2: occurrence of Hydromatching

Question 2 was tested by comparing the net growth rates and the top-bottom growth partitioning between sampling dates on three selected periods with major precipitation events. From now on we will refer to these three periods as "September 2022", "June 2023" and "July/August 2023".
Overall, the largest fluctuations in soil water head over the entire study period were observable at 10 cm, where values ranged from saturation (0 m) to a minimum of -30 m in July/August 2023. Already at 20 cm the fluctuations were much less intense, with soil water head reaching a minimum level of -4 m in July/August 2023. Interestingly, the lowest levels of soil water head were recorded in summer 2023 and not during the summer drought of 2022. Soil at 60 cm was found to be at saturation for the entirety of the study. It is important to note that the highly clayey texture of the soil at this depth could have led to tight water retention leading to constant readings of 0 m, but also that the heavy clay itself could have affected the readings of the sensors.
The rain events in September 2022 and July/August 2023 led to different water replenishing patterns than in June 2023. The levels of soil moisture at 10 and 20 cm increased strongly and simultaneously shortly after the onset of the precipitation periods on 31/08/2022 and 25/07/2023 respectively, indicating a rapid percolation of the water front into the soil profile in these two periods. In June 2023 the levels of soil moisture at 10 cm increased more gradually over a rain period of 4 days, starting on 19/06/2023, slowing down between 20/06/2023 and 21/06/2023 and resuming on 22/06/2023. The soil then started immediately to dry up again. At 20 cm soil water head barely changed, with a maximum increase of only 1 m visible on 29/06/2023.
In all three periods and at all the depths considered we observed clear changes in root growth rates and in top-bottom growth partitioning following the rain events, although at different intensities (Fig 2.4). The comparison between

growth rates on 27/08/2022 and 02/09/2022 was not possible due to sudden changes in image contrasts between the two dates, affecting the root recognition capability. In this case, we disregarded the day of the change in contrast and considered the date right after for the comparison (i.e., between 27/08/22 and 05/09/22).

In September 2022 the net growth rates at 10 cm (Fig. 2.4a) increased significantly (p-value<0.05) between 27/08/2022 and 05/09/2022 (0.05 mm day^{-1} to 2.33 mm day^{-1}) and between 02/09/2022 and 05/09/2022 (-0.03 mm day^{-1} to 2.33 mm day^{-1}, fig. 2.5a and b), showing a reactive root growth promotion 3 to 5 days after the soil wetting. The change in image contrast between 28/08/2022 and 02/09/2022 does not allow us to conclude whether the response occurred earlier already on 02/09/2022. Growth rates kept increasing to 9.50 mm day^{-1} on 07/09/2022, which was the highest growth rate recorded at 10 cm out of the three periods. Surprisingly, on 09/09/2022 growth rates decreased significantly and abruptly, reaching a negative median of -3.44 mm day^{-1} indicating root disappearance (Fig. 2.5f and g).

Net growth rates at 20 cm (Fig. 2.4b) followed a similar pattern as at 10 cm, increasing significantly from -0.11 mm day^{-1} (median value) on 02/09/2022 to 2.69 mm day^{-1} on 05/09/2022. The growth rates then slightly increased to a median of 3.81 mm day^{-1} on 07/09/2022 and decreased to a negative median of -1.35 mm day^{-1} on 09/09/2022.

Interestingly, at 60 cm growth rates increased simultaneously with the growth rates in the topsoil and went from negative (on 27/08/2022) to positive with a median of 1.76 mm day^{-1} on 05/09/2022 (Fig. 2.5c, d and e). However, growth rates decreased to -0.45 mm day^{-1} on 07/09/2022, the day when growth rates at 10 cm were at their highest and kept decreasing down to -5.04 mm day^{-1} on 09/09/2022.

The differences between top-bottom growth partitioning (blue bars in Fig. 2.4) indicate a clear change in the partitioning between shallow and deep soil after the re-wetting. Between one to two days after the rain event

(02/09/2022) the partitioning between top and bottom significantly decreased, meaning that root allocation was promoted towards the 60 cm depth while none was established in the topsoil. Then, it started increasing in the following sampling days and the allocation switched to the 10 and 20 cm depths (while declining at 60 cm). On 09/09/2022 root growth partitioning was once again no longer prioritized in the topsoil.

In June 2023 the net growth rates at 10 cm increased significantly and reached positive values on 22/06/2023, that is 1 to 3 days after the soil wetting from the first rain event. Specifically, the median of the growth rates increased from -2.38 mm day^{-1} on 19/06/2023 to 2.99 mm day^{-1} on 22/06/2023. In the following days soil dryness started to build up again and root growth at 10 cm halted, even reaching medians of -1.55 mm day^{-1} and of 0.93 mm day^{-1} on 26/06/2023 and 28/06/2023, respectively. At 20 cm a positive and significant increase in root growth was observed only at the end of the period on 28/06/2023, when it increased to 5.72 mm day^{-1} from -2.03 mm day^{-1} on 26/06/2023.

At 60 cm growth rate went from 16.1 mm day^{-1} to a significant decline on the following days, reaching negative values and a minimum of -25.76 mm day^{-1} on 22/06/2023, 1 to 3 days after the soil wetting. This was the same day when we observed the maximum positive growth rate reached at 10 cm. When soil started drying up, root growth at 60 cm progressively increased until reaching 12.44 mm day^{-1} on 28/06/2023, significantly higher than -10.94 mm day^{-1} on 26/06/2023.

The top-bottom growth partitioning increased significantly between 19/06/2023 and 22/06/2023, 1 to 3 days after the soil wetting from the first rain event, suggesting root growth promotion in the topsoil at the expense of the growth in the subsoil. With the progressive decrease in soil moisture between 22/06/2023 and 26/06/2023, the partitioning between top and bottom significantly decreased and reached negative values on 28/06/2023. This indicates that root promotion progressively switched from the top to the bottom of the profile

when dry conditions developed again.

In July/August 2023 growth rates at 10, 20 and 60 cm all increased significantly within 1 day from the topsoil wetting following the beginning of a long rainy period (lasting from 24/07/2023 to 06/08/2023). Specifically, between 21/07/2023 and 25/07/2023 the growth rate medians turned from negative to slightly positive at the three depths, going from -1.49 mm day^{-1} to 0.07 mm day^{-1} at 10 cm, from -1.00 mm day^{-1} to 0.18 mm day^{-1} at 20 cm and from -6.43 mm day^{-1} to 0.49 mm day^{-1} at 60 cm. On the following sampling dates the growth rates at 10 and 20 cm remained near-zero until 04/08/2023, when conditions of soil saturation were reached at both depths and growth rates declined and became negative again. After 25/07/2023 root growth at 60 cm became negative and kept decreasing. From 04/08/2023 onward growth rates at each depth started increasing significantly again and on 11/08/2023 they reached medians of 2.31 mm day^{-1} at 10 cm, 1.71 mm day^{-1} at 20 cm and 1.03 mm day^{-1} at 60 cm.

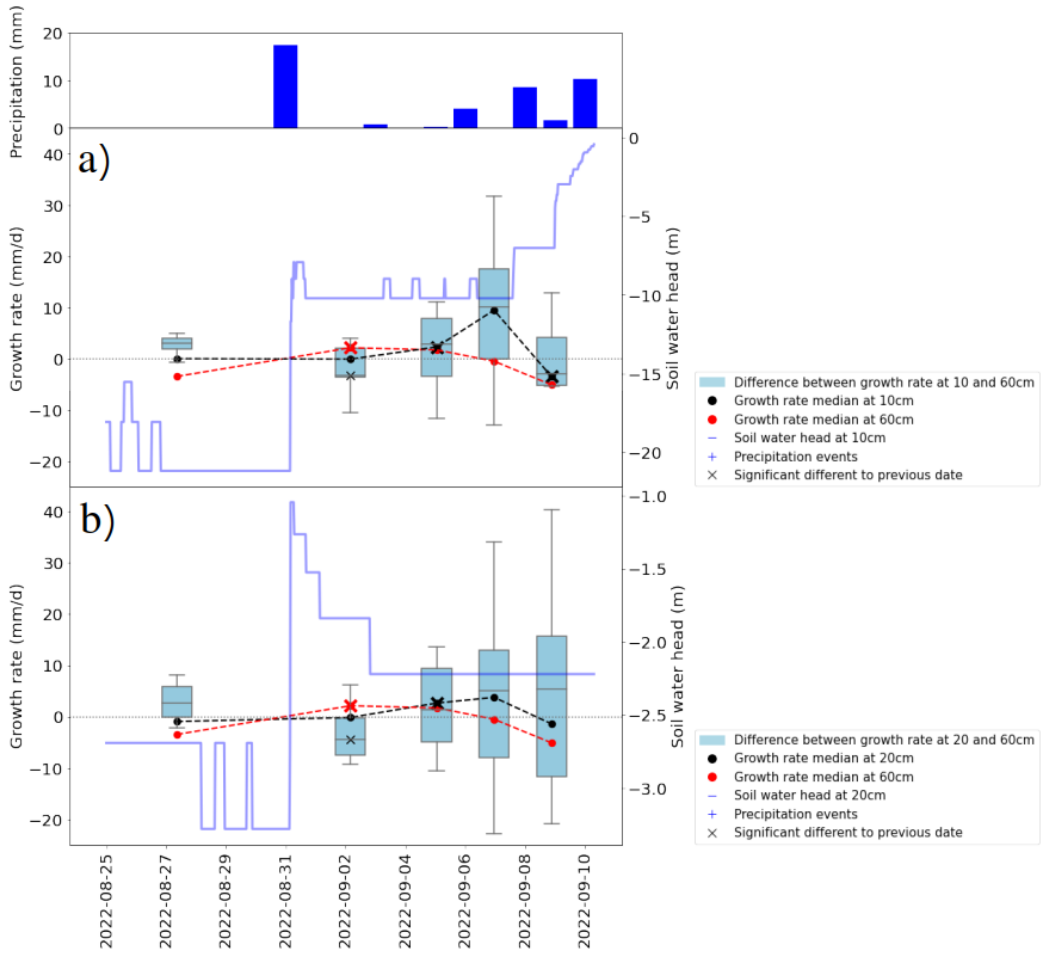

Figure 2.4: Growth rates during the three selected precipitation events of September 2022 (a and b), June 2023 (c and d) and July/August 2023 (e and f). Plots at the top represent the net growth rates at 10 cm (dashed black line), at 60 cm (dashed red line) and the growth rate partitioning between 10 and 60 cm (light blue boxes). Plots at the bottom represent the net growth rates at 20 cm (dashed black line), at 60 cm (dashed red line) and the growth rate partitioning between 20 and 60 cm (light blue boxes). Blue lines depict the soil water head and the blue bars represent precipitation. Crosses on the growth rate medians and on the partitioning bars indicate a significant increase or decline on that date compared to the previous sampling date (p-value<0.05).

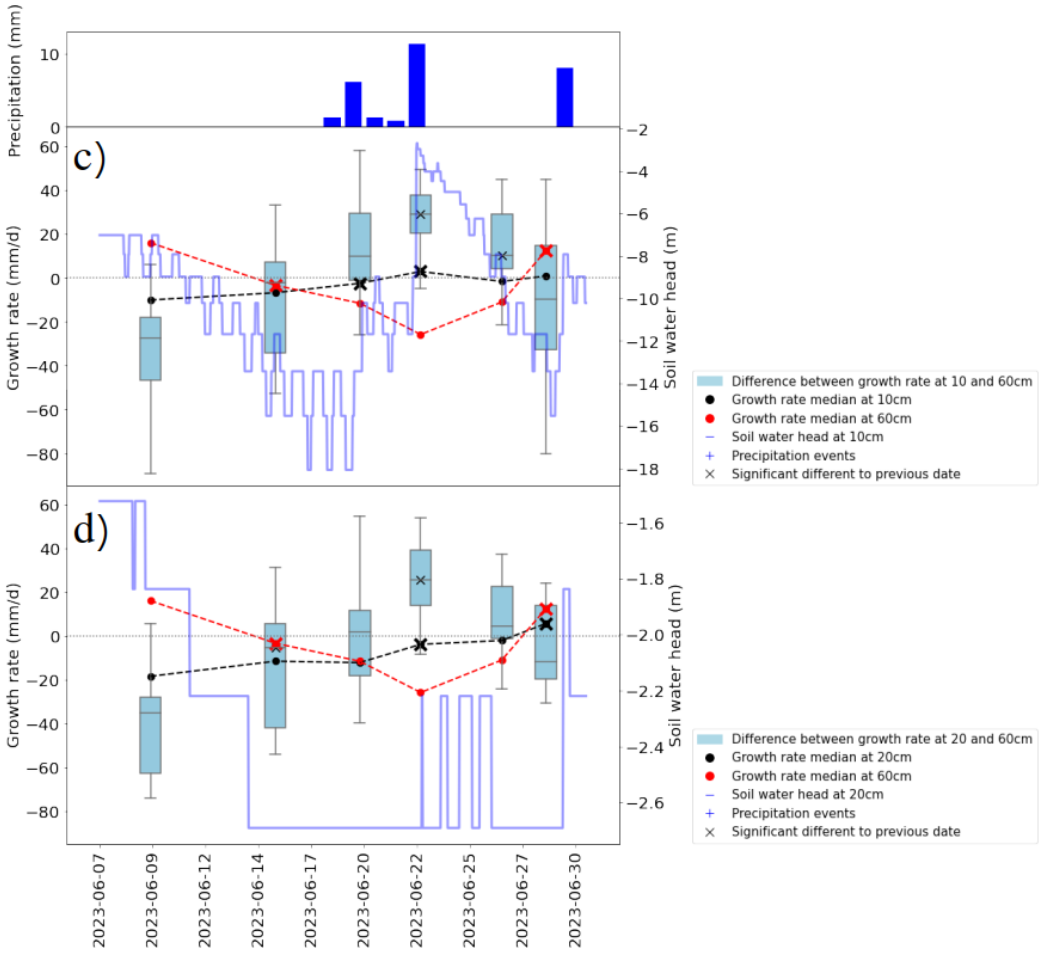

Figure 2.4: Refer to previous caption.

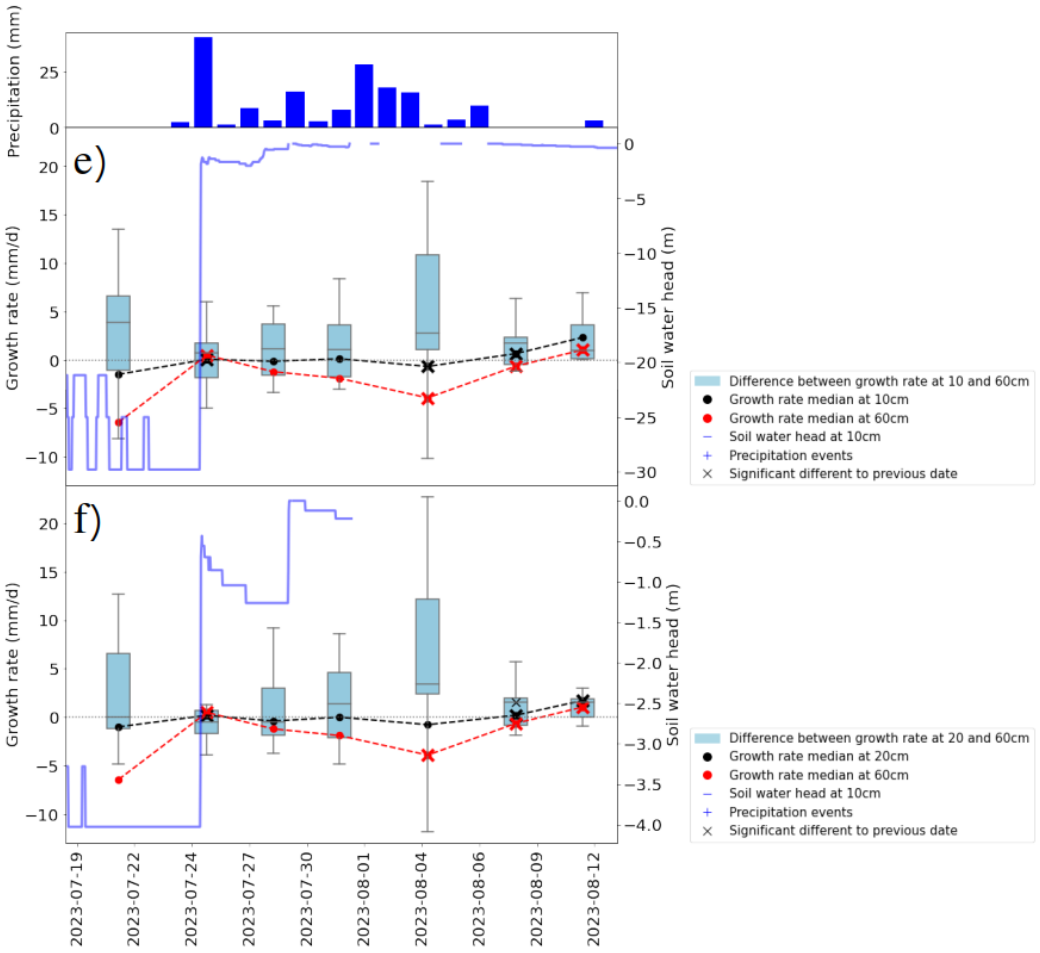

Figure 2.4: Refer to previous caption.

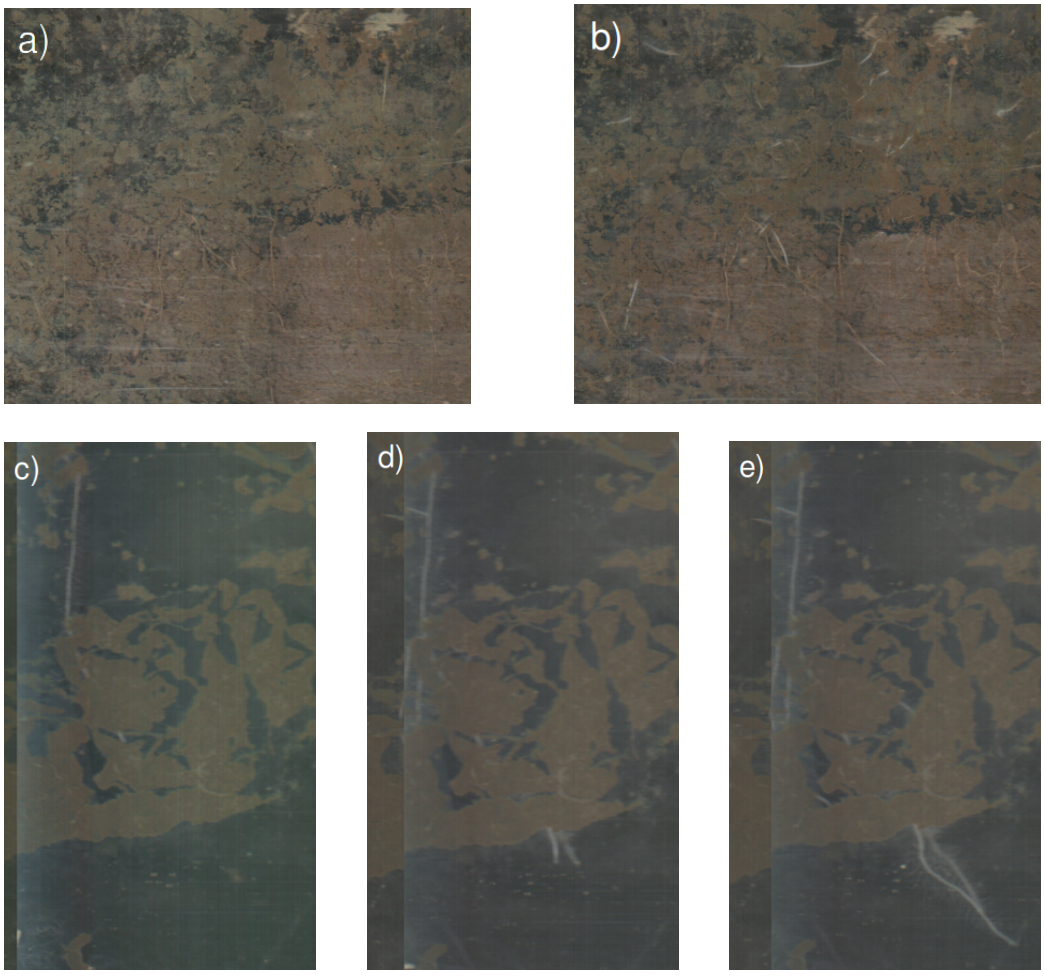

Figure 2.5: Stages of root development (a-b, c-d-e) and of root disappearance (f-g). a) and b) show the same location (10 cm depth) on 02/09/2022 and on 05/09/2022, respectively. Several new roots appeared on b). c), d) and e) show the same location (60 cm depth) on 27/08/2022, 02/09/2022 and 05/09/2022, respectively. Root elongation occurred between sampling dates. f) and g) show the same location (10 cm depth) on 07/09/2022 and 09/09/2022, respectively. Several roots visible in f) are no longer present in g). Unidentified invertebrates were detected in other images during this period which might have fed on the roots.

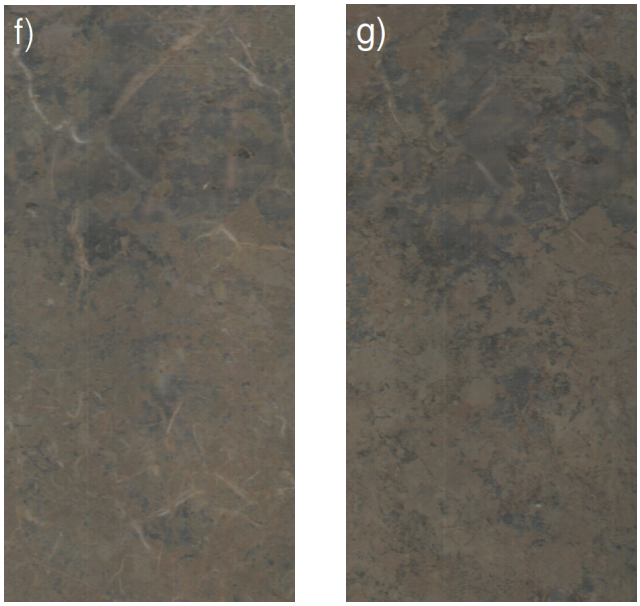

Figure 2.5: Refer to previous caption.

2.4.3 Question 3: root vertical shift from spring to summer

Question 3 was tested by comparing the whole root system profiles in May 2022 and June 2022 and in May 2023 and June 2023 (transitioning from a wetter late spring to a drier early summer). From May 2022 to June 2022 soil water head progressively decreased at 10 cm. One of the two sensors detected a decrease from -1.5 m to -2.7 m and the other from -4 m to -9 m. From May 2023 to June 2023 soil water head decreased much more intensely, from close to saturation (0 m) to approximately -15 m (corresponding to approximately -150 kPa), as measured by both sensors at 10 cm. Such soil tension was shown to impair plant growth (Mackie et al., 2019). Despite dryness building up at different intensities in the two years, in both 2022 and 2023 we observed a similar and significant shift in root length from the shallower soil depths to the deeper soil depths with the progression of the dry

season (Fig. 2.6). The shift consisted of a decline in root length at shallow depths and a promotion of root growth in the deeper layers. Specifically, root length decreased significantly shifting from May 2022 to June 2022 at 5, 10, 15, 20, 25 and 30 cm and increased significantly at 60, 70 and 80 cm (Fig. 2.6a and b). Root length decreased significantly shifting from May 2023 to June 2023 at 5, 10, 15, 20, 25, 30 and 35 cm and increased significantly at 60, 70 and 80 cm (Fig. 2.6b and c).

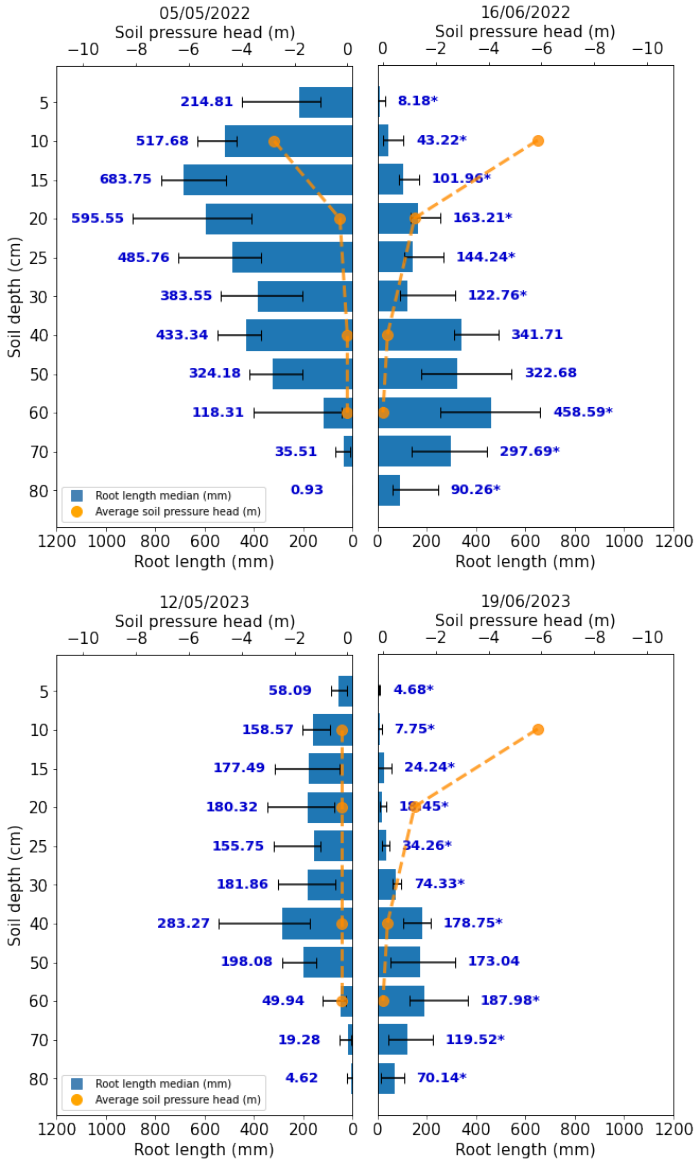

Figure 2.6: Seasonal shift in vertical root distribution. a) and b) represent the shift from May 2022 to June 2022 while c) and d) show the shift from May 2023 to June 2023. Blue bars indicate root length medians obtained from the 12 tubes at all the measured depths. Ticks at the ends of the black lines represent the 25^{th} and 75^{th} percentiles for each bar. Numbers report the value of root length median and stars indicate a significant change in root length between May and June. Orange dots represent soil water head measurements at 10, 20, 40 and 60 cm.

2.5 Discussion

2.5.1 Moisture controls growth rates

Random Forest, Ridge regression and PLS ranked soil moisture (as VWC and soil water head) as the overall strongest controller of root growth rate in our grassland. This result deviates from prior research that found other environmental and phenological factors to be stronger controllers of root growth in grasslands and tree stands (Joslin et al., 2001; Edwards et al., 2004; Wedderburn et al., 2010). However, it is worth noting that these studies did not use an adaptive sampling frequency, but followed a fixed sampling schedule. Furthermore, this result indicates that soil moisture is a key driver of root growth also under natural variations in temperature and not only under controlled conditions (as observed in Chapter 1).
Soil moisture seemed to be particularly important in determining root growth at 10 and 20 cm, where the largest predictors were VWC at 10 and 20 cm. The importance of the interactions between temperature and soil moisture at shallower depths in controlling growth rates at 60 cm does not necessarily indicate a correlation between them. In fact, the apparent higher influence of conditions from the upper layers likely resulted from the constant saturation and the smaller fluctuations in soil temperature at 60 cm. Possibly, it might only reflect the effects of seasonal cycles on the deeper layers.

The data clearly indicates that soil moisture had a higher control over root growth rates than temperature during the study period as a whole. However, the small dataset did not allow to analyze subsets of data, preventing the distinction of effects on root growth given by seasonality/phenology and the effects dictated by rapid and isolated soil environmental changes.
Answering Question 2 (occurrence of Hydromatching) will allow us to better understand root growth dynamics at daily time scales, otherwise invisible when looking at the experimental period as a whole.

2.5.2 Occurrence of Hydromatching

In September 2022 there was an increase in soil water head at 10 and 20 cm following the onset of the rain event, yet we observed an increase in growth rate at all depths (including 60 cm) on 05/09/2022, that is 3 to 5 days after the soil wetting (Fig. 2.4a and b). We do not know whether the response already occurred on 02/09/2022 due to image contrast issues. Post-drought increase in growth rate in both shallow and deep soil layers was an unexpected result and potentially due a overall regain of vitality after a drought-induced latency, requiring a re-establishment of the root system at the whole profile level.

Increased root growth at 60 cm 3 to 5 days after the rain event is an indication that the plants survived the drought (Fig. 2.5c, d and e). In fact, it is highly unlikely that newly sprouted plants could grow roots down to 60 cm in 5 days. This also means that the increase in growth rate observed at shallow depths on 05/09/2022 and later on 07/09/2022 likely originated from pre-existing plants and not from plants sprouted and established after the end of the drought. On 07/09/2022 the growth rates at 10 and 20 cm kept increasing while growth interrupted at 60 cm. Such root growth promotion in a newly wetted layer accompanied by an interrupted promotion in a less beneficial layer suggests the occurrence of Hydromatching. When soil at 10 cm was moist, soil at 60 cm became a less beneficial and a more "costly" source of water. This was due to its heavy clay composition, likely retaining water more tightly, imposing a higher mechanical resistance and creating conditions of low aeration (da Silva and Kay, 1997). Later on 09/09/2022 we observed an unexpected decline in root length both at 10 cm and 60 cm, with a significant reduction especially at 10 cm (Fig. 2.5f and g). We attribute this sudden root disappearance to herbivory, given the presence of unidentified invertebrates in several images taken at shallow depths in this period. Root disappearance due to predation might then represent a potential limitation

in minirhizotron studies focusing on root dynamics.

in June 2023 we captured two phases of precipitation, gradually increasing soil water head first at 10 cm (20/06/2023) and then at 20 cm (22/06/2023). This gradual increase in water potential was also accompanied by a gradual increase in root growth according to the moving water front.
Overall, the significant increase in net growth rates on 19/06/2023 at 10 cm and on 22/06/2023 at 20 cm indicates that growth rate responded to the re-wetting potentially already within 1 day from its establishment, although the growth rate medians were still below zero on these dates. Growth rates at 10 cm reached a positive median on 22/06/2023 while root length simultaneously declined at 60 cm, indicating a rapid vertical shift in root allocation which once again suggests Hydromatching. Net growth rates at 60 cm significantly increased to a positive median once more on 28/06/2023, after soil moisture at 10 cm had started to decline again for six days. It is noteworthy how root growth partitioning between topsoil and subsoil switched twice within a 20-days period, from subsoil on 09/06/2023 to topsoil on 19/06/2023 and 22/06/2023 and back to subsoil on 28/06/2023. The timing at which these significant switches occurred indicates a highly dynamic nature of the root systems in this grassland.

In July/August 2023 the prolonged and intense rainy period lasting from 24/07/2023 to 06/08/2023 increased the soil water head rapidly (within 1 day of the onset) and heavily (up to saturation). There was a significant and quick response in each depth one day after the beginning of the rainy period. We argue that, as in September 2022, this positive response shortly after the end of the dry period could have been due to a vitality resurgence. This would have led to a root system re-establishment after a period of inactivity and decay. However, the growth rates stopped their rising trend immediately after this initial increase, and root length declined significantly at 10 and 60 cm on 04/08/2023. The lack of responsiveness following the topsoil re-wetting could have been due to decreased irradiance and/or temperature due

to the prolonged rainy period that continued for 14 days (blue bars in Fig. 2.4e and f). Also, it might have been caused by conditions of soil saturation generated after the heavy rain. Soil saturation is known to restrict root growth due to lack of aeration (Drew, 1992). It was only after the end of the rainy period when we observed a promotion of root growth both in the top and subsoil (08/08/2023 and 11/08/2023), when irradiance and temperature increased (data not shown) and soil became less saturated. Hence, these results highlight the importance that energy limitation might still have in affecting Hydromatching. Root investment was guided not only by shoot water and nutrient demand but also governed by shoot carbon supply.

The switch in root growth from subsoil to topsoil after the precipitation events was faster in June 2023 compared to September 2022, although the intensity of post-rain re-wetting was similar in both events (from -21 to -9 m on 31/08/2022 and from -18 to -9 m on 20/06/2023, Fig. 2.4). Such switch in root growth following the topsoil re-wetting was absent in July/August 2023. The different response speeds between September 2022 and June 2023 were likely related to the different intensities of plant water stress prior to the rain events. In September 2022 and July/August 2023 dryness persisted for weeks, reaching levels largely exceeding those known to hinder plant growth (Mackie et al., 2019). High levels of water stress could have caused a decrease in photosynthetic rates and a reduction of carbon allocation to roots (Zwetsloot and Bauerle, 2021). This was not the case in June 2022, when soil dryness did not persist as long prior to the rain event. In the lab experiment from Chapter 1 we observed Hydromatching within 48 hours from the soil wetting, but avoided severely dry conditions and kept the soil moisture at a minimum of 6% at all times. This further supports our observation of rapid vertical growth shifts in June 2023 and delayed shifts (or no shift at all) after the re-wetting following very dry periods in September 2022 and July/August 2023.

The fast switch in root growth distribution in June 2023 could have also been

implemented for scavenging nutrients in the topsoil (normally nutrient-rich), mobilized by the re-wetting (Armas et al., 2012). At that point nutrient limitation might have influenced root growth more than water limitation and root growth could have adjusted accordingly following the "functional balance theory" (growth rate adjusts according to the most limiting resource, Thornley, 1972.

At the same time as growth rate increased in the topsoil, root length declined strongly and quickly at 60 cm. Such a significant and rapid shift in growth rates from subsoil to topsoil shortly after the re-wetting was probably less of a "risk factor" in June 2023 than it could have been in September 2022. In September 2022 the root growth shift towards the topsoil could have been delayed to mitigate the risk of losing newly grown roots due to potentially renewed drought conditions. (Wedderburn et al., 2010). This theory does not apply for the July/August 2023 event, when root inactivity and root length decline following the long precipitation period was likely caused by soil saturation and low levels of solar radiation.

Hydromatching was observed within 2-5 days in September 2022 and June 2023 (Fig. 2.4a and b). Root growth was promoted in the most resourceful layers and interrupted in the less beneficial and more costly layers. The role of "resourceful" and "less beneficial" layer was interchanged between top and subsoil in a matter of days, mostly depending on the moisture conditions of the topsoil. These results are in line with with the ones from Chapter 1, where we observed rapid switches in root growth distribution within 48 hours from the wetting. It then appears that the phenomenon of Hydromatching is not only observable at the individual plant level, but likely occurring at the plant community level of a temperate grassland as well. We observed it as a collective response as we did not discriminate between roots belonging to different species or ecological groups. Hydromatching occurred despite niche separations and differences between forbs and grasses in dealing with drought (Nippert and Knapp, 2007). If Hydromatching was not a collective response,

we would have observed consistent levels of root length both in shallow layers (for forbs) and at deeper depths (for grasses), rather than rapid shifts in root distribution between sub and topsoil.

While previous studies focused on larger scales that mostly captured seasonal or even annual dynamics of root growth (Hayes and Seastedt, 1987; Wan et al., 2002; Peek et al., 2006; Wedderburn et al., 2010; Saelim et al., 2019; Zhang et al., 2019a), such large scales overshadowed the daily time scale adjustments to quick changes in soil moisture. Our results show how root growth is orchestrated dynamically and rapidly along the whole profile depending on water availability in a naturally occurring plant community. Therefore, such short scale dynamics should be considered in the context of carbon and nutrient cycling, ecosystem productivity and in soil-vegetation-atmosphere transfer models.

2.5.3 Root vertical shift from spring to summer

We observed a clear full-scale shift in root distribution from shallow soil layers to deeper layers during the transition from late Spring to early Summer in both 2022 and 2023 (Fig 2.6). Root length both significantly increased in the subsoil and significantly decreased in the topsoil after entering summer. This finding is consistent with previous studies observing such shifts and suggesting that plants can relocate roots according to long-term seasonality of water distribution in the soil profile (Hayes and Seastedt, 1987; Wan et al., 2002; Peek et al., 2006; Saelim et al., 2019; Zhang et al., 2019a). Generally, we detected lower root length values in May 2023 compared to May 2022. Root growth could have been impacted by conditions close to saturation (known to hinder root growth, Drew, 1992) that characterized the soil at each depth from March 2023 till the end of May 2023. Another explanation for the overall lower root length in 2023 could be seedbank depletion caused by the intense drought of summer 2022 (Zhou et al., 2022). Additionally,

studies demonstrated how droughts can lead to legacy effects impacting root production in the following years (Zhou et al., 2022; Slette et al., 2023).

While root length decline was not accurately measured in our study, the significant reduction observed consistently in both years suggests that root disappearance in the topsoil likely occurred and was not given by inaccuracies in the image analysis. Interestingly, root length significantly diminished at 20 cm in both 2022 and 2023 despite the non-pronounced dryness (-1.2 m in 2022 and -2.7 m in 2023, Fig. 2.6b and d). This indicates that root senescence occurring over a month in the upper layers was not caused by water deprivation but was a programmed mechanism. This could be seen as a way to cut costs of root maintenance and save resources to be used for growing and maintaining roots in the subsoil. The observed shifts indicate a top-bottom resource transfer, with a clear separation between shallow and deep parts of the root system. The similar intensities of the shifts from May to June in both 2022 and 2023 despite the different levels of dryness suggest that these shifts are phenologically-driven processes.

Overall, our findings suggest the existence of two types of root morphological adaptations occurring under different time scales. At the short time scale and at local, small spatial scales (within a soil layer of few cm), root growth rates appear to be strongly influenced by rapidly changing environmental cues, such as soil moisture availability. Such daily-scale local adjustments in growth rates could be guided by both local changes in soil moisture and potentially by changes in soil moisture occurring elsewhere, according to the theory of the "whole-root system coordination" described at the end of Chapter 1. On the other hand, in the long-term (seasonal) and at the whole-root system scale, root distribution appear to undergo deep and significant adjustments occurring as programmed, phenologically-dictated processes independent of rapidly changing environmental cues.

2.6 Conclusions

Soil moisture was the strongest controller of growth rate in the investigated temperate grassland, confirming that this parameter is one of the most important to consider when investigating drivers of root growth.
Growth rates of root systems in a temperate grassland community adjusted according to both seasonality and daily changes in water availability. Seasonal adjustments (spring to summer) involved the entire root systems and were driven by phenological and genetic factors. Daily adjustments to rapid changes in soil moisture were more localized and dictated by sensed environmental cues. These adjustments corresponded to the "Hydromatching" phenomenon described in Chapter 1, which likely occurred in two out of our three selected periods. However, energy limitation (given by lower solar radiation and temperature), soil saturation and prolonged conditions of water deficit prior to the rain event could have been important limitations to Hydromatching. Also, we cannot fully rule out the potential role of nutrients in influencing root growth dynamics, especially when nutrient-deprivation might have been higher than water-deprivation.
Our results still suggest that Hydromatching is a naturally occurring phenomenon. It appears to be visible not only in individual young plants but also at a grassland community level, among competing species and plants occupying different ecological niches. Such finding could also hold important implications for the understanding of biogeochemical processes, as daily-time scale root distribution shifts implemented collectively within a plant population can affect carbon and nutrient cycling.

The significant variations in root growth to changes in soil moisture indicate the importance that these have in influencing plant carbon budget. Both observed long-term and short-term growth rate modifications might represent strategies evolved to cope with water heterogeneity alongside carbon budgeting. Such economizing strategies seem to lead to a promotion of

root growth in the more resourceful areas and to a root decay in "costly" areas that are no longer fruitful. Further evidence is needed to confirm this hypothesis.

Future studies should optimize root decay detection, as it seems to be deeply integrated in the root growth dynamics as a response to moisture heterogeneity. The research community should also investigate to what extent these adjustments facilitate the fulfillment of the transpiration demand. Additionally, they should consider plant water deficit indicators to better understand how much this might impact the responsiveness to re-hydration. Finally, they should rule out the influence of external factors on the root dynamics, such as nutrient limitation and prolonged periods of lower temperature and solar radiation. This could be achieved with environmental manipulation techniques.

Chapter 3

Dynamics of garlic root respiration in response to pulses of nitrate and ammonium

This chapter is currently not ready for publication. The study should be repeated with improved methodology and additional measurements (for a related discussion, see section 3.6). The work presented in this chapter was made possible by the contributions of Dr. Stanislaus Schymanski (SJS) and Dr. Julian Klaus (JK).
Contribution in concept and experimental design: SC (me), SJS, JK. Contribution in experimental preparation and measurements: SC, SJS. Contribution in data analysis: SC. Contribution in results interpretation and discussion: SC, SJS, JK.

3.1 Abstract

Plants invest a substantial part of carbon acquired by photosynthesis into acquiring nutrients from the soil. It is crucial to understand the processes operated by plants to meet their nutrient needs under limitation and to understand the associated carbon costs.

Plants can implement physiological changes to facilitate the uptake of nutrients under limitation. These changes include the activity of membrane proteins, such as aquaporins (adjusting root hydraulic conductivity) and proton-pumping ATPases (creating electrochemical gradients across membranes).

NH_4^+ and NO_3^- sensing and uptake lead to different physiological changes that alter water uptake trends. NO_3^- uptake is associated with increased hydraulic conductivity, facilitated by aquaporins, and enhanced water uptake. NH_4^+ uptake is instead associated with a decrease in both parameters. However, the C costs of these N species-specific uptake mechanisms is unclear, especially at short (hourly) time scales.

The goal of this study is to investigate the real-time root respiration dynamics after exposing roots to NH_4^+ and NO_3^-. We also intend to assess the promptness and reversibility of the response after a rapid change in N local availability. In order to do so we utilized garlic roots and placed them in a 2-compartment hydroponic split-root system. We monitored the respiration rates and the water uptake rates of roots in both compartments, with compartment 1 receiving first a weak NH_4^+ pulse and compartment 2 receiving later a strong NH_4^+ pulse. We did the same for NO_3^-.

No clear trends were observed in NO_3^--exposed roots, likely due to the low NO_3^- concentration used. In NH_4^+-exposed roots, respiration rates increased following the exposure to both the weak and strong NH_4^+ treatments, while water uptake decreased in the treated compartment and/or increased in the untreated compartment. These responses are likely linked to a rapid promotion of NH_4^+ uptake in the treated compartments. The results also suggest a high responsiveness to rapidly changing local NH_4^+ availability.

This study provides useful insights for the study of vegetation trade-offs. Our results elucidate the link between physiological adjustments in response to NH_4^+ supply and their respiratory costs. They also indicate that nutrient uptake can occur independently of water uptake, highlighting the necessity

of follow-up experiments to unravel the links between water and nutrient uptake and the associated carbon costs.

3.2 Introduction

Root nutrient uptake is a crucial process for plant health and its mechanisms are thoroughly studied, especially in the context of agricultural productivity (Eshel and Beeckman, 2013). Optimization of fertilizers use to meet plant requirements while preventing excessive nutrient mobilization in the soil is a current and important topic of discussion (Tsachidou et al., 2019). In this line of thinking, it is of primary importance to study the mechanisms adopted by roots to acquire nutrients from the surroundings, especially in environments under nutrient scarcity and heterogeneity. Previous studies showed that roots are able to locally proliferate in areas with richer NO_3^- and NH_4^+ availability, both in hydroponic medium and in soil (Drew, 1975; Pregitzer et al., 1993; Scheible et al., 1997; Linkohr et al., 2002; Guo et al., 2007b; Ishikawa-Sakurai et al., 2014). The studies not only observed a promotion of root growth in nutrient-rich patches, but also an inhibition of growth in nutrient-poor areas. According to Linkohr et al. (2002), plants seems to follow an "optimal allocation" strategy, allowing roots to chase nutrient availability while suppressing root investment in soil areas that are no longer fruitful. This behavior was already observed for water patches in what we described as "Hydromatching" in the previous chapters.

Studies also documented changes in root hydraulic and physiological properties depending on nutrient availability. Such changes could be driven by aquaporin activity, demonstrated to be closely linked to nutrient acquisition (Wang et al., 2016). Some of the studies highlighted the importance of aquaporins for quick and localized changes in hydraulic conductivity following a local exposure to nitrogen in split root experiments on tomatoes, cucumbers and rice (Gorska et al., 2008; Ishikawa-Sakurai et al., 2014). Root hydraulic

conductivity increased shortly (hours to minutes) following the exposure to N, resulting in improved nutrient acquisition. In Gorska et al. (2008) specifically, they removed nutrients from a previously treated compartment of the split-root system and added NO_3^- in another compartment. Within minutes, the root conductivity levels promptly switched and increased in the newly treated compartment. Such studies show the level of dynamism that characterizes roots from a physiological and molecular perspective under rapid changes in nutrient availability.

Incorporating such dynamics and in general considering aquaporin regulation in vegetation models could improve their robustness and predictive power (Schymanski et al., 2008). Studying the root respiration rates related to changes in physiological properties for improved nutrient uptake holds significant promise in both the agricultural and modeling contexts. As a matter of fact previous vegetation and biosphere models overly simplified the nutrient uptake costs, which lacked empirical foundation (Fisher et al., 2010; Brzostek et al., 2014). A characterization of real-life C costs linked to nutrient uptake has the potential of improving the accuracy of vegetation models in predicting nutrient uptake, carbon balance and overall plant performance. One of the potential C cost linked to nutrient uptake is the ATP expenditure by proton-pumping ATPases, specific proteins that generate electrochemical gradients across cellular membranes. This process is crucial for the uptake of nutrient molecules, as it generates the proton motive force used by proton-coupled transporters to allow solutes to enter the root cell. (Crawford and Glass, 1998; Taylor and Bloom, 1998; Palmgren, 2001; Bloom et al., 2002; Zhang et al., 2021).

However, to complicate matters, there appear to be different root hydraulics and physiological changes when dealing with different types of N-based nutrients. Several studies compared the effects of NO_3^- and NH_4^+ additions on the same individuals and have demonstrated that roots exhibit distinct physiological and biochemical responses when taking up NO_3^- com-

pared to NH_4^+. Under NO_3^- exposure, aquaporin activity increases, enhancing hydraulic conductivity and facilitating the mass flow of water and NO_3^- molecules to the root surface. Conversely, NH_4^+ exposure tends to decrease root hydraulic conductivity, thereby reducing water uptake rates. These responses were consistently observed in beans, tomatoes, muskmelons, maize and cucumbers .(Adler et al., 1996; Guo et al., 2002; Guo et al., 2007a; Guo et al., 2007b; Gorska et al., 2008; Souri et al., 2009; Pou et al., 2022). Numerous studies have reported that NH_4^+ uptake tends to acidify the rhizosphere, while NO_3^- uptake tends to alkalinize it. This is because NH_4^+ uptake generally leads to H+ secretion, whereas NO_3^- uptake leads to H+ intake (Imas et al., 1997; Hinsinger et al., 2003; Zaccheo et al., 2006; Xie et al., 2009; Imler et al., 2019; Zhang et al., 2019b). Solution acidification is known to inhibit aquaporin activity (Gerbeau et al., 2002; Guo et al., 2007a), which may explain the decrease in root hydraulic conductivity observed under NH_4^+ exposure.

In the context of nutrient uptake, several studies seem to agree that nutrient uptake of NH_4^+ could be more energy-efficient in satisfying the plant N requirements compared to NO_3^-. This is because of the high costs of NO_3^- assimilation, as demonstrated in experiments on maize, rice and barley (Bloom et al., 1992; Colmer and Bloom, 1998; Taylor and Bloom, 1998). It was even suggested that addition of NH_4^+ could inhibit the net uptake of NO_3^- (Colmer and Bloom, 1998). Notably, NO_3^- requires to be transformed into ammonia before it can be converted into amino-acids (Jackson et al., 2008). These reactions involve a dispendious amount of energy equaling to 12 ATPs per molecule of NO_3^- assimilated (Bloom et al., 1989).

In general, Guo et al. (2007a) suggested that a deeper understanding of the relationship between carbon and N metabolism is needed. Investigating the "costs" of N uptake processes in terms of CO_2 produced through root respiration could provide precious insights in the context of plant carbon budgeting and trade-offs. Bloom et al., 1992 did investigate the carbon catabolism dif-

ferences between NH_4^+ and NO_3^- plant nutrition, finding that C catabolism for NO_3^- absorption and assimilation is overall higher than the one for NH_4^+ (23% of total root carbon catabolism against 14%). Interestingly, Cramer and Lewis, 1993 observed higher O_2 consumption at the root level in NH_4^+-treated plants and attributed this to a high activity of the enzyme PEPc (phosphoenol-pyruvate carboxylase) which could be involved in the assimilation of NH_4^+ and its transformation into aminoacids directly in the roots. On the other hand, NO_3^- assimilation tends to occur at the shoot level. Although such studies managed to obtain an overall assessment of the carbon catabolism and root oxygen consumption differences between NH_4^+ and NO_3^- assimilation, none looked at the actual real-time dynamics of the respiration rates linked to aquaporin and/or proton-pumping reaction following rapid changes in N availability.

In our study we used a split-root system to (1) determine short-term changes in root respiration rate and their relation to variations in root hydraulic properties as a response to NO_3^- and NH_4^+. We them aimed to (2) determine the speed of the response and the intensity of the changes in respiration rate and/or root hydraulic properties after applying a higher concentration of N in the untreated part of the root system. Specifically, our goal is to answer the following questions:

- Question 1 (respiration and water uptake to NO_3^-): Does root respiration rate change in parallel with water uptake rate in a portion of the root system exposed to NO_3^-? If yes, how?
- Question 2 (respiration and water uptake to NH_4^+): Does root respiration rate change in parallel with water uptake rate in a portion of the root system exposed to NH_4^+? If yes, how?
- Question 3 (reversibility of response): Following 1) and 2), how are water uptake and/or root respiration rates affected once the untreated portion of the root system is exposed to a higher concentration of N?

3.3 Materials and methods

3.3.1 Experimental setup and steps

In our experiment we used roots of garlic cloves (*Allium sativum*) in a hydroponic split root system equipped with scales for water uptake inference and CO_2 sensor foils for the measurement of CO_2 concentrations (Fig. 3.1). The split root system consisted of two plastic and transparent rectangular boxes defined as "Compartment 1" (C1) and "Compartment 2" (C2), each filled with 72 ml of distilled water and containing approximately half of the root system. Each container was connected to a sealed water reservoir through a plastic tube. We created a siphon system between the compartments and the water reservoirs in order to maintain a constant water level in the compartments. The water reservoirs were placed on scales (precision of 0.01 g) used to infer water uptake based on the weight loss observed. Weights were measured every 5s. On the inner vertical surface of both containers we applied a chemical optical CO_2 sensor foil (SF-CD2R, VisiSens, PreSens GmbH, Regensburg, Germany) of the size of approximately 1.5 cm $\times$ 1 cm. The foils are made of dyes sensitive to fluorescent light, taking on different colors depending on the CO_2 concentration sensed. These sensors allow non-invasive and continuous 2D mapping of CO_2 concentrations. Roots were placed in close proximity to the sensors to map the gradients forming around them. The Visisens TD camera was placed right in front of the sensor foils. The camera emits a fluorescent light which excites the dyes and allows a visual detection of the CO_2 gradients. The camera was programmed to capture an image of the illuminated foils every 30s.

We chose to use garlic as it developed sturdy and thick roots, which were easy to handle. Their roots also led to clear and strong CO_2 signals during preliminary tests. In our split root hydroponic setup, a portion of the roots was inevitably exposed to the air for the entire duration of the exper-

iment (approximately 9 hours). Initially, we attempted to use cucumber, a species commonly employed in hydroponic experiments (Gorska et al., 2008; Roosta and Schjoerring, 2008). However, the exposed cucumber roots dried out within a few hours, likely compromising the root system's vitality. On the other hand, garlic roots remained vital and functional throughout the entire duration of the experiment (as evidenced by their stable respiration and water uptake rates).

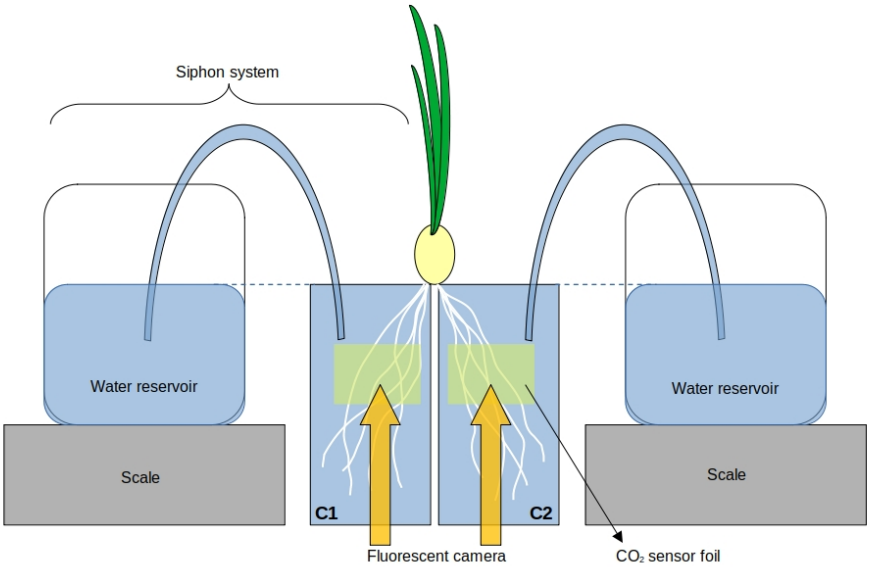

Figure 3.1: Hydroponic split root system used in the study. It consists of two compartments connected to water reservoirs through tubes, which maintain a constant water level thanks to a siphon system. Reservoirs are placed on scales for weight measurements. Each compartment contains half of the roots, which are in close proximity to the sensor foils for CO_2 gradients mapping. A fluorescent camera placed in front of the sensors emits a light that excite the dyes and capture images allowing visual detection of the CO_2 concentrations.

Garlic cloves used in our experiment were first sprouted in tap water and grown for a period ranging from 2 to 3 weeks under a PAR of approximately 35μmol s^{-1} m^{-2} at a room temperature range of 20-22 °C. The experiment was carried out on one plant at a time, for a total of 12 plants. The experi-

ment duration for each plant was of approximately 9 hours. 5 plants received NH_4^+ treatments, 5 plants received NO_3^- treatments and 2 plants were used as controls (not receiving any nutrients).

For the NH_4^+ treatments we used the Hakaphos Grün fertilizer, containing 13% Ammonium (NH_4), 7% Nitrate (NO_3), 5% phosphorus pentoxide (P_2O_5), 10% Potassium oxide (K_2O), 2% Magnesium oxide (MgO), 27% sulfur trioxide (SO_3) and trace elements (Dünger Experte, Kipfenberg/Attenzell, Germany). For the NO_3^- treatments we used a calcium nitrate mix, containing 14.4% Nitrate (NO_3), 1.1% Ammonium (NH_4), 19% Calcium (Ca) and 26.5% Calcium oxide (CaO) (Hydroponics Europe, Eindhoven, The Netherlands).

The experiment consisted of three phases: the pre-pulse phase, the post-pulse1 phase and the post-pulse2 phase. The prepulse-phase lasted approximately 2 h while the post-pulse1 and post-pulse2 phase lasted approximately 3.5 h each. During the pre-pulse phase the plants were allowed to acclimate and water uptake and respiration rates were allowed to establish under nutrient absence. At the end of the pre-pulse phase a first "weak" nutrient pulse was applied in C1, entering the post-pulse1 phase. At the end of the post-pulse1 phase a second "strong" nutrient pulse was applied in C2, entering the post-pulse2 phase. For the NH_4^+-treated plants, the first nutrient pulse consisted of 0.02 g of NH_4^+-based fertilizer which led to a concentration of 50 mg l^{-1} of total N in C1 (2 mM of NH_4^+ and 3.1×10^{-4} mM of NO_3^-). The second pulse consisted of 0.04 g of fertilizer leading to a concentration of 100 mg l^{-1} of total N in C2 (4 mM of NH_4^+ and 6.3×10^{-4} mM of NO_3^-). For the NO_3^- plants we used the same masses of NO_3^--based fertilizer which led to a concentration of 43 mg l^{-1} of total N after the first pulse in C1 (0.6 mM of NO_3^- and 1.7×10^{-4} mM of NH_4^+) and of 86 mg l^{-1} after the second pulse in C2 (1.2 mM of NO_3^- and 3.4×10^{-4} mM of NH_4^+). We defined the amounts of fertilizer according to the dosage used for growing garlic in hydroponic solutions (Naznin et al., 2010). At the same time we were also

mindful to avoid potential NH_4^+ toxicity. Studies found that levels of 5 mM of NH_4^+ and above were toxic to cucumbers, classified as a NH_4^+ sensitive species. *Aliaceae*, the family which garlic belongs to, was classified as more NH_4^+ tolerant (Britto et al., 2001). Furthermore, it was documented that the presence of NO_3^- could alleviate the NH_4^+ toxicity (Roosta and Schjoerring, 2007; Roosta and Schjoerring, 2008).
The fertilizer was dissolved in 5 ml of distilled water before being added into the compartment. Before applying it, 5 ml of solution were removed from the treated compartment in order to keep the same solution volume pre and post injection. After the pulse was applied, the solution was quickly stirred to allow uniform dispersion of solutes. This created conditions of disturbance, during which values of water uptake and respiration were neglected.
In the controls we did the same but using pulses of distilled water. For them we defined the three experimental periods as "fake" pre-pulse, fake post-pulse1 and fake post-pulse2.

During the experiment we collected solution samples to be analyzed for ion concentrations in order to infer nutrient uptake rates. We took one sample per compartment during the pre-pulse phase (considered as "blank") and three samples per compartment during both the post-pulse1 and post-pulse2 phase. The first sample was collected approximately 45 minutes into the experiment. Subsequent samples were spaced 45 minutes apart from each other and from the nutrient pulses. A sample consisted of 2 ml of solution retrieved from the compartment. We used 0.5 ml of the solution to fill glass vials through 0.45 µm Acrodisc syringe filters (Pall Corporation, New York, United States). Ion chromatography was used to analyze the ion concentrations. The analysis results were not available yet at the time of writing of this thesis chapter.
After retrieving the 2 ml of solution, 2 ml with the same concentration of the compartment solution were replenished in order to maintain the same water level. In the controls we also simulated the sample collection and their

disturbance by extracting and injecting 2 ml of distilled water at the same frequency as in the treatments. As for the pulse application, sample collection created disturbance in the system. Specific intervals of undisturbed water uptake and respiration rates were chosen for the analysis. For water uptake, we considered values once they stabilized after each disturbance until the subsequent disturbance. Value stabilization was assessed without mathematical criteria but it was intuitively evident. For root respiration, we considered values recorded after the 25 minutes following each disturbance until the subsequent disturbance.

It was important for the NH_4^+ and NO_3^- solutions to have similar levels of osmotic potential to prevent osmotically driven responses in only one of the two treatments, which would have interfered with the interpretation of the results. In an attempt to avoid this circumstance, we decided to use the same quantities of NH_4^+-based fertilizer and NO_3^--based fertilizer. Further tests carried out at the end of the experiment with a Psychrometer (PSY1, ICT International, Armidale, Australia) revealed that the osmotic potentials did not change significantly following the application of both the weak and strong pulse in water (data not shown).

3.3.2 Data analysis

Before extrapolating the water uptake values from the weight loss data of the reservoirs, we first selected undisturbed intervals within each phase. We avoided the disturbance caused by the solution sampling and by the nutrient pulse injections by considering the weight loss values after they stabilized following the perturbation. We then smoothed and reduced the noise of the weight measurements during the undisturbed intervals by using a moving average approach with an averaging window of 20 values (i.e. 1 minute and 40 seconds). Smoothed data was used to calculate water uptake rates in ml per 10 minutes, in order to yield higher values of water uptake to use

in the analysis (otherwise too small if considered on a 5-seconds interval). Since no clear trends could be observed when looking at the evolution of the absolute water uptake levels in individual compartments during the three phases, relative water uptake rates between C1 and C2 were calculated for each phase and plant. The use of relative water uptake rates allowed to separate changes in water uptake due to nutrient addition from changes due to varying shoot water demand.

For the CO_2 analysis, we utilized the Visisens ScientifiCal Software to measure the mean CO_2 concentration within the area of the sensor foils in C1 and C2 for each picture taken. We used calibration data to convert the raw values provided by the Software into pCO_2 (partial pressure exerted by dissolved CO_2 in equilibrium with the atmospheric CO_2 and the other species of the carbonic acid cycle). pCO_2 is expressed as %, with 100% indicating the maximum partial pressure that dissolved CO_2 could exert at saturation (equaling to approximately 1.5 g of CO_2 per kg of water at 22 °C) (The Engineering ToolBox, 2008; Solubility of Gases in Water vs Temperature [online] available at: https://www.engineeringtoolbox.com). We then converted the pCO_2 % into g kg^{-1} of water. For the analysis, we considered the CO_2 concentrations 25 minutes after the disturbance caused by each solution sampling and pulse injection and until right before the next perturbation. The CO_2 levels tended to naturally follow a logistic growth in the controls (Fig. 3.6e and f), continuously increasing but eventually reaching a plateau (indicating equilibrium). In the analysis we calculated a linear fit between the CO_2 concentration values for each phase separately, including the 95% confidence interval of slope and intercept. We decided to fit the data linearly and not logistically because the noise in the data was too high to allow a proper fitting of the logistic function. For each plant we plotted the CO_2 concentration data from each phase with the respective fitted function and confidence intervals. In the controls, we expected to see the upper confidence margin of the fitted linear function during the pre-pulse

phase positioned above the first undisturbed segment of CO_2 measurements in the post-pulse1 phase in both C1 and C2. We expected the same between post-pulse1 and post-pulse2 phase. In the treatments, if in C1 the upper confidence margin of the pre-pulse fit laid below the first CO_2 concentrations of the post-pulse1 phase, then we considered the CO_2 response to the first pulse to be positive. The same applied between post-pulse1 and post-pulse2 phase to test for the responsiveness to pulse 2 in C2.
The use of a linear fitting allowed us to decrease the likelihood of detecting "false positives", and rather increased the likelihood of detecting "false negatives". This, in turn, would enhance the reliability of our analysis if we detected a majority of positive responses.

The dataset of Chapter 3 can be found on Zenodo at https://zenodo.org/records/10600943 .

3.4 Results

3.4.1 Respiration rates

The respiration rates following the additions of NH_4^+ generally increased both after the first pulse in C1 and after the second pulse in C2 (Fig. 3.2 and Fig. 3.4a and b). Specifically, in three out five plants the respiration rates in C1 during the beginning of the post-pulse1 period were above the upper confidence margin of the pre-pulse fit (Fig. 3.4a). The same plants plus one additional plant (four out of five) increased their respiration rates in C2 after receiving the second pulse during the beginning of the post-pulse2 phase (Fig. 3.4b).
The respiration rates were not responsive to the first pulse of NO_3^- (Fig. 3.3 and Fig. 3.5c and d). In fact, in C1 only one plant out of five increased its respiration rates following the first pulse compared to the end of the pre-pulse

period (Fig. 3.5c). On the other hand, the same plant plus two additional plants (three out of five) increased their respiration rates after receiving the second NO_3^- pulse compared to the end of the post-pulse1 period (Fig. 3.5d). As expected, in the controls the respiration rates did not increase between phases in both C1 and C2 (Fig. 3.6e and f).

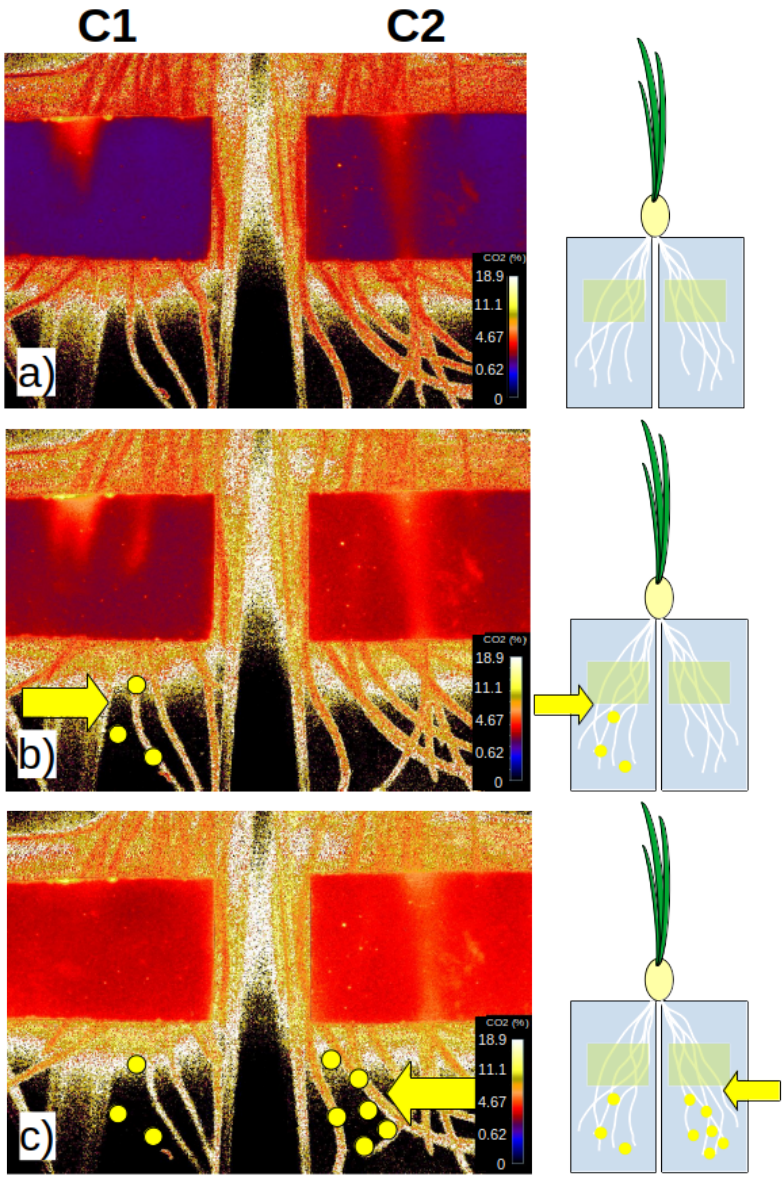

Figure 3.2: Sensor foils CO_2 measurements during the three experimental phases in C1 and C2 of a NH_4^+-treated plant. a) shows the CO_2 concentrations (%) detected during the pre-pulse phase. b) depicts the CO_2 concentrations measured during the post-pulse1 phase (after adding the weak NH_4^+ pulse in C1). c) shows the CO_2 concentrations detected during the post-pulse 2 phase (after adding the strong NH_4^+ pulse in C2)

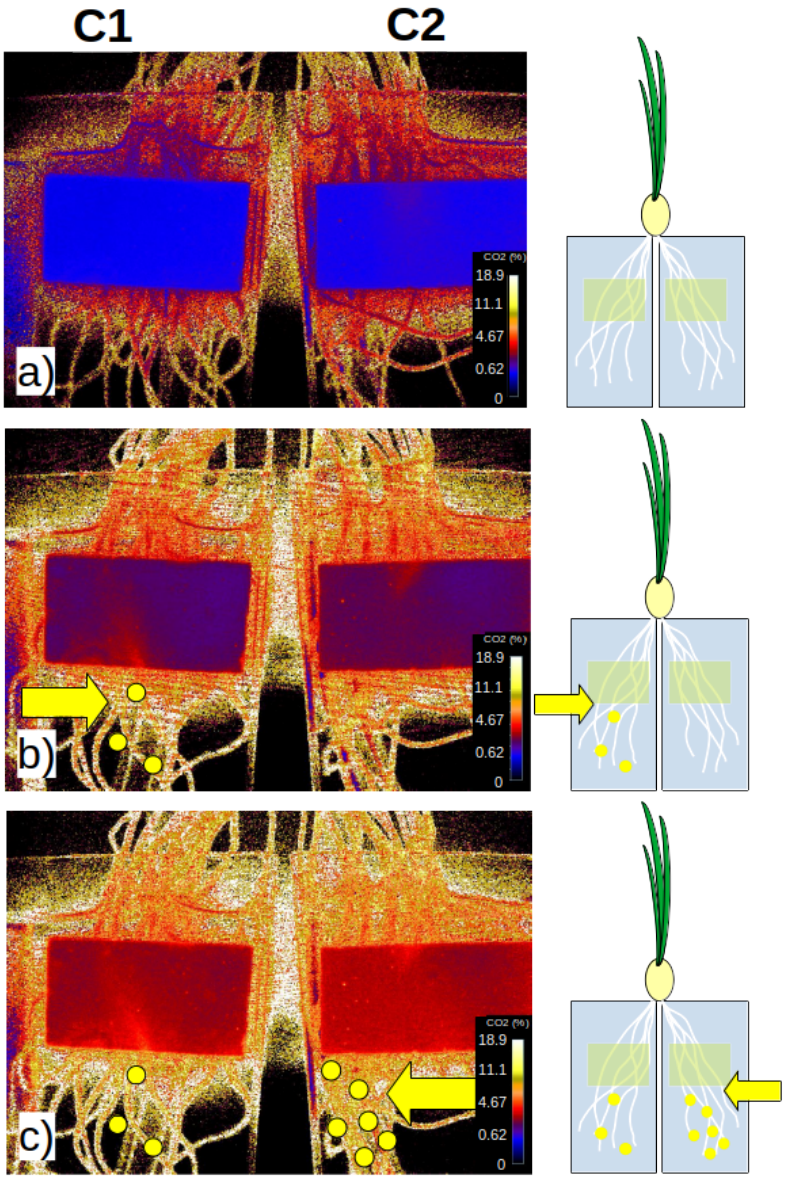

Figure 3.3: Sensor foils CO_2 measurements during the three experimental phases in C1 and C2 of a NO_3^--treated plant. a), b) and c) convey the same concepts as in Fig. 2 but considering NO_3^- pulses instead of NH_4^+.

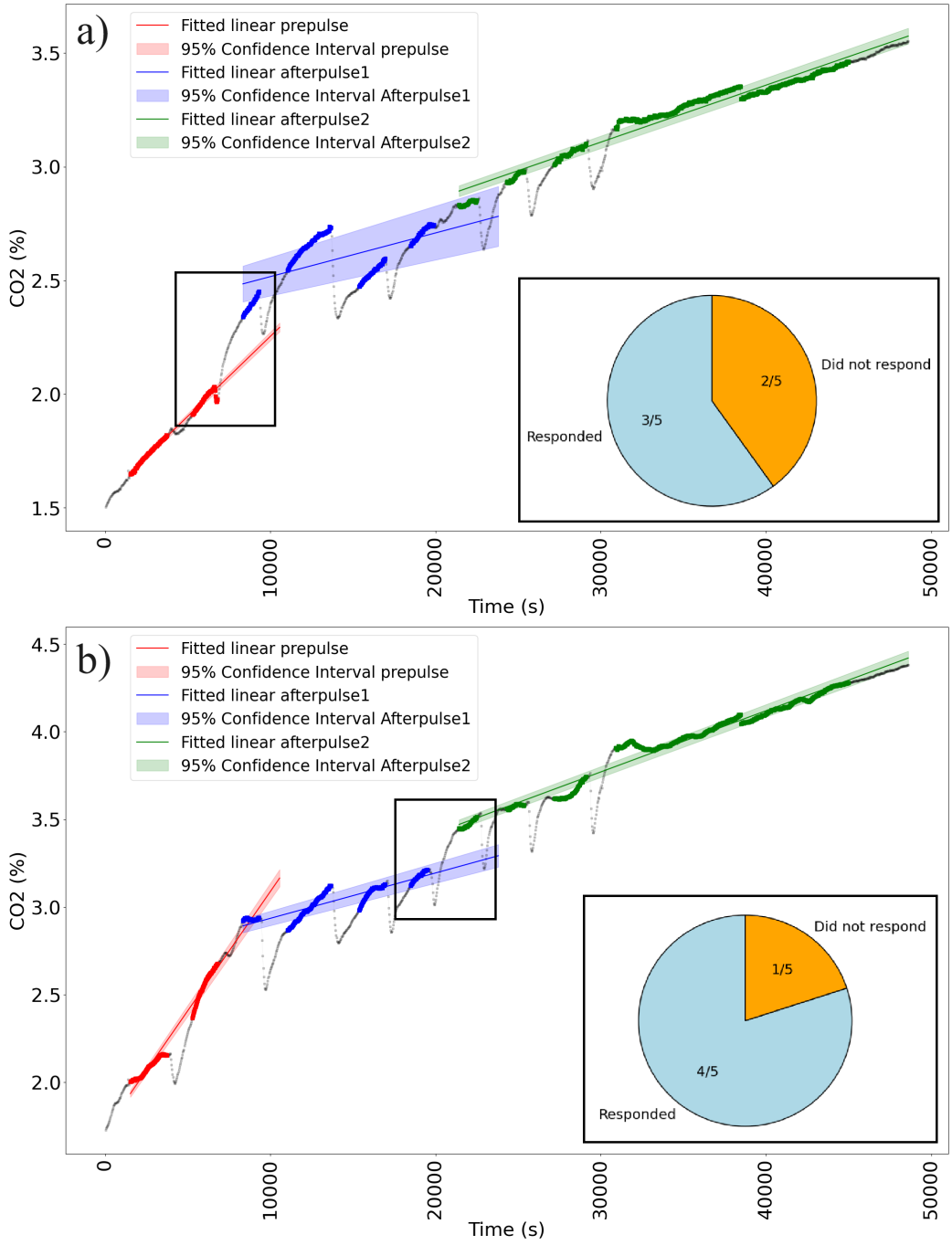

Figure 3.4: CO_2 concentrations over the three experimental phases in (a-b) one NH_4^+-treated plant, in (c-d) one NO_3^--treated plant and in (e-f) one control plant. a), c) and e) show the respiration rates in C1 and b), d) and f) in C2. X-axis represents the time in seconds and the y-axis displays the CO_2 concentration in % of gas mixture.

Continuation of previous caption: the black line behind the colored points represent all the recorded CO_2 values, including the disturbed periods. Red points represent the CO_2 concentrations recorded during the undisturbed intervals of the prepulse phase, the blue points are the CO_2 concentrations during the undisturbed intervals of the post-pulse1 phase and the green points are the CO_2 concentrations during the undisturbed intervals of the post-pulse2 phase. The straight red, blue and green lines represent the linear fit of the CO_2 concentrations of the prepulse, post-pulse1 and post-pulse2 phases respectively. The upper and lower limit of the colored areas represent the 95% confidence intervals of the linear fits of the respective phase. The pie charts report how many positive responses to CO_2 have been detected in each compartment of each treatment. Rectangular areas show the interval of data considered for the evaluation.

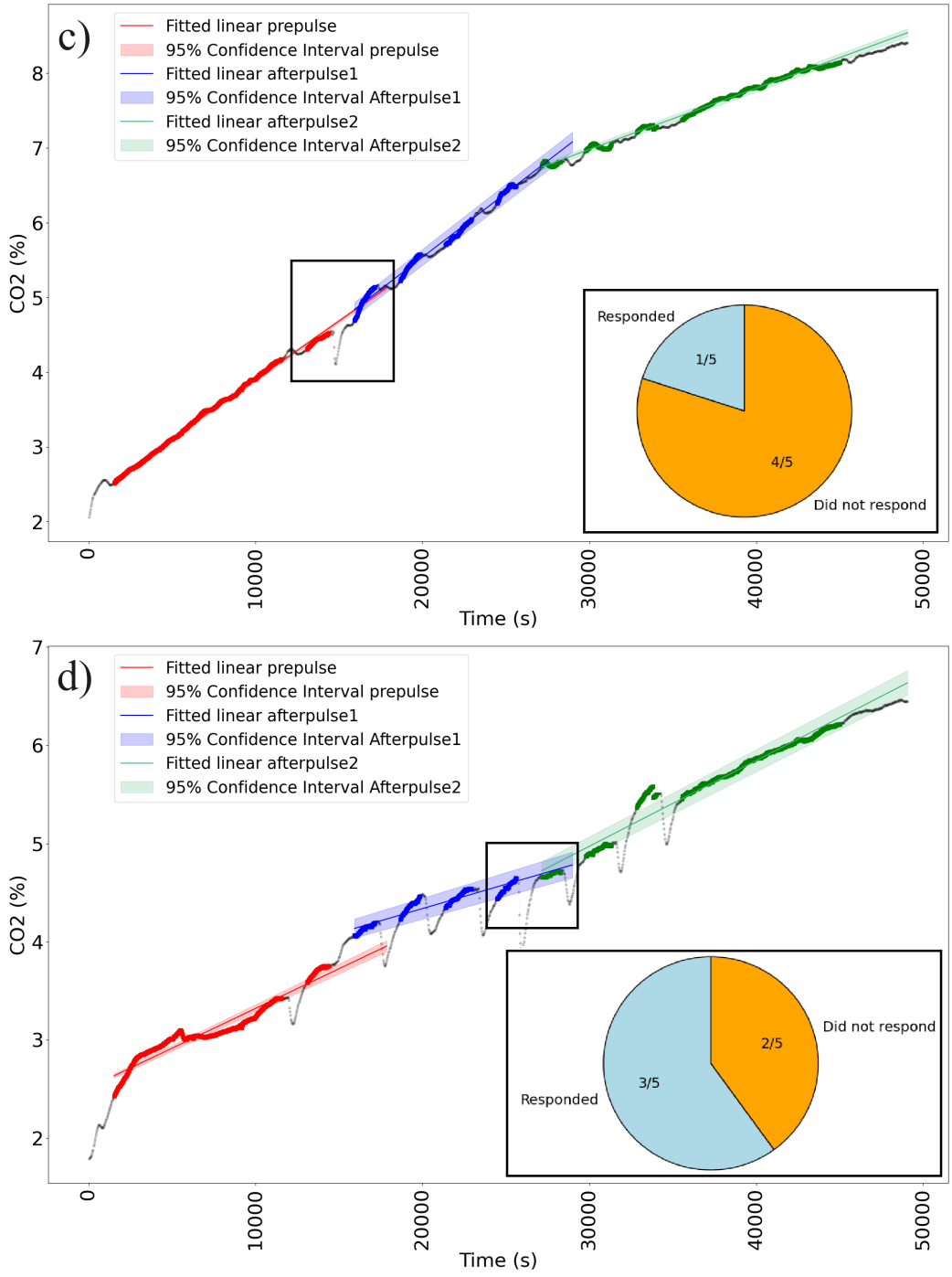

Figure 3.5: CO_2 concentrations over the three experimental phases in one NO_3^--treated plant. c) show the respiration rates in C1 and d) in C2. For details, refer to the caption of Fig. 3.4

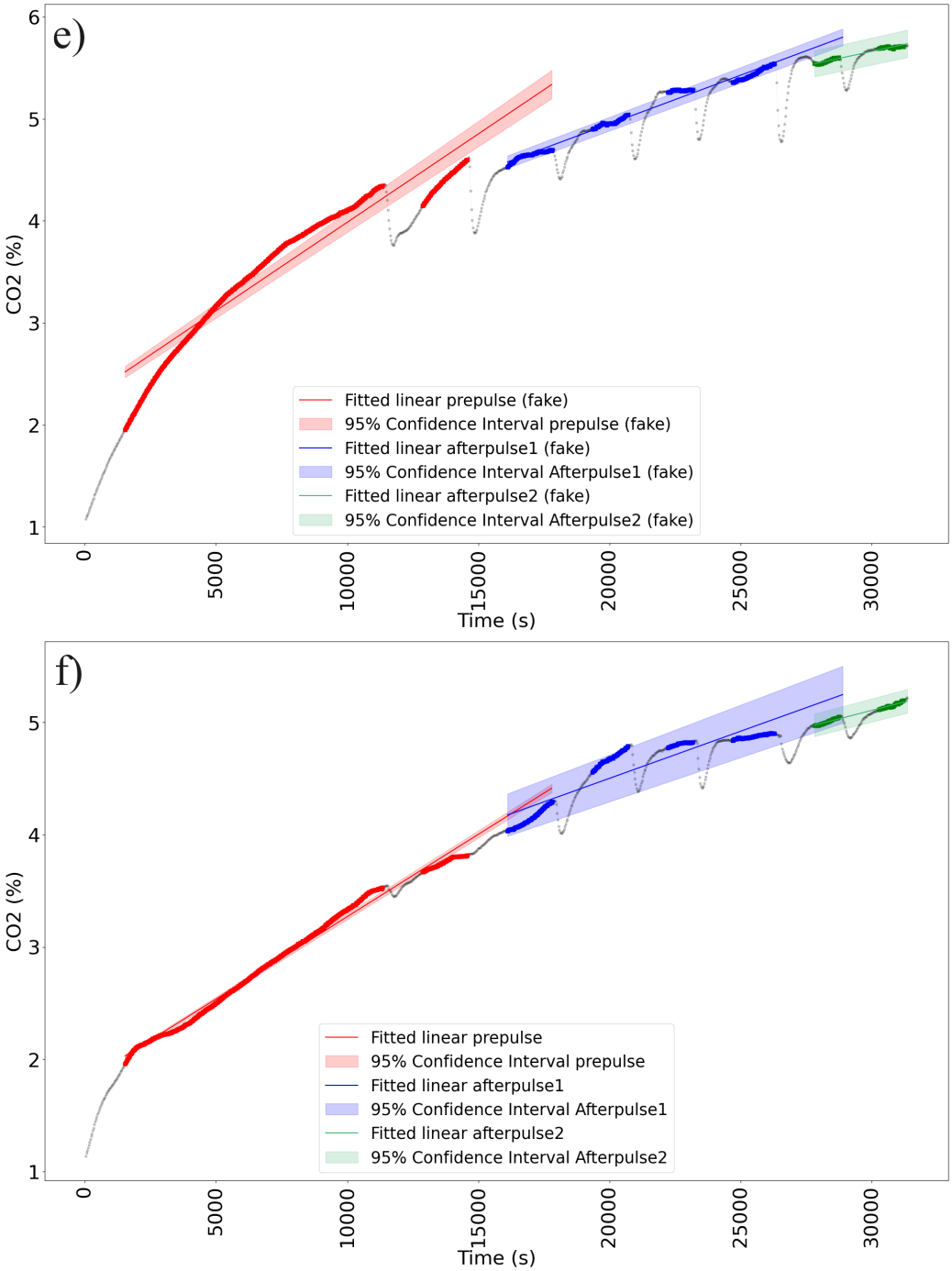

Figure 3.6: CO_2 concentrations over the three experimental phases in one control plant. e) show the respiration rates in C1 and f) in C2. For details, refer to the caption of Fig. 3.4

3.4.2 Relative water uptake rates

The relative water uptake rates between compartments following the first pulse of NH_4^+ in C1 indicate a general decrease in the water uptake in C1 and/or an increase in the water uptake in C2 (Fig. 3.7a). Four out of five plants displayed this behavior. Following the second pulse in C2, two of the same plants plus one additional plant increased their water uptake in C1 and/or decreased it in C2.

The relative water uptake between compartments in NO_3^--treated plants did not appear to adhere to any particular trend (Fig. 3.7b). Nevertheless, it was interesting to observe that the relative water uptake rates decreased in C1 and/or increased in C2 following the first pulse only in one plant. This indicates that the roots responded differently to the first pulse of NH_4^+ compared to the first pulse of NO_3^-.

Out of the two controls, one slightly increased its water uptake in C1 and/or decreased it in C2 when moving from the fake pre-pulse phase to the fake post-pulse1 phase. Other than that, no apparent change in relative water uptake rates between compartments was observed (Fig. 3.7c).

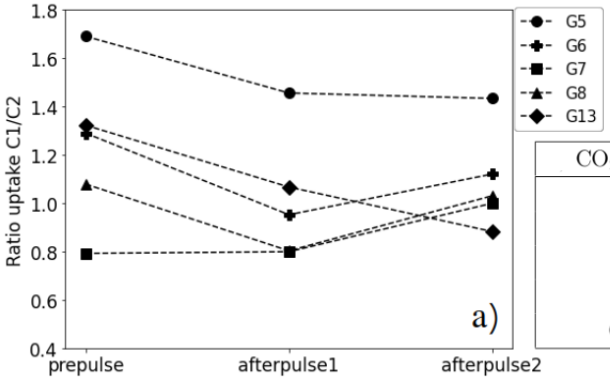

CO_2 response	Pulse 1 (C1)	Pulse 2 (C2)
G5	✓	✓
G6	✓	✓
G7		✓
G8		
G13	✓	✓

Figure 3.7: Relative water uptake rates between compartments in a) NH_4^+-treated plants, b) NO_3^--treated plants and c) controls. Markers represent the ratio between the 10-minute average uptake in C1 and the 10-minute average uptake in C2 during the same phase. Different markers represent different plants. The y-axis displays the C1/C2 ratio values. Tables next to each plot indicate for which plant of that group we observed an increase in the CO_2 concentrations in C1 after receiving the first pulse and in C2 after the second pulse.

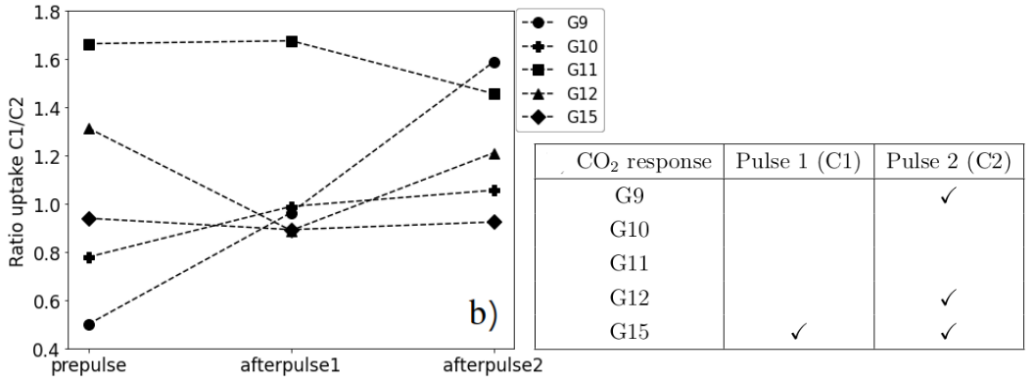

CO_2 response	Pulse 1 (C1)	Pulse 2 (C2)
G9		✓
G10		
G11		
G12		✓
G15	✓	✓

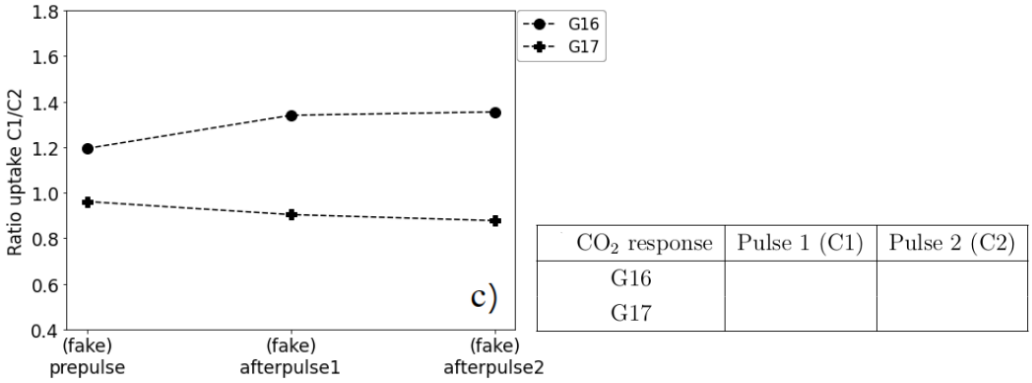

CO_2 response	Pulse 1 (C1)	Pulse 2 (C2)
G16		
G17		

Figure 3.7: Refer to previous caption.

3.5 Discussion

Overall, we observed clearer trends in water uptake and root respiration in NH_4^+-treated plants compared to NO_3^--treated plants. The possible decrease in water uptake in NH_4^+-treated compartments (Fig. 3.7a) is consistent with previous studies (Adler et al., 1996; Guo et al., 2002; Guo et al., 2007a; Guo

et al., 2007b; Souri et al., 2009), although in our case the changes were detectable within hours from the treatment. Specifically, roots of NH_4^+-treated plants increased their respiration rates after receiving both the weak pulse in C1 and the strong pulse in C2 (Fig. 3.4a and b). The plants displaying this behavior also decreased the water uptake in the treated compartment (and/or increased it in the untreated compartment) (Fig. 3.7a). On the other hand, in NO_3^--treated roots we detected an increased release of CO_2 only after applying the strong pulse in C2 (Fig. 3.5d). In this case, such increase did not relate to any trend in water uptake (Fig. 3.7b). We hypothesize that one possible cause of the higher CO_2 levels measured after NH_4^+ additions might be an increase in proton-pumping ATPase activity, needed to create the proton motive force allowing the uptake of NH_4^+. ATPases requires energy to function, and their activity potentially led to higher respiration rates downstream. NH_4^+ uptake could then explain the decline in water uptake in the treated compartments, as NH_4^+ intake leads to rhizosphere acidification (Imas et al., 1997; Hinsinger et al., 2003; Zaccheo et al., 2006; Xie et al., 2009; Imler et al., 2019; Zhang et al., 2019b), which in turn can block aquaporins and decrease root hydraulic conductivity (Gerbeau et al., 2002; Guo et al., 2007a). The potential increase in water uptake in the untreated compartment accompanying the decrease in the NH_4^+-treated compartment would be consistent with previous results (Adler et al., 1996; Guo et al., 2002; Guo et al., 2007a; Souri et al., 2009). For instance, bean plants in split root systems were seen decreasing water uptake in a NH_4^+-supplied compartment while increasing it in a N-free compartment, to compensate (Guo et al., 2007b).

Another possible explanation for the higher respiration rates observed in response to NH_4^+ addition could be linked to NH_4^+ assimilation processes involving their transformation into amino-acids. NH_4^+ is assimilated directly in the roots and the process is mediated through PEPc (phosphoenol-pyruvate carboxylase) activity at the root level, requiring carbohydrates to synthesize amino-acids from NH_4^+. This, in turn, could lead to an intensification of the

tricarboxylic acid cycle (TCA) cycle and to an increase in respiration rates (Cramer and Lewis, 1993). On the other hand, NO_3^- is often assimilated at the leaf level, potentially explaining the lower respiration rates observed at the root level of NO_3^--treated plants compared to NH_4^+. Such results might indicate fast NH_4^+ assimilation rates following the nutrient addition, as CO_2 levels increased at sub-hourly time scales following the pulses.

Assimilation of NH_4^+ directly at the root level was also described as a detoxifying mechanism in the presence of toxic levels of NH_4^+ in soil solution. Toxicity is usually associated with presence of free NH_4^+ in plant tissues, which was shown to hinder plant growth (Schortemeyer et al., 1997). A strategy to avoid this consists in enhanced NH_4^+ assimilation and transformation into non-toxic amids and amino-acids directly at the root level, which was shown to consume large amounts of energy in the form of carbohydrates (Schortemeyer et al., 1997; Hachiya et al., 2012). This could be another explanation for the increased root respiration rates in NH_4^+-treated plants as per the TCA mechanism explained earlier. However, toxicity-related changes in respiration rates were unlikely due to the use of a NH_4^+-tolerant species and sub-toxic NH_4^+ concentrations (<5 mM compared to >10 mM in NH_4^+ detoxification studies).

Ultimately, there is a chance that the detected CO_2 levels in the NH_4^+-treated plants might not derive from changes in root respiration rates but from an imbalance of the carbonic acid cycle. Proton extrusion occurs as NH_4^+ is taken up, decreasing the solution pH. At pH<7 HCO_3^- already begins to progressively transform into CO_2 (König et al., 2019). Unfortunately, pH measurements were not included in our study, impeding us from establishing whether this process influenced the measured CO_2 levels. However, supposing this imbalance led to higher CO_2 levels not derived from respiring roots, this would still indicate that NH_4^+ uptake was rapid and high enough to alter the pH. In this scenario, defining a direct relation between NH_4^+ uptake and respiration rates would not be possible. Follow-up studies should

include pH measurements to detect when variations in CO_2 concentrations are likely given by pH-induced chemical transformations and not by changes in respiration rates.

Surprisingly, we did not observe clear trends in water uptake rates following either of the pulses in NO_3^--treated plants, unlike previous studies (Guo et al., 2007b; Gorska et al., 2008; Pou et al., 2022). The increase in CO levels observed in three out of five NO_3^--treated plants following the strong pulse could be attributed to proton-pumping ATPase activity, necessary to establish the electrochemical gradient used by NO_3^- transporters for NO_3^- uptake. Instead, the NO_3^- concentration following the weak pulse was likely too low to trigger any physiological response. Additionally, the promotion of ATPase activity after the strong NO_3^- pulse may have also been influenced by the presence of NH_4^+, for the reasons explained before. NH_4^+ was in fact still present in small amounts in the NO_3^--based fertilizer. Following the application of the strong NO_3^--based pulse, the NH_4^+ concentration in solution corresponded to 0.34 mM. Studies have shown increases in respiration rate due to root-level NH_4^+ assimilation processes at NH_4^+ concentrations as low as 0.05 mM (Bloom et al., 1992). We did not find evidence of garlic being more responsive to NH_4^+ compared to NO_3^-, nor to exhibit a preference for NH_4^+ uptake. We therefore hypothesize that the absence of clear trends under NO_3^- treatment was due to inadequate amounts of NO_3^- to trigger a significant aquaporin activation and increase in hydraulic conductivity. We defined the amounts of fertilizer for our treatments according to a study about growing garlic in a hydroponic system (Naznin et al., 2010). Such amounts were also suitable to avoid NH_4^+ toxicity. In addition, we adjusted the amounts of NH_4^+-based and NO_3^--based fertilizers in order for them to lead to similar osmotic potentials in solution. By following these criteria we most likely applied an insufficient quantity of NO_3^-. Studies observing significant aquaporin activation and increase in root hydraulic conductivity administered enough NO_3^- to generate concentrations $300\ \mathrm{mg\ l^{-1}}$ (Guo et al.,

2007b; Gorska et al., 2008; Pou et al., 2022), in contrast to 86 mg l^{-1} reached in our system after the strong pulse. Also, NO_3^--based fertilizers used in such studies did not contain NH_4^+ but ours did. Hence, another possible explanation for the unresponsiveness to the NO_3^- treatment could be found in a potential deactivation of aquaporins due to H+ extrusion, mediated to favor the uptake of NH_4^+ even if present in small quantities.

NH_4^+-treated roots responded, both in terms of respiration rates and relative water uptake rates, to both pulses applied in the two compartments in different moments (Fig. 3.2, Fig. 3.4a and b and Fig. 3.7a). This indicates a degree of responsiveness that is maintained through time and a promptness in the reaction time to changes in NH_4^+ availability. After the application of the strong pulse in compartment 2, compartment 1 went abruptly from most beneficial (in terms of N availability) to least beneficial. A similar sudden shift in favorability between areas of the rhizosphere occurred in the studies from Chapter 1 and 2, although in terms of soil moisture. While in Chapter 1 and 2 we were able to observe a clear decline in root growth after a soil layer shifted from most to least beneficial, here we cannot answer Question 3 (reversibility of response) and determine whether there was a reversal in resource allocation from compartment 1 to compartment 2 after applying the strong pulse. The impossibility is given by the fact that change in respiration rates was not a reliable proxy to assess a shift in resource allocation, both due to the type of data analysis chosen (reliable to detect an increase in respiration rates but not a decline) and due to the nature of the sensor foils. As we never replaced the hydroponic solutions during the experiment, the sensors tended to display an overall continuous buildup of CO_2 concentrations (tending to saturation). While rapid accelerations in the CO_2 buildup were easily identifiable, this tendency made it challenging to clearly detect reductions in respiration rates.

Relative water uptake seemed to progressively decrease in the NH_4^+-treated compartment and/or increase in the untreated compartment (Fig. 3.7). How-

ever, this did not reflect a shift in resource allocation from least to most beneficial compartment but a passive adjustment to continue meeting the canopy water demand.

Once the solution samples will be analyzed for ion concentrations, we may be able to obtain a rough estimate of nutrient uptake in C1 and C2 after the weak and strong pulse application. By linking nutrient uptake rates to respiration and water uptake rates, we will gain a better understanding on the underlying mechanisms of NH_4^+ and NO_3^- acquisition and of the related carbon expenditure.

3.6 Conclusions

In this study we observed higher respiration rates and lower water uptake rates from NH_4^+-treated roots (and/or higher water uptake rates from untreated roots). No clear trends were observed in NO_3^--treated roots. Higher CO_2 levels following NH_4^+ addition could be explained by a fast (sub-hourly) and local promotion of nutrient uptake in the treated compartment. Such promotion could have been aided by proton-pumping ATPase activity and by assimilation at the root level through PEPc (phosphoenol-pyruvate carboxylase) enzyme activity. Increased NH_4^+ uptake could also explain the reduced water uptake in the treated compartment, as it would lead to H+ extrusion and rhizosphere acidification which can deactivate aquaporins and decrease root hydraulic conductivity. Water uptake rates would then adjust accordingly and increase in the untreated compartment to meet the canopy water demand. However, there could be a chance that a low pH-induced imbalance of the carbonic acid cycle could have affected the CO_2 measurements. This demonstrates that measuring pH is fundamental to determine the influence of this process on the CO_2 measurements. Response to NH_4^+ addition was observed for both weak and strong pulse, indicating that the roots were highly responsive to multiple nutrient pulses applied in different

locations in different moments.
The reversibility of the response, described as a switch in resource allocation from least beneficial area to most beneficial area, was impossible to determine due to analysis and setup constraints.
The lack of trends to the NO_3^- treatment was unexpected, as studies consistently showed pronounced aquaporin activation and increased hydraulic conductance to NO_3^- exposition. This was likely caused by the low NO_3^- concentration in solution (one order of magnitude lower than the one used in previous studies) or by the simultaneous presence of NH_4^+, potentially causing aquaporin suppression.
Our investigation would have benefited from further parameters measurements such as pH and root hydraulic conductivity. Still, in this study we managed to shed light on the real-time dynamics of respiration rates in relation to changes in nutrient availability, which could contribute in improving the knowledge on the scavenging tactics operated by plants. Furthermore, if it is proven that CO_2 measurements derived from root respiration and not from chemical imbalances in solution, our study could be employed to estimate C costs related to NH_4^+ uptake. Such finding would largely benefit the study of vegetation trade-offs and could strengthen the performance of vegetation models.

General discussion and outlook

The three chapters composing this thesis improved our understanding of the short-term root morphological and physiological dynamics occurring under rapid changes in water and nutrient availability. Chapter 1 and 2 were centered around the influence of soil moisture on root growth dynamics at daily time scales while Chapter 3 focused on the effect of nutrients in modifying root physiological properties at sub-hourly time scales. The results from all three chapters highlighted the high degree of dynamicity that characterize root systems and that enables them to chase and capture resources under high levels of spatial and temporal heterogeneity.

In all three chapters I strove to assess the promptness and speed of response following an abrupt change in resource availability. In Chapter 1 and 2 I successfully managed to observe significant adjustments in morphology (defined as "Hydromatching") within days from the change in water availability. In Chapter 3 I observed significant adjustments in physiology (with CO_2 serving as a proxy) within 1 hour from the change in nutrient availability.

In all chapters I also aimed at assessing the reversibility of the observed adjustments. Reversibility was regarded as a shift in resource allocation from an initially resourceful area to another area that initially was less beneficial but has then become more resource-rich than the former area. In Chapter 1 and 2 I obtained strong indications of the reversibility of the Hydromatch-

ing phenomenon occurring on a daily time scale. Such results highlight how short-time scale dynamics could account for a large portion of the trade-offs and might be overlooked in studies. In Chapter 3 it was not possible to determine the reversibility of the physiological adjustments due to experimental and statistical constraints.

The root growth dynamics observed in Chapter 1 and 2 indicate an ability to sense moisture at the whole root-system level and to invest C budget to promote growth (and uptake) in water-rich areas while economizing in water-poor areas. The observation of similar root growth dynamics in both individual young plants (Chapter 1) and at the plant community level (Chapter 2) suggests that Hydromatching is a naturally occuring phenomenon. It was intriguing to observe clear and rapid shifts in root growth in the grassland despite the potential presence of plant species occupying different ecological niches.

Chapter 2 also allowed us to understand the constraints of Hydromatching in nature. The phenomenon was not observable under energy limitation (caused by lower temperature and solar radiation) and it was less quick and less pronounced when the plant community previously experienced severe water deficit. This study also offered insights for differentiating between the factors controlling Hydromatching and the ones driving seasonal shifts in root distribution. The former appear to be fully guided by environmental cues while the latter, widely reported in literature, is controlled by genetic and phenological factors.

In Chapter 3 the results were not as clear and conclusive as in the previous chapters. Nonetheless, the rapid and significant increases in root respiration after both NH_4^+ weak and strong pulses indicate a high degree of responsiveness to rapid NH_4^+ spatial and temporal variations, similar to the reactivity for moisture variations in Chapter 1 and 2. The link between CO_2 and water uptake measurements suggests that the higher respiration rates post-treatment likely derived from processes of NH_4^+ uptake. After further

refinement, these rates can be potentially used for the estimation of NH_4^+ uptake-related C costs.

My studies, although insightful, had limitations that impacted the collectivity, quality and interpretability of the results. The studies would have also benefited from additional parameters measurements to increase the cohesiveness and integrity and to draw less speculative conclusions. My findings also raised new questions and paved the way for new studies to expand upon them. Specifically, the experiment described in Chapter 1 was affected by time constraints that forced me to start the experiment prematurely, when roots were still in the process of exploring the layers below the topsoil. This potentially hindered the effectiveness of the treatments. Future studies should ensure that the root systems have established in each layer and have depleted water levels consistently before proceeding with the treatments.

In Chapter 2 I faced problems of imprecise root detection from the images, impacting the accuracy of root decline measurements. Furthermore, additional parameters such as plant water stress and the control over nutrient availability should have been considered to reinforce the hypothesized explanations with further evidence.

The observed similarity in root growth dynamics in response to rapid and localized moisture changes between Chapter 1 (lab experiment) and Chapter 2 (field experiment) suggests that the results I derived from controlled laboratory conditions are likely transferable to real-world plant communities. Still, studies on the dynamics of Hydromatching should be repeated considering different plant species and different plant communities to further validate the results and potentially demonstrate the universality of the observed dynamics. For example, follow-up research could test whether the quick root dynamics that I observed in herbaceous plants are also detectable in woody species, which typically experience higher transpiration demand but also exhibit deeper rooting depth (Wang et al., 2020). Pulsed water experiments should be carried out on plant species adapted to energy-limited

and water-limited environments, to understand if fast root distribution shifts are expressed only in species accustomed to periods of water scarcity. More pulsed water experiments should also be conducted on species of high food security value. In such species, leveraging Hydromatching under patchy water supply could improve their water use efficiency while ensuring yield.
Both in Chapter 1 and Chapter 2 I observed rapid and significant rates of root decay. Researchers should explore more deeply into the possibility of root decay to be an active mechanism and an important part of the dynamic adjustments, implemented to cut C costs which are then allocated for improved resource acquisition. Such investigations could involve measurements of below and aboveground C fluxes, water and nutrient status and overall plant performance to estimate the net benefit by considering resource acquisition per carbon expenditure.
Future investigations should also analyze the effect of rapid nutrient fluctuations on root growth dynamics in a similar way as I did for water fluctuations in Chapter 1 and 2. As creating quick fluctuations in nutrient availability could be challenging in soil, hydroponic mediums may be an effective alternative.

The study described in Chapter 3 should be repeated with improved methodology. While the findings are promising, they opened up too many possible interpretations and did not permit clear conclusions. In the study, the unexpected absence of clear trends in water uptake and respiration rates under NO_3^- treatment was likely given by an inadequate NO_3^- concentration in solution, too low to trigger significant aquaporin activation and changes in hydraulic conductivity. The experiment should be repeated with an increased number of replicates and adjustments to the quantity and type of fertilizer used. Specifically, pure NH_4^+ and NO_3^- fertilizers should be utilized, with a higher NO_3^- concentration established in solution. The experiment would have benefited from additional parameters measurements, including pH and root hydraulic conductivity. The former could be measured with pH sensor

foils while the latter could be estimated by using high pressure flow meters (Pou et al., 2022) or assessed through osmotic potential measurements of sap and soil solution coupled with sap flow rates (Ishikawa-Sakurai et al., 2014). Furthermore, while garlic was chosen for the experiment primarily due to practical convenience given by root sturdiness and ease of handling, further tests should be conducted on species with fibrous root systems, as opposed to the adventitious root system of garlic. Additionally, investigating species that are more extensively studied in root physiology and morphology (e.g. *Arabidopsis thaliana*, *Zea mays*, *Oryza sativa*, *Solanum lycopersicum*) could enhance the transferability of the findings across different species. Repeating the experiment with the recommended additions and further measurements would enhance the results' quality and clarity, reducing the number of interpretations and increasing the likelihood of obtaining clearer insights suitable for publication.

Follow-up studies could also consider the role played by other stressors, such as soil compaction, in influencing root properties adjustments to varying water and nutrient supply. Such investigations could also delve deep into monitoring the effects of soil compaction on the utilization of different nutrient pools or on the symbiosis with arbuscular mycorrhiza, which play a crucial role in facilitating tree nutrient uptake (Anthony et al., 2022).

In conclusion, all the three chapters provided useful insights in the field of plant morphodynamics and development. The results showcased an exceptional level of short-term root system dynamicity and plasticity dictated by surrounding resource availability. My results can serve as a solid base to further investigate species-specific abilities to modify their root system morphological and physiological traits to benefit from sparse and pulsing resource availability. In turn, such investigations could pave the way towards the formulation of plant breeding programs and cropping methods to enhance input use efficiency. From an ecological perspective, the detection of clear root growth responses to rapidly varying soil moisture at a plant community

level is an impactful finding to be considered in plant population dynamics and plant resource competition studies. Vegetation, hydrological and climate models can potentially grow upon our findings and consider the incorporation of the root dynamics reported in this thesis for more accurate predictions of resource uptake and plant trade-offs and, consequently, of plant performance and water fluxes.

Bibliography

Adler, P., Wilcox, G., and III, A. (1996). Ammonium decreases muskmelon root system hydraulic conductivity. *Journal of Plant Nutrition*, 19:1395–1403.

Amenu, G. G. and Kumar, P. (2007). A model for hydraulic redistribution. *Hydrology and Earth System Sciences Discussions*, 4:3719–3769.

Anthony, M. A., Crowther, T. W., Van Der Linde, S., Suz, L. M., Bidartondo, M. I., Cox, F., Schaub, M., Rautio, P., Ferretti, M., Vesterdal, L., et al. (2022). Forest tree growth is linked to mycorrhizal fungal composition and function across europe. *The ISME journal*, 16(5):1327–1336.

Armas, C., Kim, J. H., Bleby, T. M., and Jackson, R. B. (2012). The effect of hydraulic lift on organic matter decomposition, soil nitrogen cycling, and nitrogen acquisition by a grass species. *Oecologia*, 168(1):11–22.

Bauerle, T. L., Smart, D. R., Bauerle, W. L., Stockert, C., and Eissenstat, D. M. (2008). Root foraging in response to heterogeneous soil moisture in two grapevines that differ in potential growth rate. *New Phytologist*, 179(3):857–866. _eprint: https://nph.onlinelibrary.wiley.com/doi/pdf/10.1111/j.1469-8137.2008.02489.x.

Bloom, A. J., Caldwell, R. M., Finazzo, J., Warner, R. L., and Weissbart, J. (1989). Oxygen and Carbon Dioxide Fluxes from Barley Shoots Depend on Nitrate Assimilation. *Plant Physiology*, 91(1):352–356.

Bloom, A. J., Meyerhoff, P. A., Taylor, A. R., and Rost, T. L. (2002). Root Development and Absorption of Ammonium and Nitrate from the Rhizosphere. *Journal of Plant Growth Regulation*, 21(4):416–431.

Bloom, A. J., Sukrapanna, S. S., and Warner, R. L. (1992). Root Respiration Associated with Ammonium and Nitrate Absorption and Assimilation by Barley. *Plant Physiology*, 99(4):1294–1301.

Britto, D. T., Siddiqi, M. Y., Glass, A. D. M., and Kronzucker, H. J. (2001). Futile transmembrane NH $_4$ $^+$ cycling: A cellular hypothesis to explain ammonium toxicity in plants. *Proceedings of the National Academy of Sciences*, 98(7):4255–4258.

Brzostek, E. R., Fisher, J. B., and Phillips, R. P. (2014). Modeling the carbon cost of plant nitrogen acquisition: Mycorrhizal trade-offs and multipath resistance uptake improve predictions of retranslocation. *Journal of Geophysical Research: Biogeosciences*, 119(8):1684–1697.

Carsel, R. F. and Parrish, R. S. (1988). Developing joint probability distributions of soil water retention characteristics. *Water resources research*, 24(5):755–769.

Carvajal, M., Cooke, D., and Clarkson, D. (1996). Responses of wheat plants to nutrient deprivation may involve the regulation of water-channel function. *Planta*, 199(3).

Chaves, M. and Davies, B. (2010). Drought effects and water use efficiency: improving crop production in dry environments. *Functional Plant Biology*, 37(2):iii.

Colmer, T. D. and Bloom, A. J. (1998). A comparison of NH4+ and NO3– net fluxes along roots of rice and maize. *Plant, Cell & Environment*, 21(2):240–246. _eprint: https://onlinelibrary.wiley.com/doi/pdf/10.1046/j.1365-3040.1998.00261.x.

Conant, R. T., Paustian, K., and Elliott, E. T. (2001). Grassland Management and Conversion into Grassland: Effects on Soil Carbon. *Ecological Applications*, 11(2):343–355.

Cordell, D., Drangert, J.-O., and White, S. (2009). The story of phosphorus: global food security and food for thought. *Global environmental change*, 19(2):292–305.

Cramer, M. and Lewis, O. (1993). The influence of no-3 and nh+ 4 nutrition on the gas exchange characteristics of the roots of wheat (triticum aestivum) and maize (zea mays) plants. *Annals of Botany*, 72(1):37–46.

Craven, D., Isbell, F., Manning, P., Connolly, J., Bruelheide, H., Ebeling, A., Roscher, C., Van Ruijven, J., Weigelt, A., Wilsey, B., et al. (2016). Plant diversity effects on grassland productivity are robust to both nutrient enrichment and drought. *Philosophical Transactions of the Royal Society B: Biological Sciences*, 371(1694):20150277.

Crawford, N. M. and Glass, A. D. (1998). Molecular and physiological aspects of nitrate uptake in plants. *Trends in plant science*, 3(10):389–395.

da Silva, A. P. and Kay, B. D. (1997). Estimating the Least Limiting Water Range of Soils from Properties and Management. *Soil Science Society of America Journal*, 61(3):877–883.

Daryanto, S., Wang, L., and Jacinthe, P.-A. (2017). Global synthesis of drought effects on cereal, legume, tuber and root crops production: A review. *Agricultural Water Management*, 179:18–33.

Dekker, L. W., Doerr, S. H., Oostindie, K., Ziogas, A. K., and Ritsema, C. J. (2001). Water repellency and critical soil water content in a dune sand. *Soil Science Society of America Journal*, 65(6):1667–1674.

Drew, M. (1975). Comparison of the effects of a localised supply of phosphate, nitrate, ammonium and potassium on the growth of the seminal root system, and the shoot, in barley. *New Phytologist*, 75(3):479–490.

Drew, M. C. (1992). Soil aeration and plant root metabolism. *Soil Science*, 154(4):259–268.

Dusschoten, D. v., Metzner, R., Kochs, J., Postma, J. A., Pflugfelder, D., Bühler, J., Schurr, U., and Jahnke, S. (2016). Quantitative 3D Analysis of Plant Roots Growing in Soil Using Magnetic Resonance Imaging. *Plant Physiology*, 170(3):1176–1188.

Edwards, E. J., Benham, D. G., Marland, L. A., and Fitter, A. H. (2004). Root production is determined by radiation flux in a temperate grassland community. *Global Change Biology*, 10(2):209–227.

Eissenstat, D. M. (1992). Costs and benefits of constructing roots of small diameter. *Journal of plant nutrition*, 15(6-7):763–782.

Engels, C., Mollenkopf, M., and Marschner, H. (1994). Effect of drying and rewetting the topsoil on root growth of maize and rape in different soil depths. *Zeitschrift für Pflanzenernährung und Bodenkunde*, 157(2):139–144. _eprint: https://onlinelibrary.wiley.com/doi/pdf/10.1002/jpln.19941570213.

Eshel, A. and Beeckman, T., editors (2013). *Plant Roots: The Hidden Half, Fourth Edition*. CRC Press, Boca Raton, FL, 4 edition edition.

Farley, R. and Fitter, A. (1999). Temporal and spatial variation in soil resources in a deciduous woodland. *Journal of Ecology*, 87(4):688–696.

Farrant, J. M. and Hilhorst, H. (2022). Crops for dry environments. *Current Opinion in Biotechnology*, 74:84–91.

Fay, P. A., Prober, S. M., Harpole, W. S., Knops, J. M. H., Bakker, J. D., Borer, E. T., Lind, E. M., MacDougall, A. S., Seabloom, E. W., Wragg, P. D., Adler, P. B., Blumenthal, D. M., Buckley, Y. M., Chu, C., Cleland, E. E., Collins, S. L., Davies, K. F., Du, G., Feng, X., Firn, J., Gruner, D. S., Hagenah, N., Hautier, Y., Heckman, R. W., Jin, V. L., Kirkman, K. P., Klein, J., Ladwig, L. M., Li, Q., McCulley, R. L., Melbourne, B. A., Mitchell, C. E., Moore, J. L., Morgan, J. W., Risch, A. C., Schütz, M., Stevens, C. J., Wedin, D. A., and Yang, L. H. (2015). Grassland productivity limited by multiple nutrients. *Nature Plants*, 1(7):1–5.

Fisher, J., Sitch, S., Malhi, Y., Fisher, R., Huntingford, C., and Tan, S.-Y. (2010). Carbon cost of plant nitrogen acquisition: A mechanistic, globally applicable model of plant nitrogen uptake, retranslocation, and fixation. *Global Biogeochemical Cycles*, 24(1).

Fransen, B., Blijjenberg, J., and de Kroon, H. (1999). Root morphological and physiological plasticity of perennial grass species and the exploitation of spatial and temporal heterogeneous nutrient patches. *Plant and Soil*, 211:179–189.

Fromm, H. (2019). Root Plasticity in the Pursuit of Water. *Plants*, 8(7):236.

Gallardo, M., Turner, N., and Ludwig, C. (1994). Water relations, gas exchange and abscisic acid content of *Lupinus cosentinii* leaves in response to drying different proportions of the root system. *Journal of Experimental Botany*, 45(7):909–918.

Gerbeau, P., Amodeo, G., Henzler, T., Santoni, V., Ripoche, P., and Maurel, C. (2002). The water permeability of arabidopsis plasma membrane is regulated by divalent cations and ph. *The Plant Journal*, 30(1):71–81.

Giehl, R. F. H. and von Wirén, N. (2018). Hydropatterning—how roots test the waters. *Science*, 362(6421):1358–1359.

Gill, R. A., Burke, I. C., Lauenroth, W. K., and Milchunas, D. G. (2002a). Longevity and turnover of roots in the shortgrass steppe: influence of diameter and depth. page 12.

Gill, R. A., Burke, I. C., Lauenroth, W. K., and Milchunas, D. G. (2002b). Longevity and turnover of roots in the shortgrass steppe: influence of diameter and depth. *Plant Ecology*, 159:241–251.

Goergen, K., Beersma, J., Hoffmann, L., and Junk, J. (2013). ENSEMBLES-based assessment of regional climate effects in Luxembourg and their impact on vegetation. *Climatic Change*, 119(3):761–773.

Gorska, A., Ye, Q., Holbrook, N. M., and Zwieniecki, M. A. (2008). Nitrate Control of Root Hydraulic Properties in Plants: Translating Local Information to Whole Plant Response. *Plant Physiology*, 148(2):1159–1167.

Green, S. R. and Clothier, B. E. (1995). Root water uptake by kiwifruit vines following partial wetting of the root zone. *Plant and Soil*, 173(2):317–328.

Guo, S., Brück, H., and Sattelmacher, B. (2002). Effects of supplied nitrogen form on growth and water uptake of French bean (Phaseolus vulgaris L.) plants. *Plant and Soil*, 239(2):267–275.

Guo, S., Kaldenhoff, R., Uehlein, N., Sattelmacher, B., and Brueck, H. (2007a). Relationship between water and nitrogen uptake in nitrate- and ammonium-supplied Phaseolus vulgaris L. plants. *Journal of Plant Nutrition and Soil Science*, 170(1):73–80. _eprint: https://onlinelibrary.wiley.com/doi/pdf/10.1002/jpln.200625073.

Guo, S., Shen, Q., and Brueck, H. (2007b). Effects of Local Nitrogen Supply on Water Uptake of Bean Plants in a Split Root System. *Journal of Integrative Plant Biology*, 49(4):472–480.

Hachiya, T., Watanabe, C. K., Fujimoto, M., Ishikawa, T., Takahara, K., Kawai-Yamada, M., Uchimiya, H., Uesono, Y., Terashima, I., and Noguchi, K. (2012). Nitrate addition alleviates ammonium toxicity without lessening ammonium accumulation, organic acid depletion and inorganic cation depletion in arabidopsis thaliana shoots. *Plant and Cell Physiology*, 53(3):577–591.

Hayes, D. C. and Seastedt, T. R. (1987). Root dynamics of tallgrass prairie in wet and dry years. *Canadian Journal of Botany*, 65(4):787–791.

Hinsinger, P., Plassard, C., Tang, C., and Jaillard, B. (2003). Origins of root-mediated ph changes in the rhizosphere and their responses to environmental constraints: a review. *Plant and soil*, 248:43–59.

Ho, M. D., Rosas, J. C., Brown, K. M., and Lynch, J. P. (2005). Root architectural tradeoffs for water and phosphorus acquisition. *Functional Plant Biology*, 32(8):737.

Hodge, A. (2004). The plastic plant: root responses to heterogeneous supplies of nutrients. *New Phytologist*, 162(1):9–24. _eprint: https://nph.onlinelibrary.wiley.com/doi/pdf/10.1111/j.1469-8137.2004.01015.x.

Hodge, A. (2010). Roots: The Acquisition of Water and Nutrients from the Heterogeneous Soil Environment. In Lüttge, U., Beyschlag, W., Büdel, B., and Francis, D., editors, *Progress in Botany 71*, Progress in Botany, pages 307–337. Springer, Berlin, Heidelberg.

Hodge, A., Berta, G., Doussan, C., Merchan, F., and Crespi, M. (2009). Plant root growth, architecture and function. *Plant and Soil*, 321(1-2):153–187.

Hu, Y., Wei, X., Hao, M., Fu, W., Zhao, J., and Wang, Z. (2018). Partial Least Squares Regression for Determining Factors Controlling Winter Wheat Yield. *Agronomy Journal*, 110(1):281–292.

Hutchings, M. J., John, E. A., and Wijesinghe, D. K. (2003). Toward understanding the consequences of soil heterogeneity for plant populations and communities. *Ecology*, 84(9):2322–2334.

Imas, P., Bar-Yosef, B., Kafkafi, U., and Ganmore-Neumann, R. (1997). Release of carboxylic anions and protons by tomato roots in response to ammonium nitrate ratio and ph in nutrient solution. *Plant and Soil*, 191:27–34.

Imler, C. S., Arzola, C. I., and Nunez, G. H. (2019). Ammonium uptake is the main driver of rhizosphere ph in southern highbush blueberry. *HortScience*, 54(5):955–959.

Isbell, F., Craven, D., Connolly, J., Loreau, M., Schmid, B., Beierkuhnlein, C., Bezemer, T. M., Bonin, C., Bruelheide, H., de Luca, E., Ebeling, A., Griffin, J. N., Guo, Q., Hautier, Y., Hector, A., Jentsch, A., Kreyling, J., Lanta, V., Manning, P., and Meyer, S. T. (2015). Biodiversity increases the resistance of ecosystem productivity to climate extremes. *Nature*, 526(7574):574–577. Publisher: Springer Nature.

Ishikawa-Sakurai, J., Hayashi, H., and Murai-Hatano, M. (2014). Nitrogen availability affects hydraulic conductivity of rice roots, possibly through changes in aquaporin gene expression. *Plant & Soil*, 379(1/2):289–300.

Jackson, L. E., Burger, M., and Cavagnaro, T. R. (2008). Roots, nitrogen transformations, and ecosystem services. *Annu. Rev. Plant Biol.*, 59:341–363.

Jackson, R. B., Schenk, H., Jobbagy, E., Canadell, J., Colello, G., Dickinson, R., Field, C., Friedlingstein, P., Heimann, M., Hibbard, K., et al. (2000). Belowground consequences of vegetation change and their treatment in models. *Ecological applications*, 10(2):470–483.

Jarvis, N. J. (2011). Simple physics-based models of compensatory plant water uptake: concepts and eco-hydrological consequences. *Hydrology and Earth System Sciences*, 15(11):3431–3446.

Javot, H. and Maurel, C. (2002). The role of aquaporins in root water uptake. *Annals of Botany*, 90(3):301–313.

Joslin, J. D., Wolfe, M. H., and Hanson, P. J. (2001). Factors controlling the timing of root elongation intensity in a mature upland oak stand. page 12.

Klaus, J., Monk, W. A., Zhang, L., and Hannah, D. M. (2022). Ecohydrological interactions during drought. *Ecohydrology*, 15(5):e2456. _eprint: https://onlinelibrary.wiley.com/doi/pdf/10.1002/eco.2456.

Kleidon, A. and Heimann, M. (1998). A method of determining rooting depth from a terrestrial biosphere model and its impacts on the global water and carbon cycle. *Global Change Biology*, 4(3):275–286.

König, M., Vaes, J., Klemm, E., and Pant, D. (2019). Solvents and supporting electrolytes in the electrocatalytic reduction of co2. *Iscience*, 19:135–160.

Kulmatiski, A., Adler, P. B., Stark, J. M., and Tredennick, A. T. (2017). Water and nitrogen uptake are better associated with resource availability than root biomass. *Ecosphere*, 8(3):e01738. _eprint: https://esajournals.onlinelibrary.wiley.com/doi/pdf/10.1002/ecs2.1738.

Leuschner, C., Backes, K., Hertel, D., Schipka, F., Schmitt, U., Terborg, O., and Runge, M. (2001). Drought responses at leaf, stem and fine root levels of competitive Fagus sylvatica L. and Quercus petraea (Matt.) Liebl. trees in dry and wet years. *Forest Ecology and Management*, 149(1):33–46.

Linkohr, B. I., Williamson, L. C., Fitter, A. H., and Leyser, H. O. (2002). Nitrate and phosphate availability and distribution have different effects on root system architecture of *Arabidopsis*. *The Plant Journal*, 29(6):751–760.

Mackie, K. A., Zeiter, M., Bloor, J. M. G., and Stampfli, A. (2019). Plant functional groups mediate drought resistance and recovery in a multisite grassland experiment. *Journal of Ecology*, 107(2):937–949.

Majdi, H. and Andersson, P. (2005). Fine Root Production and Turnover in a Norway Spruce Stand in Northern Sweden: Effects of Nitrogen and Water Manipulation. *Ecosystems*, 8(2):191–199.

Marx, S. and Flammang, F. (2015). La cartographie des sols au Grand-Duché de Luxembourg.

Metcalfe, D. B., Meir, P., Aragão, L. E. O. C., da Costa, A. C. L., Braga, A. P., Gonçalves, P. H. L., de Athaydes Silva Junior, J., de Almeida, S. S., Dawson, L. A., Malhi, Y., and Williams, M. (2008). The effects of water availability on root growth and morphology in an Amazon rainforest. *Plant and Soil*, 311(1):189–199.

Müllers, Y., Postma, J. A., Poorter, H., and van Dusschoten, D. (2023). Deep-water uptake under drought improved due to locally increased root conductivity in maize, but not in faba bean. *Plant, Cell & Environment*, 46(7):2046–2060. _eprint: https://onlinelibrary.wiley.com/doi/pdf/10.1111/pce.14587.

Nakagawa, S. and Schielzeth, H. (2013). A general and simple method for obtaining r2 from generalized linear mixed-effects models. *Methods in ecology and evolution*, 4(2):133–142.

Naznin, M., Kitaya, Y., Shibuya, T., and Hirai, H. (2010). Growth and ajoene concentrations in garlic plants cultured hydroponically with different aeration regimes. *The Journal of Horticultural Science and Biotechnology*, 85(2):161–165.

Nguyen, M. A., Larson, J. E., Blair, M. D., Hardwick, D. D., Khurana, N., Kim, J. S., Rosenfield, M. V., and Funk, J. L. (2017).

Rapid root responses of seedlings exposed to a postdrought water pulse. *American Journal of Botany*, 104(12):1816–1824. _eprint: https://bsapubs.onlinelibrary.wiley.com/doi/pdf/10.3732/ajb.1700282.

Nippert, J. B. and Knapp, A. K. (2007). Soil water partitioning contributes to species coexistence in tallgrass prairie. *Oikos*, 116(6):1017–1029.

North, G. B. and Nobel, P. S. (1998). Water uptake and structural plasticity along roots of a desert succulent during prolonged drought. *Plant, Cell & Environment*, 21(7):705–713. _eprint: https://onlinelibrary.wiley.com/doi/pdf/10.1046/j.1365-3040.1998.00317.x.

Padilla, F. M., Aarts, B. H. J., Roijendijk, Y. O. A., de Caluwe, H., Mommer, L., Visser, E. J. W., and de Kroon, H. (2013). Root plasticity maintains growth of temperate grassland species under pulsed water supply. *Plant and Soil*, 369(1-2):377–386.

Palmgren, M. G. (2001). Plant plasma membrane h+-atpases: powerhouses for nutrient uptake. *Annual review of plant biology*, 52(1):817–845.

Pardales, J. R. and Yamauchi, A. (2003). Regulation of root development in sweetpotato and cassava by soil moisture during their establishment period. *Plant and Soil*, 255(1):201–208.

Peek, M. S., Leffler, A. J., Hipps, L., Ivans, S., Ryel, R. J., and Caldwell, M. M. (2006). Root turnover and relocation in the soil profile in response to seasonal soil water variation in a natural stand of Utah juniper (Juniperus osteosperma). *Tree Physiology*, 26(11):1469–1476.

Pou, A., Hachez, C., Couvreur, V., Maistriaux, L. C., Ismail, A., and Chaumont, F. (2022). Exposure to high nitrogen triggered a genotype-dependent modulation of cell and root hydraulics, which can involve

aquaporin regulation. *Physiologia Plantarum*, 174(1):e13640. _eprint: https://onlinelibrary.wiley.com/doi/pdf/10.1111/ppl.13640.

Pregitzer, K. S., Hendrick, R. L., and Fogel, R. (1993). The demography of fine roots in response to patches of water and nitrogen. *New Phytologist*, 125(3):575–580.

Richter, K., Atzberger, C., Hank, T. B., and Mauser, W. (2012). Derivation of biophysical variables from earth observation data: validation and statistical measures. *Journal of Applied Remote Sensing*, 6(1):063557–063557.

Ritsema, C. J. and Dekker, L. W. (1994). How water moves in a water repellent sandy soil: 2. dynamics of fingered flow. *Water resources research*, 30(9):2519–2531.

Robbins, N. E. and Dinneny, J. R. (2015). The divining root: moisture-driven responses of roots at the micro- and macro-scale. *Journal of Experimental Botany*, 66(8):2145–2154.

Roosta, H. R. and Schjoerring, J. K. (2007). Effects of ammonium toxicity on nitrogen metabolism and elemental profile of cucumber plants. *Journal of Plant Nutrition*, 30(11):1933–1951.

Roosta, H. R. and Schjoerring, J. K. (2008). Effects of nitrate and potassium on ammonium toxicity in cucumber plants. *Journal of Plant Nutrition*, 31(7):1270–1283.

Saelim, S., Sdoodee, S., and Chiarawipa, R. (2019). Monitoring seasonal fine root dynamics of Hevea brasiliensis clone RRIM 600 in Southern Thailand using minirhizotron technique. *Songklanakarin Journal of Science & Technology*, 41(2):8.

Scheible, W.-R., Lauerer, M., Schulze, E.-D., Caboche, M., and Stitt, M. (1997). Accumulation of nitrate in the shoot acts as a signal to regulate shoot-root allocation in tobacco+. *The Plant Journal*, 11(4):671–691.

Schortemeyer, M., Stamp, P., and Feil, B. (1997). Ammonium tolerance and carbohydrate status in maize cultivars. *Annals of Botany*, 79(1):25–30.

Schwinning, S. and Ehleringer, J. R. (2001). Water use trade-offs and optimal adaptations to pulse-driven arid ecosystems. *Journal of Ecology*, 89(3):464–480.

Schymanski, S. J. (2008). Optimality as a Concept to Understand and Model Vegetation at Different Scales. *Geography Compass*, 2(5):1580–1598.

Schymanski, S. J., Sivapalan, M., Roderick, M. L., Beringer, J., and Hutley, L. B. (2008). An optimality-based model of the coupled soil moisture and root dynamics. *Hydrology and Earth System Sciences*, 12(3):913–932.

Sebastian, J., Yee, M.-C., Viana, W. G., Álvarez, R. R., Feldman, M., Priest, H. D., Trontin, C., Lee, T., Jiang, H., Baxter, I., Mockler, T. C., Hochholdinger, F., Brutnell, T. P., and Dinneny, J. R. (2016). Grasses suppress shoot-borne roots to conserve water during drought. *Proceedings of the National Academy of Sciences of the United States of America*, 113(31):8861–8866. Publisher: National Academy of Sciences.

Shahhosseini, M., Martinez-Feria, R. A., Hu, G., and Archontoulis, S. V. (2019). Maize yield and nitrate loss prediction with machine learning algorithms. *Environmental Research Letters*, 14(12):124026.

Singh, R. K., Deshmukh, R., Muthamilarasan, M., Rani, R., and Prasad, M. (2020). Versatile roles of aquaporin in physiological processes and stress tolerance in plants. *Plant Physiology and Biochemistry*, 149:178–189.

Slette, I. J., Hoover, D. L., Smith, M. D., and Knapp, A. K. (2023). Repeated extreme droughts decrease root production, but not the potential for post-drought recovery of root production, in a mesic grassland. *Oikos*, 2023(1):e08899. _eprint: https://onlinelibrary.wiley.com/doi/pdf/10.1111/oik.08899.

Smith, A. G., Han, E., Petersen, J., Olsen, N. A. F., Giese, C., Athmann, M., Dresbøll, D. B., and Thorup-Kristensen, K. (2020). RootPainter: Deep Learning Segmentation of Biological Images with Corrective Annotation. preprint, Plant Biology.

Souri, M. K., Neumann, G., and Roemheld, V. (2009). Nitrogen forms and water consumption in tomato plants. *Hort. Environ. Biotechnol*, 50:377–383.

Stewart, A. M. and Frank, D. A. (2008). Short sampling intervals reveal very rapid root turnover in a temperate grassland. *Oecologia*, 157(3):453–458.

Taylor, A. R. and Bloom, A. J. (1998). Ammonium, nitrate, and proton fluxes along the maize root. *Plant, Cell & Environment*, 21(12):1255–1263. _eprint: https://onlinelibrary.wiley.com/doi/pdf/10.1046/j.1365-3040.1998.00357.x.

Teskey, R. O. and Hinckley, T. M. (1981). Influence of temperature and water potential on root growth of white oak. *Physiologia plantarum*, 52(3):363–369.

Thomas, A. (2020). Root water uptake under heterogeneous soil moisture conditions: an experimental study for unraveling compensatory root water uptake and hydraulic redistribution. *Plant Soil*, page 15.

Thornley, J. (1972). A balanced quantitative model for root: shoot ratios in vegetative plants. *Annals of Botany*, 36(2):431–441.

Toğaçar, M., Ergen, B., and Cömert, Z. (2020). Application of breast cancer diagnosis based on a combination of convolutional neural networks, ridge regression and linear discriminant analysis using invasive breast cancer images processed with autoencoders. *Medical Hypotheses*, 135:109503.

Torbenson, M. C. A., Büntgen, U., Esper, J., Urban, O., Balek, J., Reinig, F., Krusic, P. J., Del Castillo, E. M., Brázdil, R., Semerádová, D., Štěpánek,

P., Pernicová, N., Kolář, T., Rybníček, M., Koňasová, E., Arbelaez, J., and TRNKAc, M. (2023). Central European Agroclimate over the Past 2000 Years. *Journal of Climate*, 36(13):4429–4441. Publisher: American Meteorological Society.

Tripathy, K. P. and Mishra, A. K. (2023). How Unusual Is the 2022 European Compound Drought and Heatwave Event? *Geophysical Research Letters*, 50(15):e2023GL105453.

Tsachidou, B., Scheuren, M., Gennen, J., Debbaut, V., Toussaint, B., Hissler, C., George, I., and Delfosse, P. (2019). Biogas residues in substitution for chemical fertilizers: A comparative study on a grassland in the Walloon Region. *Science of The Total Environment*, 666:212–225.

Tzohar, D., Moshelion, M., and Ben-Gal, A. (2021). Compensatory hydraulic uptake of water by tomato due to variable root-zone salinity. *Vadose Zone Journal*.

van Dusschoten, D., Kochs, J., Kuppe, C., Sydoruk, V. A., Couvreur, V., Pflugfelder, D., and Postma, J. A. (2020). Spatially resolved root water uptake determination using a precise soil water sensor. *Plant Physiology*, page pp.00488.2020.

Van Genuchten, M. T. (1980). A closed-form equation for predicting the hydraulic conductivity of unsaturated soils. *Soil science society of America journal*, 44(5):892–898.

Van Loon, A. F., Gleeson, T., Clark, J., Van Dijk, A. I. J. M., Stahl, K., Hannaford, J., Di Baldassarre, G., Teuling, A. J., Tallaksen, L. M., Uijlenhoet, R., Hannah, D. M., Sheffield, J., Svoboda, M., Verbeiren, B., Wagener, T., Rangecroft, S., Wanders, N., and Van Lanen, H. A. J. (2016). Drought in the Anthropocene. *Nature Geoscience*, 9(2):89–91. Number: 2 Publisher: Nature Publishing Group.

Van Vuuren, M., Robinson, D., and Griffiths, B. (1996). Nutrient inflow and root proliferation during the exploitation of a temporally and spatially discrete source of nitrogen in soil. *Plant and Soil*, 178:185–192.

Virtanen, P., Gommers, R., Oliphant, T. E., Haberland, M., Reddy, T., Cournapeau, D., Burovski, E., Peterson, P., Weckesser, W., Bright, J., van der Walt, S. J., Brett, M., Wilson, J., Millman, K. J., Mayorov, N., Nelson, A. R. J., Jones, E., Kern, R., Larson, E., Carey, C. J., Polat, İ., Feng, Y., Moore, E. W., VanderPlas, J., Laxalde, D., Perktold, J., Cimrman, R., Henriksen, I., Quintero, E. A., Harris, C. R., Archibald, A. M., Ribeiro, A. H., Pedregosa, F., van Mulbregt, P., and SciPy 1.0 Contributors (2020). SciPy 1.0: Fundamental Algorithms for Scientific Computing in Python. *Nature Methods*, 17:261–272.

Wan, C., Yilmaz, I., and Sosebee, R. E. (2002). Seasonal soil–water availability influences snakeweed root dynamics. *Journal of Arid Environments*, 51(2):255–264.

Wang, L., de Kroon, H., Bögemann, G. M., and Smits, A. J. M. (2005). Partial Root Drying Effects on Biomass Production in Brassica napus and the Significance of Root Responses. *Plant & Soil*, 276(1/2):313–326. Publisher: Springer Nature.

Wang, M., Ding, L., Gao, L., Li, Y., Shen, Q., and Guo, S. (2016). The Interactions of Aquaporins and Mineral Nutrients in Higher Plants. *International Journal of Molecular Sciences*, 17(8):1229.

Wang, P., Huang, K., and Hu, S. (2020). Distinct fine-root responses to precipitation changes in herbaceous and woody plants: a meta-analysis. *New Phytologist*, 225(4):1491–1499.

Wang, P., Niu, G., Fang, Y., Wu, R., Yu, J., Yuan, G., Pozdniakov, S. P., and Scott, R. L. (2018). Implementing Dynamic Root Optimization in Noah-

MP for Simulating Phreatophytic Root Water Uptake. *Water Resources Research*, 54(3):1560–1575.

Wedderburn, M., Crush, J., Pengelly, W., and Walcroft, J. (2010). Root growth patterns of perennial ryegrasses under well-watered and drought conditions. *New Zealand Journal of Agricultural Research*, 53(4):377–388. Publisher: Taylor & Francis _eprint: https://doi.org/10.1080/00288233.2010.514927.

Weißhuhn, K., Auge, H., and Prati, D. (2011). Geographic variation in the response to drought in nine grassland species. *Basic and Applied Ecology*, 12(1):21–28.

Wilcox, C. S., Ferguson, J. W., Fernandez, G. C. J., and Nowak, R. S. (2004). Fine root growth dynamics of four Mojave Desert shrubs as related to soil moisture and microsite. *Journal of Arid Environments*, 56(1):129–148.

Xie, H., Jiang, R., Zhang, F., McGrath, S., and Zhao, F. (2009). Effect of nitrogen form on the rhizosphere dynamics and uptake of cadmium and zinc by the hyperaccumulator thlaspi caerulescens. *Plant and Soil*, 318:205–215.

Yu, P. and Li, C. (2019). Plasticity of Lateral Root Branching in Maize. *Frontiers in Plant Science*, 10:5.

Zaccheo, P., Crippa, L., and Pasta, V. D. M. (2006). Ammonium nutrition as a strategy for cadmium mobilisation in the rhizosphere of sunflower. *Plant and Soil*, 283:43–56.

Zhang, B., Cadotte, M. W., Chen, S., Tan, X., You, C., Ren, T., Chen, M., Wang, S., Li, W., Chu, C., Jiang, L., Bai, Y., Huang, J., and Han, X. (2019a). Plants alter their vertical root distribution rather than biomass allocation in response

to changing precipitation. *Ecology*, 100(11):e02828. _eprint: https://esajournals.onlinelibrary.wiley.com/doi/pdf/10.1002/ecy.2828.

Zhang, K., Wu, Y., and Hang, H. (2019b). Differential contributions of no 3-/nh 4+ to nitrogen use in response to a variable inorganic nitrogen supply in plantlets of two brassicaceae species in vitro. *Plant Methods*, 15:1–12.

Zhang, M., Wang, Y., Chen, X., Xu, F., Ding, M., Ye, W., Kawai, Y., Toda, Y., Hayashi, Y., Suzuki, T., Zeng, H., Xiao, L., Xiao, X., Xu, J., Guo, S., Yan, F., Shen, Q., Xu, G., Kinoshita, T., and Zhu, Y. (2021). Plasma membrane H+-ATPase overexpression increases rice yield via simultaneous enhancement of nutrient uptake and photosynthesis. *Nature Communications*, 12(1):735. Number: 1 Publisher: Nature Publishing Group.

Zheng, C., Bochmann, H., Liu, Z., Kant, J., Schrey, S. D., Wojciechowski, T., and Postma, J. A. (2023). Plant root plasticity during drought and recovery: What do we know and where to go? *Frontiers in Plant Science*, 14.

Zhou, H., Hou, L., Lv, X., Yang, G., Wang, Y., and Wang, X. (2022). Compensatory growth as a response to post-drought in grassland. *Frontiers in Plant Science*, 13.

Zwetsloot, M. J. and Bauerle, T. L. (2021). Repetitive seasonal drought causes substantial species-specific shifts in fine-root longevity and spatio-temporal production patterns in mature temperate forest trees. *New Phytologist*, 231(3):974–986. _eprint: https://onlinelibrary.wiley.com/doi/pdf/10.1111/nph.17432.